The Institute of Paper Chemistry

Appleton, Wisconsin

Doctor's Dissertation

A Study of the Diffusion into and Adsorption of Polyethylenimine onto Silica Gel

Ronald E. Hostetler

June, 1973

A STUDY OF THE DIFFUSION INTO AND ADSORPTION OF POLYETHYLENIMINE ONTO SILICA GEL

A thesis submitted by

Ronald E. Hostetler

B.S. 1968 Western Michigan University

M.S. 1970, Lawrence University

in partial fulfillment of the requirements
of The Institute of Paper Chemistry
for the degree of Doctor of Philosophy
from Lawrence University,
Appleton, Wisconsin

June, 1973

TABLE OF CONTENTS

SUMMARY

Previous studies have suggested that the inability of large cationic polymers to diffuse into the microporous structure of cellulose fibers is the cause of the experimentally observed decrease in adsorption with increased molecular weight and the slow adsorption rates. Other investigators conclude that larger molecules are adsorbed to a lesser extent as a result of the greater repulsive domain between the larger molecules.

This study was conducted with the polyethylenimine (PEI)-water-silica gel adsorption system. This system was used as a model for the PEI-water-cellulose fiber adsorption system to investigate the effect of the adsorbate molecular size and adsorbent pore size on equilibrium adsorption. Equilibrium adsorption isotherms (EAI) were interpreted with respect to the solution size of the adsorbate molecule and the pore size distribution of the adsorbent.

The size of the PEI molecule was controlled in adsorption experiments by changing its charge or the ionic strength of the solution and by using narrow molecular weight fractions. The size of polyethylenimine fractions was calculated using the Seely, Einstein-Stokes, and Stokes equations from intrinsic viscosity, molecular weight, and diffusion coefficient determinations. To facilitate these determinations, polyelectrolyte charge effects were suppressed by using as solvent an aqueous solution containing 0.109$\underline{N}$ NaCl and $4.25 \times 10^{-5}\underline{N}$ NaOH. Changes in the charge and size of the molecule were found by H ion titration, light-scattering, and electrophoretic mobility determinations.

The pore size of the adsorbent was varied in adsorption experiments by using three chromatographic silica gel types, Porasil A, B, and C. The pore size, area, and volume distributions of these silica gels were determined by mercury intrusion porosimetry (MIP) and nitrogen gas adsorption isotherms (NAI).

Equilibrium adsorption isotherms for the adsorption of PEI onto silica gel were obtained, in most cases, at times less than 72 hr. The amount of PEI adsorbed onto Porasil A, which had the majority of its pore apertures less than approximately twice the solution diameter of the adsorbing molecule, was found to be substantially controlled by molecular exclusion. Adsorption increased greatly as the size of the adsorbing molecule was decreased.

In contrast, the adsorption onto Porasil C, which contains the majority of its porous volume with apertures greater than about twice the size of the adsorbing molecule, changed only slightly with molecular size changes.

The following summary of experimental evidence is given to support these findings. The adsorption of PEI onto Porasil A increased greatly with increases in concentration, ionic strength (up to 0.218N NaCl) and pH (up to pH 10.8). Adsorption decreased with increased molecular weight over a molecular weight range from 2140 to 18,000. The Langmuir form describes the adsorption data when the pH is 10.8 where maximum adsorption takes place. At lower pH and with addition of simple electrolyte, adsorption is described by the Freundlich isotherm.

The adsorption of PEI onto Porasil C increased slightly with molecular weight up to 10,000. Only very slight increases in adsorption occurred thereafter up to 20,000 molecular weight. Langmuirian isotherms were obtained. Adsorption increased slightly with ionic strength increases as compared to very large increases for Porasil A. Isotherms for Porasil C in contrast to Porasil A were approximately the same without and with NaOH addition for pH control to the maximum adsorption pH found for Porasil A.

The diameters of the adsorbed PEI molecules on Porasil C were found to be of the same size as molecules in bulk solution over a molecular weight range from 2140 to 20,000. Molecular size calculations in this case, were based on the Brunauer, Emmett and Teller (BET) nitrogen gas adsorption isotherm surface area and the specific adsorption of PEI.

Adsorption was found to be irreversible with respect to dilution of the solution at neutral solution pH where the PEI molecule and silica gel surface are highly charged. The electrostatic bonding forces between protonated amino groups on the PEI molecule and ionized silanol groups on the silica gel surface are greater than the desorption forces of the solvent.

Polyethylenimine adsorbed at pH 10.8 was found to be partially desorbed by elution with solvent at pH 12 or by lowering the pH of the supernatant to 2-3. The amount of PEI desorbed at pH 12 was independent of the amount of PEI initially adsorbed, depending only on the solvent power of the elutriator.

This was further demonstrated by the decreased amount of desorption found at low pH (2-3) as the equilibrium concentration was increased. At pH 2 silica gel has a negligible charge and offers few sites where electrostatic bonds can form with highly cationic PEI molecules. Desorption occurs at low equilibrium concentrations where the solvation forces are greater than the adsorption forces. At higher equilibrium concentrations the solvent power is greatly reduced by the presence of the PEI molecules in solution.

Adsorption was found to be reversible with respect to molecular weight. Higher molecular weight molecules were shown to replace lower molecular weight molecules that were initially adsorbed.

Since molecular exclusion was found to greatly control adsorption on Porasil A, molecular entrapment within pores was deemed equally plausible. The equilibrium adsorption at pH 2-3 was found to be much higher if the adsorption was initially carried out at pH 10.8 then lowered, compared to the amount of PEI normally adsorbed at the low pH (2-3). At the higher pH the PEI molecule can diffuse into the porous regions of Porasil A. As the pH is lowered the molecule expands and becomes trapped. An increase in the amount of reversibility was also found at low equilibrium PEI concentrations between high (pH 10.8) and low pH (pH 2-3) by addition of simple electrolyte (0.054N NaCl). A decrease in the molecular size of the PEI molecule allowing it to diffuse out of the porous regions is apparently occurring.

INTRODUCTION

Polyelectrolytes are used extensively in the manufacture of paper, paperboard, and textiles. Cationic polyelectrolytes, such as polyethylenimine, are used to increase paper machine efficiency and impart specific properties to fibrous products. Large quantities of cationic polymers are used as strength, retention, and drainage aids. However, inherent in their use are some disadvantages. Low retention levels, high cost, and enhancement of pollution are commonly cited problems.

Current knowledge of the diffusion of cationic polyelectrolytes to the cellulose surface and/or into the intrafiber ultrastructure with subsequent adsorption is lacking. This knowledge would greatly aid in understanding the retention of cationic polyelectrolytes on cellulose. Knowledge concerning the location of polymer deposition, whether interfiber or intrafiber, is important depending on the goal in using a particular wet-end additive. Increased fiber strength may be obtained by penetration of the polyelectrolyte into the fiber. On the other hand, increased interfiber strength may be most efficiently achieved by deposition of polymer on the outer surface of cellulose fibers.

The polyethylenimine (PEI)-water-cellulose fiber system found in the paper industry is a very complex adsorption system. Kindler (1), Trout (2), and Allan and Reif (3) have studied this system.

Trout's data indicated that adsorption energies comparable with ion exchange and hydrogen bonding forces are involved. Kindler's kinetic work indicated that the rate-determining step in the adsorption of PEI onto regenerated cellulose fibers is a mass-transport process. However, the observed rates were very slow and the necessity of the polymer to penetrate into the porous structure of the fiber was postulated as the cause.

Allan and Reif (3) have postulated a new retention mechanism. Irreversible adsorption with acid washing is postulated to occur by the "Jack in the Box Effect" (JBE). Protonation of the PEI molecule leading to molecular expansion and entrapment within small aperture pores is designated the JBE.

Kindler's equilibrium adsorption data support the importance of the size of the PEI molecule in relation to pore size brought to light by Allan and Reif's work. He postulated that molecular exclusion was the cause of the observed decrease in adsorption with increased molecular weight between 8000 and 20,000. This explanation seemed reasonable, even though from thermodynamic considerations the adsorption of higher molecular weight polymers is favored (4).

Stone, et al. (5) have measured the pore size distribution of the accessible regions of textile rayon fibers by the solute exclusion technique. Pore size estimates were based on the Stokes diameters of various molecular weight dextrans. Their data indicated a median pore size of about 25 A. and a maximum of 100 A. Their data compare favorably with gas adsorption studies with other cellulosic fibers.

Gas adsorption studies by Thode, et al. (6), Haselton (7), and Sommers (8) on cellulose wood fibers and cotton fibers prepared in the expanded state by solvent exchange drying techniques have shown that the most common pore diameters are in the 36 to 40 A. equivalent pore diameter (EPD)[1] range. This pore size was postulated to be closely associated with an elementary polymer building block of cellulosic fibers since mechanical treatment of the fibers did not destroy this peak in pore size distribution curves but did increase the specific surface area (6).

---

[1]The diameter of a straight cylindrical capillary pore.

If pore size estimates of Stone, et al. are valid for the regenerated cellulose fibers used by Kindler, then Kindler's molecular size estimates for the PEI molecule by the Stokes equation must be significantly in error compared with the true solution size. Molecular diameters from 23 to 30 A. were calculated from diffusion coefficients for the molecular weight range from 8000 to 20,000. A fivefold decrease in adsorption over this range was shown by Kindler's data. This decrease is not adequately explained by decreased accessibility corresponding to 7 A. pore size change. A much larger molecular diameter range is compatible with the molecular exclusion hypothesis used to explain the adsorption data for the PEI-water-cellulose fiber system.

The irreversibility (3) may also be explained in light of adsorption studies with uncharged polymers in organic solvents. In a generalized picture of the adsorption of a polymer molecule, multiple points of segmental attachments to the adsorbent surface are thought to be involved (9-12). Looping of chain segments into solution between attachments is thought to occur. Desorption of the entire molecular chain is thought to occur only when all bonds are broken simultaneously which is statistically improbable. These authors emphasize that once adsorbed the chain segments looped into solution establish a high concentration of polymer segments near the surface. As the solution is diluted, the adsorption bonds still feel a high polymer concentration near them due to the high concentration of polymer segments looped into solution from the adsorbed molecules themselves.

The interpretation of polyelectrolyte adsorption studies on cellulose fibers is often complicated by the ill-defined surface characteristics of cellulose. A definitive surface region of highly refined chemical pulp fibers is difficult to locate. Fibrillation and hydration of fibers through beating and refining, after chemical pulping measures, create a structure that is very conformable and may be partially soluble in its surface region. Distinct surface boundaries and pore geometries may not be present.

The basic nature of the highly swollen cellulose fibers makes them unsuitable for a critical study of the pores present that are accessible to a given size of macromolecules in solution. In the case of the adsorption of PEI onto cellulose fibers, changes in the type of counter- and coions present, ionic strength, and pH may alter both the pore geometries and sizes within highly swollen cellulose fibers, as well as the molecular size of PEI. A rigid non-swelling adsorbent which lends itself to conventional pore characterization methods while still maintaining surface chemical groups similar to cellulose would be an ideal model for generating data to provide information about polymer accessibility in a porous adsorbent.

Silica gel fulfills this criteria as an adsorbent. Gels are commercially available that are known to have rather narrow pore size distributions. When placed in water, silica gels, like cellulose fibers, have primarily hydroxyl surfaces. They possess definite surface boundaries in contrast to highly hydrated cellulose fibers.

The comparison of silica gels and cellulose fibers as adsorbents may be limited. The silanol groups hydrogen ion's dissociation constant is estimated at 1×10^{-12} (13) compared to that of the most acidic hydrogen ion on cellulose 2×10^{-14} (14). Pore geometries may be very much different. Other chemical groups, such as carboxyl groups and resinous materials, are present in cellulose fibers.

The advantages of using silica gel for a critical study of pore accessibility which in turn may be related to adsorption behavior found for cellulose fibers are many. Silica gels which are commercially available, such as Porasil, have surface areas and pore sizes similar to dry cellulose fibers prepared in the expanded state. The surface area and pore size distribution are easily

obtained by conventional methods such as gas adsorption and mercury intrusion porosimetry. Porasil is a rigid, nonswelling three-dimensional structure. Pore geometries and sizes do not change with solvent conditions. Polymer adsorption studies may be directly related to the effect of pore size, since gels are available having narrow pore size distributions over a range of pore sizes. Adsorption studies on silica gels having in one case very large pores in comparison to the PEI molecule being adsorbed and having in a second case pores comparable to the molecules size will provide data which can be directly related to the accessibility of the pores present in the adsorbent.

LITERATURE REVIEW

SILICA GEL

SURFACE CHEMISTRY

It is well established that the silica surface is composed of silanol groups when placed in water (15, 16). It is believed that a layer of water molecules is hydrogen bonded to the silanol surface layer and ordering of water molecules may be many layers deep. Dissociation of H ions from the hydrogen bound water layer and/or the surface silanol groups is recognized as the mechanism by which silica particles take on a net negative charge. However, other possible mechanisms must also be considered such as isomorphous substitution and preferential adsorption of ions.

The number of hydroxyl groups that various silica gels possess has been determined by a number of investigators. Stober (17) from structural considerations proposed 4.4 OH/100 $A.^2$ as a theoretical value. Experimentally he found slightly less than 4 OH/100 $A.^2$ Fripial and Uytterhoeven (18) obtained a figure 4.2 OH/100 $A.^2$ surface area. deBoer and Vlessking (19) dehydrated and rehydrated various silica gels many times and found a maximum surface density of 4.6 OH/100 $A.^2$ This figure is in good agreement with the data of Russian investigators (20). In their work with various silica gels in their most hydroxylated state, they found a OH group content of 4.7 OH/100 $A.^2$ If the figure 4.6 OH/100 $A.^2$ is taken as the best estimate then a silica gel having a surface area (SA) of 100 $m.^2/g.$ would have a surface hydroxyl content of 0.76 mM/g.

Limited data are available about the dissolution and total solubility of amorphous silica. It is about an order of magnitude more soluble than quartz (21). At room temperature the solubility of amorphous silica in water is 2×10^{-3}

moles SiO_2 per liter. The total solubility as a function of pH is given by

$$pH - \log [(S_t - S_M)/S_M] = 9.8 \quad (1)$$

where S_M is equal to 2×10^{-3} moles SiO_2 per liter and S_t is the solubility at a given pH (21).

The rate of dissolution of quartz in water is approximately 8.5×10^{-11} g./m.^{2}/day. The rate for amorphous silica is expected to be slightly greater. At elevated temperatures the rate of dissolution is accelerated by the presence of 0.1N NaCl. At room temperature where the rate of dissolution is very slow, negligible effect is observed (22) for 0.1N NaCl.

The point of net zero surface charge for amorphous silica occurs at pH 2.0 ± 0.2. This number results as the best figure from work by 13 independent investigators (23).

ULTRASTRUCTURE

The ultrastructure of many silica gels have been investigated by electron microscopy, mercury intrusion porosimetry (MIP) and by the gas adsorption techniques. For Porasil, the silica gel used in this study, the above methods of investigation have been employed by Beau, et al. (24). The silica beads were found by electron microscopy to have a nearly spherical geometry and to be composed of small elemental, somewhat spherical, particles of varying size. The elemental particles were observed to be packed in a random fashion which formed a continuous three-dimensional network with interconnecting pores of variable shape. The average aperture size was found to be that of the elemental particles. Further work by Beau, et al. employing MIP and nitrogen gas adsorption led them to conclude that for most Porasil types the average pore aperture is smaller in diameter than the average diameter in the interior of

the pore. This conclusion is commonly found in the literature for the analysis of gas adsorption-desorption studies on many porous silica gels.

ADSORPTION FROM SOLUTION

The adsorption of molecules containing amino groups from aqueous solution onto silica gel has enjoyed some attention. The surface reactions in water are believed to be primarily confined to hydrogen bonding and cation exchange (25-27). Infrared spectroscopy also indicates that nonspecific Van der Waals forces are apparently operative in adsorption of amines on silica (26).

GENERAL ASPECTS OF POLYMER ADSORPTION

Reviews are available concerning polymer adsorption at the liquid-solid interface (28-31). Some of the generalities of polymer adsorption will be touched upon to bring to mind important aspects.

Although complex models have been proposed to explain polymer adsorption, most systems appear to fit an equation of the Langmuir type. The amount of polymer adsorbed per unit weight adsorbent or unit surface area is generally found to increase rapidly with solution concentration. At higher concentrations a saturation point is reached where no further adsorption takes place with increase in solution concentration. The saturation point is believed to correspond to the formation of a monolayer of polymer on the adsorbent surface.

Polymer-solvent interactions are found to play an important role in polymer adsorption. The amount of polymer adsorbed is generally found to be inversely related to the solvent power. Temperature dependence is small and is shown to have either a positive or negative effect on the amount of polymer adsorbed at equilibrium depending on the system being considered.

It is generally believed that only a fraction of the polymer segments are in direct contact with the adsorbent surface. The remaining segments are believed to be looped into solution. This view is also harmonious with the recent thinking that the configuration of the adsorbed molecule in many cases closely approximates that of the polymer in bulk solution.

The adsorption of polymers from solution onto solid surfaces is found to increase, decrease, or be independent of molecular weight. For example, adsorption of PEI onto regenerated cellulose fibers from an aqueous solution was found to increase with decrease in molecular weight from 20,000 to 8000, but increase with increase of molecular weight between 50,000 and 100,000 (1, 32). Howard and McConnell (33) also report a similar trend. They found that the adsorption of polyethylene oxide onto powdered nylon decreased with increase in molecular weight up to a point; further molecular weight increase was found to increase adsorption.

Heinegard and Martin-Lof (34), on the other hand, found no reversal point in the adsorption dependence on molecular weight. Their data showed that the specific adsorption of cationic polymers decreased over a molecular weight range from 20,000 to 240,000 when microcrystalline cellulose was the adsorbent.

Numerous adsorption studies are available in which the effect of molecular weight has been investigated. In the examples cited above, the adsorbents are believed to be highly porous, a factor that may have a substantial effect on the resulting specific adsorption.

PRESENTATION OF PROBLEM AND THESIS OBJECTIVES

The brief literature review and introduction points out that our present knowledge concerning the effect of the porous nature of an adsorbent on the equilibrium adsorption isotherm of macromolecules from solution needs improvement. The equilibrium adsorption isotherms for the polyethylenimine-cellulose system presented by Kindler (1) were explained in terms of the increased pore accessibility to smaller molecules. However, the polymer size and pore sizes used in the study were not characterized adequately. This study is proposed to evaluate the role exclusion plays in determining the amount of polymer adsorbed on porous material. By using a well-characterized adsorbate and adsorbent, the effect of adsorbate exclusion or entrapment within known size pores can be evaluated.

The major objective of this study is to determine the relationship between the relative molecular size of a polyelectrolyte and the pore size of the adsorbent into which the molecule can diffuse and adsorb. The extent to which this relationship determines the equilibrium adsorption isotherm will be assessed.

EXPERIMENTAL MATERIALS, EQUIPMENT AND PROCEDURES

SOLVENT

The polar solvent water was used throughout this investigation. It was deionized and distilled having a conductivity less than 1.5×10^{-6} ohm/cm.[2]

The characterization of PEI and much of the adsorption work was done in aqueous media containing analytical reagent grade 0.109N NaCl and 4.25×10^{-5}N NaOH having pH = 8. This solution will be subsequently referred to as standard aqueous solvent. This solvent was routinely vacuum filtered through Schleicher and Schuell analytical filter paper for finest precipitates. The solvent was further filtered through 0.45 μm. pore size Millipore cellulose ester filters before using in diffusion coefficient and sedimentation equilibrium determinations. The solvent was filtered through 1000 A. pore size Millipore (35) filters for light-scattering and viscosity determinations.

CHARACTERIZATION OF POLYETHYLENIMINE

SOURCE

The PEI sample used in this study was obtained from the Dow Chemical Company (control number SA1117-633974). This sample was secured by Kindler (1) and used in his investigation of the adsorption kinetics of the PEI-cellulose system. The sample is of high purity and contains no added cross-linking agents. The sample shows no visible signs of degradation or formation of colloidal aggregates. A relative viscosity determination confirmed that the PEI sample is very stable and has not changed since it was received.

GEL PERMEATION FRACTIONATION

The polyethylenimine sample was fractionated by the gel permeation technique using P-10 Bio-gel in order to obtain narrow molecular weight fractions. The materials, equipment, and procedures employed by Kindler were used in this work with the exception of the solvent which was standard aqueous solvent.

Seventeen samples were fractionated. Eighteen fractions of approximately 13.0 ml. each were collected from each fractionation run. Like fractions from separate fractionations were combined.

STRUCTURE

The PEI used in this study is a highly branched polyamine produced by the acid-catalyzed stepwise polymerization of the monomer ethylenimine (36). Recent work by Dick and Ham (37) at the Amines Research Laboratory of the Dow Chemical Company has furnished substantial information about the structure of PEI. Using infrared spectrography and nonaqueous titration methods on PEI that had been selectively substituted at select amino groups, they have found that for most PEI, branching occurs about every 3-3.5 monomer units, and the ratio of primary, secondary, and tertiary amino groups is approximately 1:2:1. This distribution of units is believed to give rise to a spherically shaped macromolecule with tertiary amines being the branch sites and primary amino nitrogens being the terminal groups (36).

HYDROGEN ION TITRATION CURVE

Polyethylenimine is a polybase and when placed in water alkaline solutions result. The amino groups act as Lewis bases to combine with H ions and shift the equilibrium to the alkaline side. For example, after being dialyzed against

constantly fresh distilled water for 16 hours, a 3.8 x 10^{-5}M PEI solution (mol. wt. ≈ 10,000) has a pH of 10.3.

The degree of protonation of PEI was determined by the hydrogen ion titration technique described by Kenchington and Tanford (38, 39). This technique yields the degree of protonation as a function of solution pH.

Briefly, the method involves a blank titration of solvent where the $[H^+]$ or $[OH^-]$ added as a function of pH is determined. A known amount of PEI is then titrated in the same solvent and the $[H^+]$ added as a function of pH is again determined. The amount of H ion bound to PEI at a given pH is then calculated by subtracting the amount of H ion required by the blank (solvent) at the given pH from the amount added to the solution. The approximation is generally made for most titration work that the pH is approximately equal to the negative logarithm of the hydrogen ion activity and that errors in the measurement are the same for the separate titrations of solution and solvent. This is thought to be nearly true when the ionic strength of the solvent and solution titrated are essentially the same.

The titrations were carried out in a stirred system at room temperature in a carbon dioxide-free nitrogen atmosphere in a 0.109N NaCl aqueous system. A solution of fraction 5 (F-5) with a mol. wt. of 10,400 at 3.84 x 10^{-2}N amino groups was titrated with 0.1000N HCl or 0.1000N NaOH in 0.109N NaCl solutions. Equilibrium was found to be established almost instantaneously; however, 3-minute intervals were used for successive points. Burets (5.000 ml.) were used to deliver accurate volumes of titrant. A Corning Research pH meter, readable to 0.001 pH units and believed reliable to the 0.01 unit was employed for pH measurements.

ELECTROPHORETIC MOBILITY

The electrophoretic mobility of PEI F-5 was determined at 25.0°C. in 0.109N NaCl aqueous solution at four pH values: 4.0, 7.0, 10.1, and 13.0. Hydrochloric acid and sodium hydroxide were used to adjust pH. Solutions and solvent were separately adjusted to a given pH and then dialyzed against each other for three days. Thirty milliliter solutions at approximately 0.2% PEI were dialyzed against 75 ml. of solvent. The solvent was exchanged three times over the dialysis period. Cellulose acetate dialysis membranes reported by their manufacturer to have a nominal pore size of 48 A. were used.

A Beckman/Spinco Model H Electrophoretic-Diffusion Instrument was employed for the measurements. It is equipped with the Tiselius apparatus and Schlieren optics to enable absolute mobility measurements to be made by the moving boundary technique. A detailed description of the moving boundary technique, Tiselius cell employed, and optical systems are readily available in many texts (40-42).

DIFFUSION COEFFICIENTS

Diffusion coefficients were determined by the free-diffusion method. A boundary is formed between solvent and solution. The concentration of solute across the boundary region is then observed as a function of time. Fick's second law is applied to this information to calculate the diffusion coefficient.

Since perfect boundaries are difficult to form and nonideality effects occur, experimental measurements are made at a number of concentrations over a period of time. A limiting diffusion coefficient is obtained by extrapolating to infinite time and zero solute concentration. Gosting (43) presents a detailed description of the techniques of measurement and interpretation of diffusion coefficients.

A Beckman Spinco Model E ultracentrifuge was employed in free diffusion experiments. Double and triple sector synthetic boundary cells were used to create the necessary boundary across which the solute concentration was monitored as a function of time using the Rayleigh optical system. The Creeth (44) method of data analysis was used. A description of its application together with a computer program designated DIFFCO, written by Kindler (1), was used for the calculations required in the analysis.

Diffusion coefficients were determined on Fractions 1, 3, 4, 5, 7, and 9 at 25.0°C. in standard aqueous solvent. Fractions 3, 5, 7, and 9 were dialyzed against solvent for four hours. F-1 and F-4 were dialyzed three days with three solvent exchanges. The dialyses were done in dialysis cells constructed of teflon having a dialyzing membrane separating 10-ml. compartments. Five milliliters of solution at about 1.5% were dialyzed against 10 ml. of solvent. This solvent was used to dilute these stock solutions to the various concentrations at which determinations were made.

Diffusion coefficients were also obtained on F-5 at about 0.2% as a function of pH. After an electrophoresis run, the boundary region between solvent and solution is easily sharpened. Rayleigh optics are then employed to monitor the solute concentration across the boundary region as a function of time. From these data the apparent diffusion coefficients are easily calculated based on Fick's second law.

MOLECULAR WEIGHT

The weight average molecular weights of F-1, 3, 4, 5, 7, and 9 were determined by the sedimentation equilibrium technique. The number average molecular weight of F-3, 5, and 7 were determined by osmometry. Both techniques, sedimentation equilibrium and osmometry are conventional routine methods for determining

the molecular weight of macromolecules. Numerous references are available on the theory, application, and analysis by these techniques. Schachman (45) and Fujita (46) may be consulted on the sedimentation equilibrium technique.

Sedimentation equilibrium runs were done on the ultracentrifuge used for diffusion measurements. Each fraction was run at a number of concentrations. This allows the extrapolation of the apparent molecular weight to zero solute concentration. Fraction 1 was run at two rotor speeds. No dependence of molecular weight on angular speed was found. All measurements were done at 25.0°C. in standard aqueous solvent. Rayleigh optics were used to determine the solute distribution across the cell at equilibrium. Photographs were taken as a function of time to ascertain when equilibrium was obtained.

Osmometry measurements were performed with a Mechrolab Model 501 High Speed Membrane Osmometer. This instrument allows the rapid measurement of osmotic pressure by applying an external pressure and noting the pressure at zero solvent flow through the membrane. A general review of osmometry is given by Wagner (47). High-speed osmometry is justified by Staverman (48) using irreversible thermodynamics measurements.

Osmometry measurements were made in standard aqueous solvent at a number of concentrations on each fraction. The reduced osmotic pressure at zero solute concentration was obtained by extrapolating π'/C versus C to zero concentration.

VISCOSITY

Viscosity determinations were done for PEI F-1, 3, 4, 5, 7, and 9 at 30,000 ± 0.001°C. in standard aqueous solvent. Duplicate viscosity determinations were made on each fraction at a number of solution concentrations by dilution in the viscometer. Two Cannon number 50 Ubbelohde semimicro viscometers requiring a

minimum of 1.0 ml. solution were used. Approximately thirty minutes were allowed for equilibration after a dilution was made. Dilutions were made using a micro-syringe constructed of glass having a teflon plugger and equipped with a ten-inch stainless steel needle. During this time the solution was drawn up into the capillary bulb reservoir at least four times to facilitate mixing. Efflux times were recorded until three successive times differed by less than 0.3 sec. The efflux times for the viscometers for the solvent were 241.8 sec. and 225.6 sec. Cannon, et al. (49) have shown that no kinetic energy correction is necessary at these large efflux times. A negligible shear rate dependence is found for this viscometer for low molecular weight polymers.

Intrinsic viscosities were calculated by the least squares method for the best fit of reduced specific viscosity (η_{sp}/C) as a function of PEI concentration (C). The combined data of the duplicate determinations were used in the calculations.

LIGHT SCATTERING

The Rayleigh ratio (R_θ) at $\theta = 90$ and the dissymmetry of F-3 PEI were measured as a function of pH in a 0.109N NaCl solution. Fifty milliliters of 0.167% PEI were placed in a conventional semioctagonal light-scattering cell which allows light-scattering readings to be obtained at 0, 45, 90, and 135°. Sodium hydroxide and hydrochloric acid in 1N solutions were added in a 250-µl. graduated syringe to change pH. The HCl and PEI solutions were filtered through a 1000 A. pore size Millipore cellulose ester filter to remove dust and particulates. The 1N NaOH was cleaned by ultracentrifugation at 50,000X g for 30 minutes. Four solutions of F-3 were used to obtain light-scattering data. The 0.167% PEI solution in standard aqueous solvent had a pH of 10.1. To obtain measurements at lower pH, HCl was added. To minimize PEI concentration changes,

NaOH was added to a second solution to obtain data above pH 10.1. Two other solutions were used to determine the pH at the various HCl and NaOH addition levels.

The PEI concentration change between pH 10.1 and 5.6 was 0.006% resulting from dilution with 1N HCl. The concentration change between pH 10.1 and 12.56 was 0.006% with 1N NaOH addition. The PEI concentration change between pH 12.56 and 13.40 was 0.020%. The R_{90} and dissymmetry measurements were taken separately on the solvent and solution, so the standard corrections for solvent scattering could be made.

In theory, the light scattered is directly proportional to the number of scattering particles per unit volume of solution and the square of the specific volume of the molecules. For systems involving charged molecules in water with added simple electrolyte, internal and external interference effects (50) cause great diminution of light scattered from theory. However, changes in the scattering at nearly constant concentration can still be related to volume changes in the molecule.

The theory of light scattering is much too complex and lengthy to be dealt with here. Stacey (51) presents an excellent treatise of the subject. He devotes a chapter to a review of the light-scattering behavior of polyelectrolytes in solution. Correlations of R_{90} and dissymmetry measurements are made with the degree of ionization, concentration of added simple electrolyte, and polyelectrolyte concentration.

Light-scattering measurements were done on a Brice-Phoenix Universal Light Scattering Photometer, series 1937 equipped with an aluminum shielded galvanometer having a sensitivity of approximately 0.6 nanoamperes per millimeter scale division. Successive measurements were made on the solution or solvent, when

the pH was changed by addition of acid or base, after allowing at least 30 minutes for equilibration of the solution. Measurements were done at room temperature using monochromatic light at 436 nm. The operating procedure for the Brice-Phoenix Photometer and method of calculation of $\underline{R}_{90}$ and dissymmetry values are given elsewhere (52). The $\underline{R}_{90}$ is equal to the ratio of the intensities of light scattered at 90° to the incident light beam times the square of the distance from which it is observed. Dissymmetry values are calculated as the ratio of $\underline{R}_{45}$ to $\underline{R}_{135}$.

DIFFUSION THROUGH MEMBRANE

Simple equilibrium diffusion experiments through a dialysis membrane were done using F-1, 3, 4, 5, 7, and 9. Cellulose acetate dialysis membranes, reported by their manufacturer to have a nominal pore size of 48 A. were initially soaked in water to remove glycerin and then autoclaved. These membranes were placed between two 10-ml. compartments of dialysis cells constructed of teflon. Five milliliters of standard aqueous solvent were placed in one compartment and 5 ml. of the appropriate fraction at 0.4% were placed in the other compartment. The dialysis was carried out under stagnant conditions at room temperature for 10 days. The volume of solution and concentration of PEI in each compartment of the dialysis cell were determined. The volume was determined with graduated microsyringes. The concentration of PEI was determined spectrophotometrically.

CHARACTERIZATION OF SILICA GEL

DESCRIPTION OF PARTICLES

Three silica gels, Porasil A, B, and C, were characterized. According to the manufacturer they are chemically the same. They differ in pore size, surface area, and apparent density.

Organic materials are present in Porasil as received from the supplier. To remove these impurities the gels were heated in a muffle furnace for 8 hr. at 640°C. This treatment has been found sufficient to remove organic materials that are present (53) and leave the gel unchanged with respect to chromatography use.

Porasil A, B, and C are manufactured in two particle size ranges. The manufacturer (Pechiney-Saint-Gobain of France) specifies a particle size range from 75 to 125 μm. for the samples used in this study. The particle size range for Porasil C was investigated using a JEOL JSM-U3 scanning electron microscope (SEM). The particle size range determined in this way was the same as the manufacturer's stated value.

The ultrastructure of the Porasil particles was observed at higher magnification on the SEM and on the RCA EMV-3F model transmission electron microscope (TEM). The TEM micrographs were made from direct carbon replicas of the Porasil particles that were preshadowed with platinum. A 20° shadowing angle was used in preparing the replicas. The Electron Microscopy Laboratory at The Institute of Paper Chemistry prepared the direct carbon replicas of Porasil A, B, and C and the SEM and TEM micrographs.

DESCRIPTION OF PORES

The pore size, surface area and volume distributions of Porasil A, B, and C were determined by two independent conventional methods: mercury intrusion porosimetry (MIP) and nitrogen gas adsorption. Approximately one gram of the appropriate Porasil was suspended in 40.0 ml. of standard aqueous solvent in 50.0-ml. screw top centrifuge tubes. The tubes were constantly agitated for five days in an adsorption apparatus, as described in the next section, then solvent exchange dried. Six, fifty-milliliter volumes of deionized and distilled water were used in the replacement of the original solvent over a 24-hour period.

Six volume changes of methyl alcohol of analytical reagent grade were used to replace the water over the next 24-hour period. In a similar fashion, high purity pentane was used to replace the methanol. The replacement procedure was accomplished by decanting the solvent and refilling the tube. After each solvent replacement, the centrifuge tubes were returned to the constant temperature bath (25°C.) and continually agitated. The Porasil samples were air dried and muffled at 640°C. for 8 hr. after decanting the final solvent. These samples were submitted to the American Instrument Company (AMINCO) Materials Technology Laboratory for determination of low-temperature nitrogen gas adsorption isotherms.

Nitrogen Adsorption Isotherms

The nitrogen adsorption isotherms (NAI) were determined on a fully automatic AMINCO Adsorptomat Instrument. Adsorption isotherms were obtained from data at 60 relative pressure values. A full description of the Adsorptomat and operating procedure may be obtained from the AMINCO Materials Technology Laboratory (54).

The pore size, area, and volume distributions were calculated by the Barrett, et al. technique (55). A computer program designated SHAZAM (56), available at the AMINCO Materials Technology Laboratory, was used to calculate the distributions. The computer program also calculates the Brunauer, Emmett, and Teller (BET) (57) total surface area.

Mercury Intrusion Porosimetry

Mercury intrusion porosimetry determinations were done on Porasil A by the AMINCO Materials Technology Laboratory. This work was done on an AMINCO Winslow Porosimeter at pressures up to 60,000 p.s.i. The MIP data on Porasil B and C were obtained on an AMINCO Porosimeter at The Institute of Paper Chemistry. A maximum pressure of 15,000 p.s.i. is the operating limit of this instrument. Previous MIP data indicated that Porasil B and C have pores in the pore size range of

inspection of the 15,000 p.s.i. instrument. The pore size, surface area, and volume distributions were calculated by the technique of Ritter and Drake (58) and Barrett, et al. (59). A slightly modified form of a computer program designated Q725E, written by Nelson (60) available at The Institute of Paper Chemistry, was used to calculate the pore size, surface area, and volume distributions of the mercury intrusion data. Program Q725E calculates the pore size and pore size distribution using the Washburn form of the Laplace equation of capillarity. Equivalent pore diameters were calculated using a contact angle of 130° and surface tension of mercury at 473 dyne/cm. (61).

ADSORPTION OF POLYETHYLENIMINE ON SILICA GEL

ADSORPTION APPARATUS

All adsorption experiments were done in 50-ml. screw cap centrifuge tubes. The caps were lined with polyethylene film over a cushioning rubber insert to provide tight seals.

The tubes were agitated in a water bath at 25.0 ± 0.1°C. Agitation was provided by mounting the tubes at the periphery between two 12-inch diameter notched wheels. The wheels were perpendicularly mounted on a horizontal shaft with the notches of one wheel advanced 15° relative to the notches on the other wheel. The tubes were rotated about the horizontal shaft at 4.5 r.p.m.

QUANTITATIVE ANALYSIS

Spectrophotometric

The concentration of PEI in adsorption experiments was determined spectrophotometrically. Polyethylenimine forms a complex with cupric ion in acidic solution. The complex has an absorbance peak at 269 nanometers. The

reaction was discovered by Perrine and Landis (62). The technique for quantitative determination of PEI was developed by Kindler (1).

The experimental technique involves the addition of 1 ml. of PEI solution containing from 30 to 300 mg. PEI/liter to 5 ml. of 2 x 10^{-3}N cupric acetate solution containing 2 x 10^{-3}N HCl. The absorbance is measured at 269 nm. on a Beckman Model DU spectrophotometer. The spectrophotometer is zeroed against a blank consisting of 1 ml. of solvent of the same type as the solution of unknown PEI concentration and 5 ml. of cupric acetate solution. A standard curve of PEI concentration versus absorbance was prepared by determining the organic nitrogen content of solutions by the Hengar technique (63, 64). The standard curve obeys Beer's law.

Organic Nitrogen

The Hengar organic nitrogen technique was used to determine both the amount of PEI adsorbed on silica gel in desorption experiments and for calibration of the spectrophotometric method. Polyethylenimine amounts were calculated from organic nitrogen determinations based on the theoretical nitrogen content of 32.53%.

In the Hengar organic nitrogen technique, samples are digested in concentrated sulfuric acid containing potassium sulfate and a selenium catalyst. Organic nitrogen is converted to the ammonium ion. The digestion mixture is neutralized with sodium hydroxide. The ammonia released is distilled into a dilute boric acid solution which is back-titrated with acid to an equivalence point. Bromcresol green is used as the end point indicator.

ADSORPTION CONDITIONS

Polymer adsorption and desorption experiments were conducted over a wide variety of conditions. A general description of the loading technique is as follows. Stock solutions of PEI, F-1, 3, 4, 5, 7, and 9, were made up at 0.4% and added directly to aqueous suspensions of Porasil. Initially, the appropriate amount of Porasil (50.0 ± 0.1 mg. of Porasil A, 120 mg. of Porasil B, and 480 mg. of Porasil C) was placed in screw top centrifuge tubes. Various amounts of solvent were added and the tubes were agitated for 12 hr. The pH of the suspensions was adjusted when necessary using 0.1N or 1.0N solutions of HCl or NaOH. Various amounts of stock PEI solutions were then added so that the suspension had a total of 40.0 ml.

The tubes were vigorously shaken after addition of polymer and placed in the adsorption apparatus for constant rate agitation. After equilibrium was established, one milliliter of solution was pipetted out for use in determining the solution's concentration spectrophotometrically.

Reversibility experiments with respect to pH were accomplished by merely adding acid or base to the above solutions that had established adsorption equilibrium. Reversibility experiments with respect to PEI solution concentration were done using solvents consisting of distilled water, an aqueous solution of 0.218N NaCl and aqueous media having 0.109N NaCl at pH 12.0. The adsorption solutions were decanted. Several exchanges of solvent were made within a several day period. The amount of PEI still adsorbed was determined by an organic nitrogen determination on the adsorbent.

Replacement experiments with respect to molecular weight were done in the following way. Fraction 10 was adsorbed onto Porasil B. At adsorption equilibrium the supernatant was decanted. The tubes were refilled with solvent and agitated.

After five minutes the supernatant was again exchanged then agitated six hours. At the end of this period the solvent was decanted. The tubes were filled with F-3 at the same concentration as the initial concentration of F-10 used in adsorption experiments. The solution was again allowed to come to adsorption equilibrium.

EXPERIMENTAL DATA AND DISCUSSION OF RESULTS

CHARACTERIZATION OF POLYETHYLENIMINE

GEL PERMEATION FRACTIONATION

The elution volume-concentration distribution is shown in Fig. 1. The values plotted are the average values for the combined fractions from 1 to 11 for the first ten fractionations. Seventeen samples were fractionated. Fraction 1 is the combined fraction of Fractionations 11 through 17. Fractions 3, 4, 5, 7, and 9 are the combined fractions of Fractionations 1 through 10. The concentration elution volume curve changed only slightly during the seventeen fractionations. Higher concentrations were observed for initial fractions, suggesting that the column packing may have compressed slightly. However, this effect was not significant, since narrow molecular weight fractions were shown to be present.

MOLECULAR WEIGHT OF FRACTIONS

The weight average molecular weight ($\underline{M}_w$) results for PEI Fractions F-1, 3, 4, 5, 7, and 9 determined by a sedimentation equilibrium technique are given in Appendix I. The number average molecular weight ($\underline{M}_n$) results of Fractions F-3, 5, and 7 determined by osmometry are given in Appendix II. Table I is a summary of those results. The molecular weights listed are for infinite dilution.

TABLE I

NUMBER AND WEIGHT AVERAGE MOLECULAR WEIGHTS

Fraction	$\underline{M}_n$	$\underline{M}_w$	$\underline{M}_w/\underline{M}_n$
1		20,000	
3	17,500	18,000	1.03
4		11,100	
5	12,680	10,400	0.82
7	5,270	5,350	1.01
9		2,140	

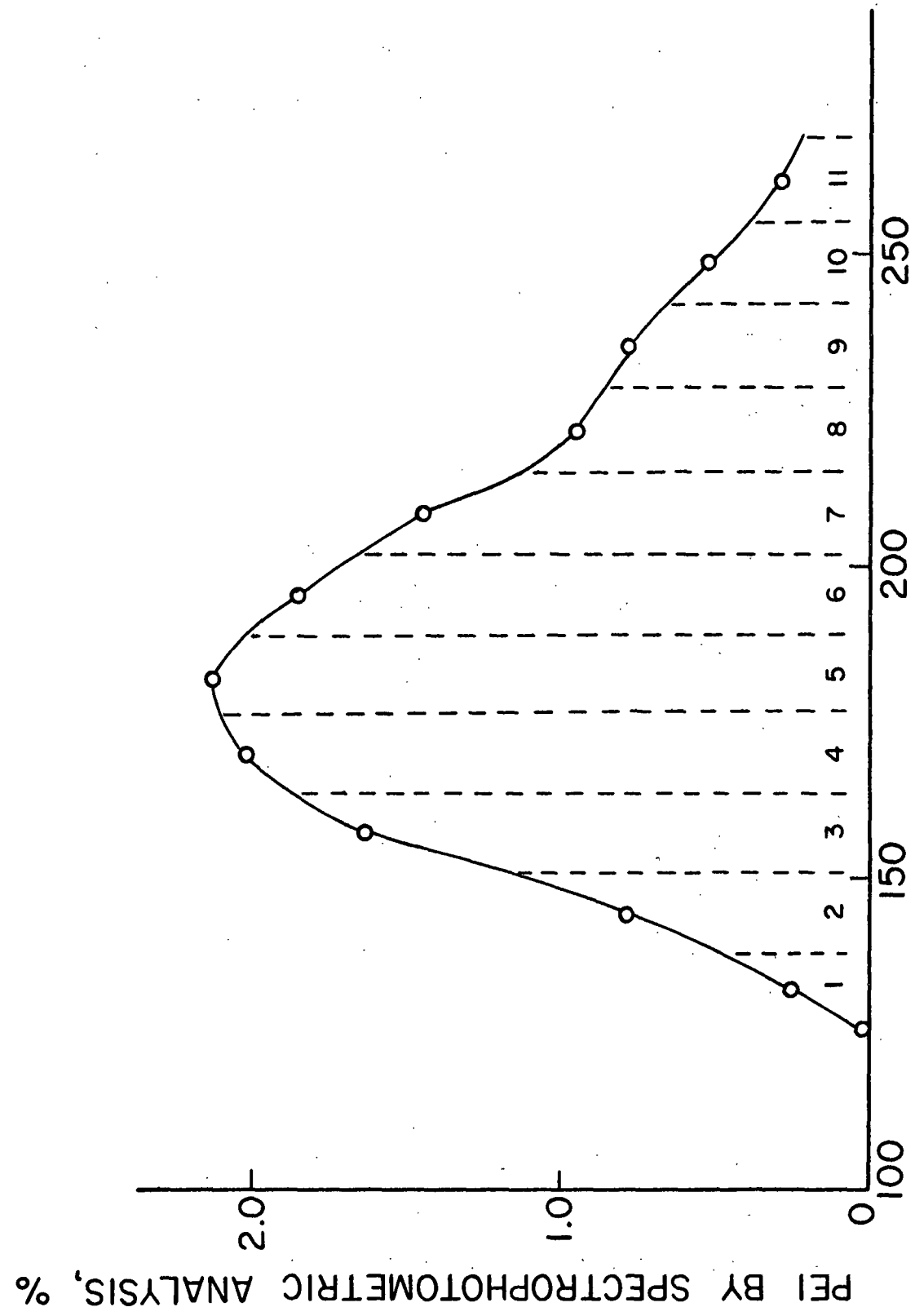

Figure 1. Elution Volume Versus PEI Concentration. Average Values for First 10 Fractionations. Numbers on Graph Refer to Fractions Collected

The $\underline{M}_w$ and $\underline{M}_n$ for F-3, 5, and 7 are within the experimental error of being equal. The $\underline{M}_w/\underline{M}_n$ ratio values are nearly equal to unity which indicates that rather narrow molecule weight fractions of PEI were obtained by the preparative gel permeation fractionation technique. The $\underline{M}_w$ values show an order of magnitude range for the six fractions.

The elution volume *versus* the logarithm of the molecular weight is shown in Fig. 2. The regression equation expressing the nearly linear relationship shown in Fig. 2 is

$$\log M_w = (-1.06)\ V/V_o + 5.95 \qquad (2)$$

where $\underline{V}/\underline{V}_o$ is the elution volume divided by the void volume. The void volume was estimated to be 100 ml. where trace amounts of PEI were eluted. It should be noted that a slightly curved line fits the data somewhat better than the linear regression line. Curvature is sometimes noted for low molecular weights in gel permeation chromatography.

A nearly linear relationship was shown by Kindler (1) over the range from 8,000 to 20,000 molecular weight. The regression equation obtained here, for 0.109$\underline{N}$ NaCl and $4.25 \times 10^{-5}\underline{N}$ NaOH solvent, has a smaller slope than that obtained previously (1) in 0.073$\underline{N}$ sodium acetate.

HYDROGEN ION TITRATION

The original titration data, pH *versus* milliequivalents of acid or base are shown in Fig. 3. No sharp inflections indicating equivalent points are prominent. However, three regions of maximum slope are apparent. Figure 4 shows the first derivative $\Delta pH/\Delta[H^+ \text{ or } OH^-]$ as a function of pH. Three point linear smoothing was applied to the original data before taking the first derivative. Three maxima are clearly visible in Fig. 4 at pH 4.7, 7.0, and 10.8.

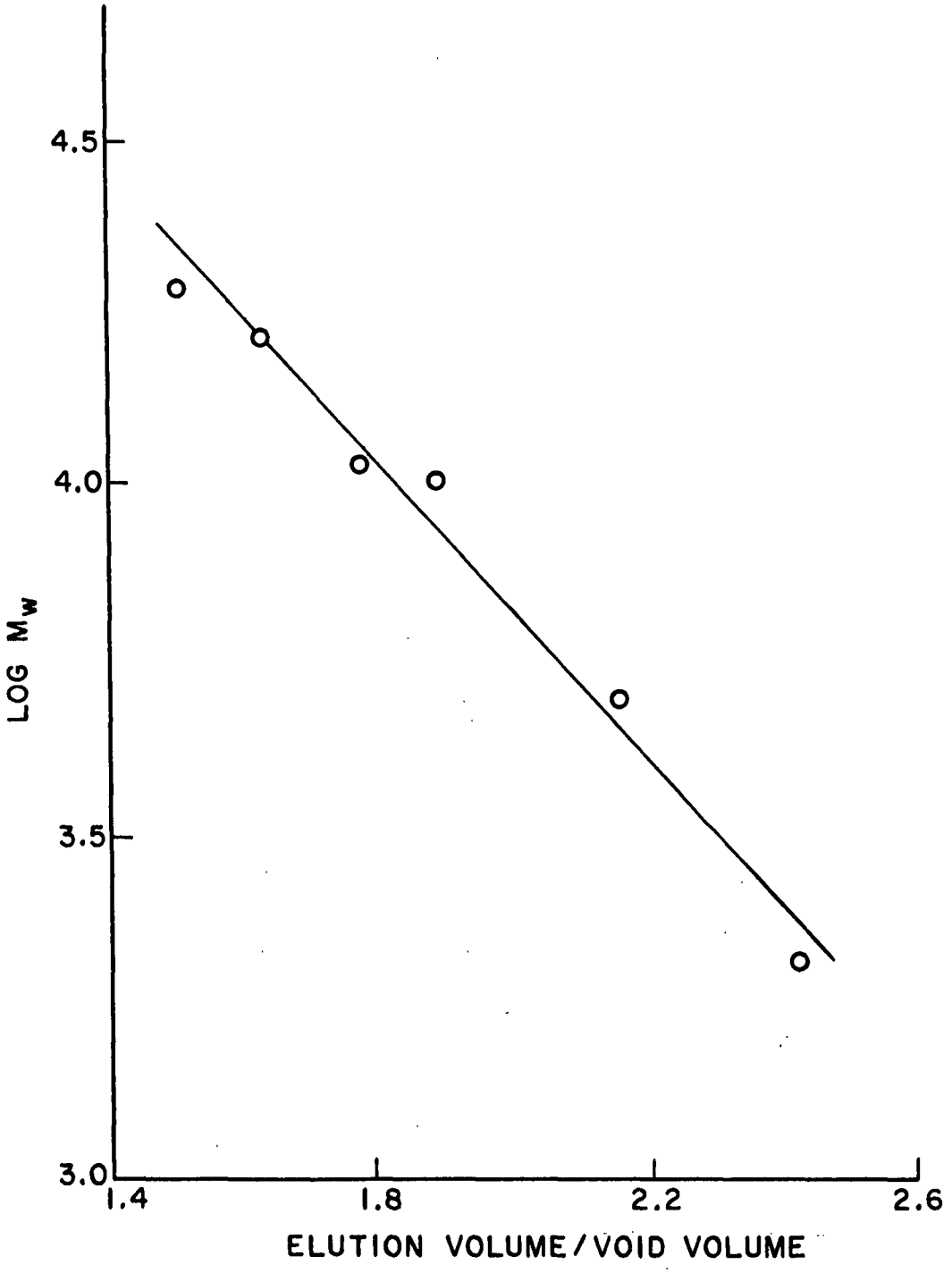

Figure 2. Log Molecular Weight Versus Reduced Elution Volume

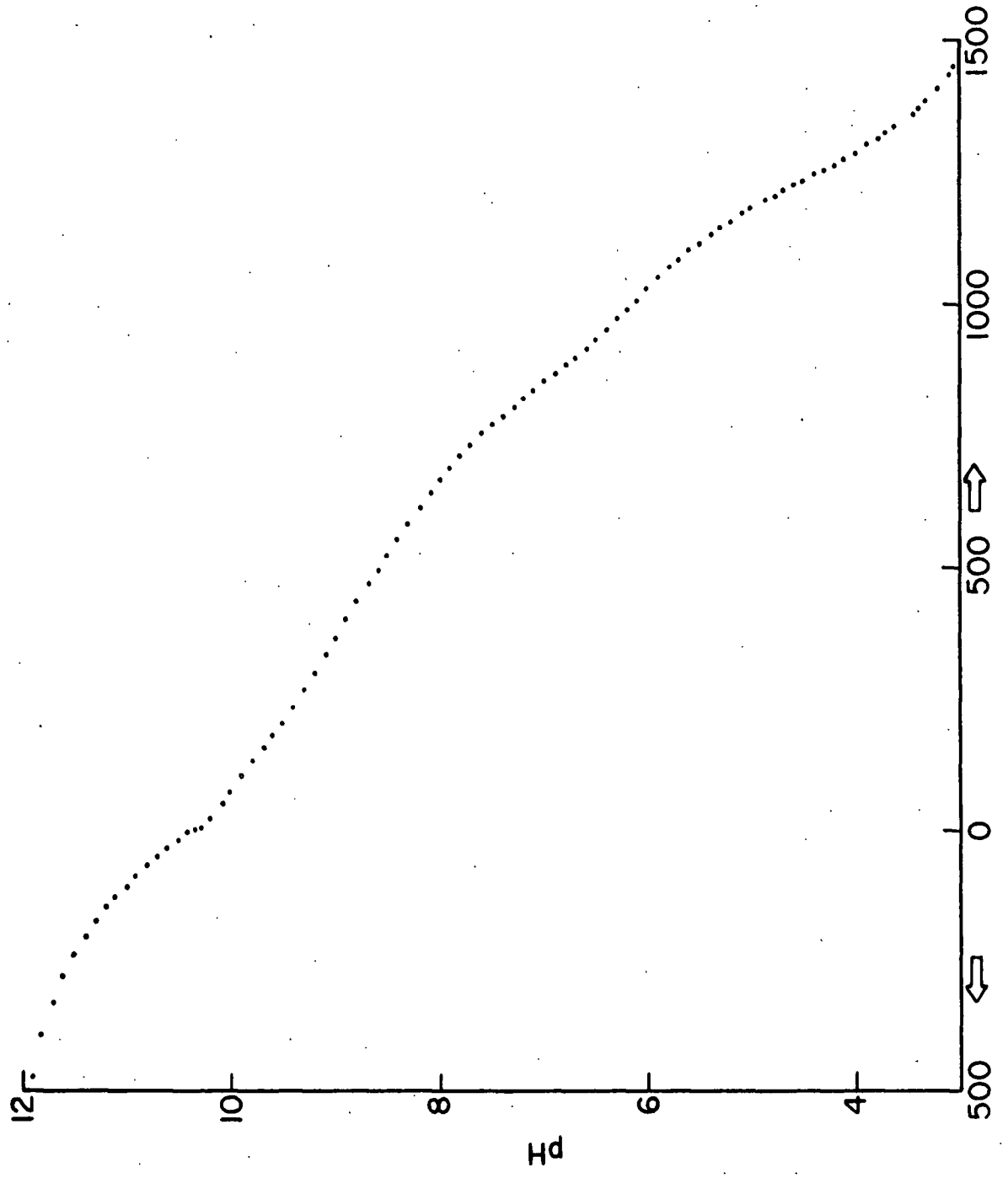

Figure 3. Milliequivalents of Acid or Base as a Function of PEI Solution pH

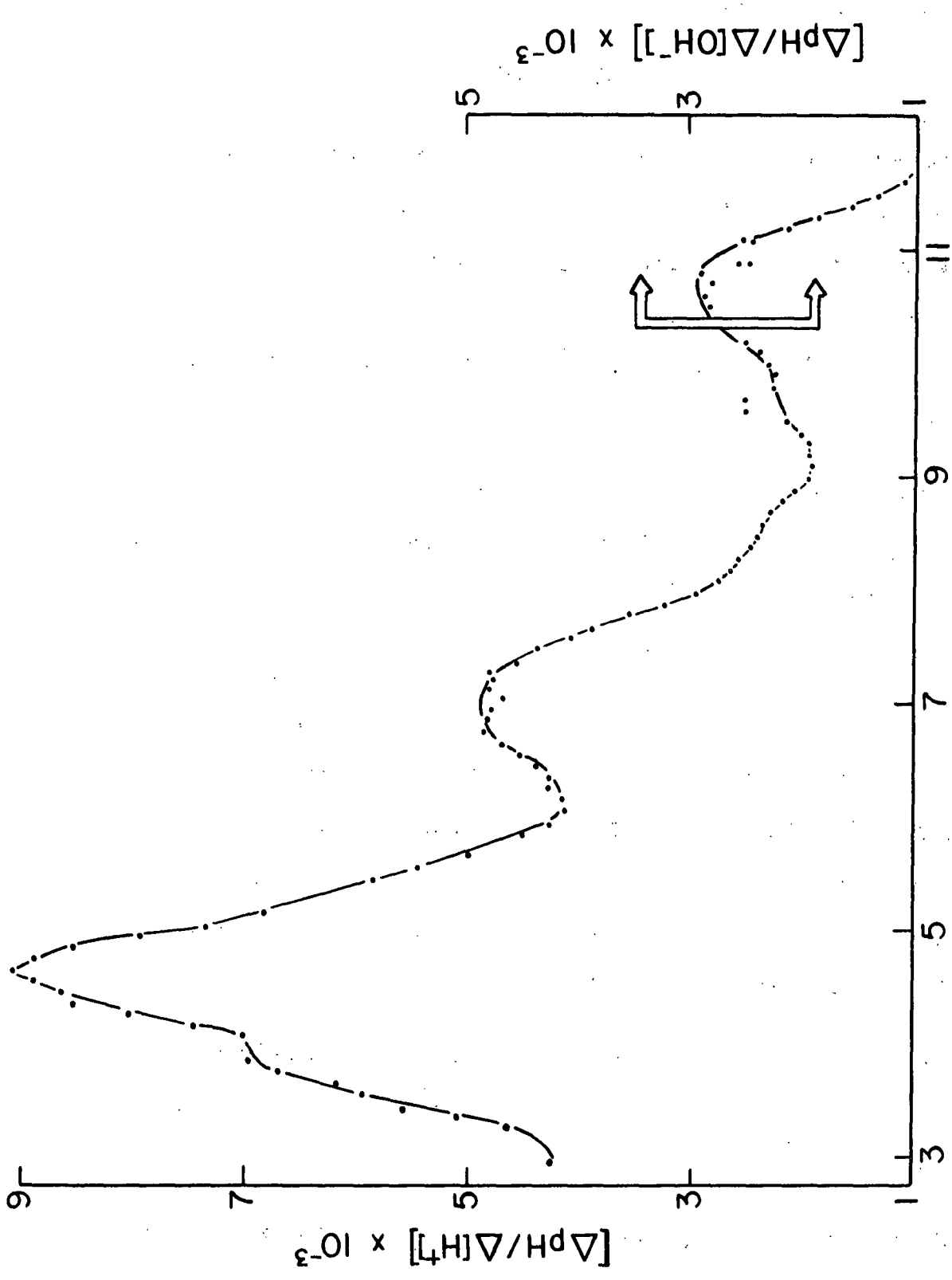

Figure 4. First Derivative of the Plot of pH Versus Milliequivalents of Acid or Base as a Function of pH

When PEI is placed in water it acts as a Lewis acid. A portion of the amino groups (RN) become protonated.

$$RN + H_2O \rightleftharpoons RNH^+ + OH^- \qquad (3)$$

As strong base is added the equilibrium is shifted to the left. The maximum shown in Fig. 4 at pH 10.8 apparently corresponds to the point of neutralization of the PEI molecule. Light-scattering and electrophoretic mobility data presented later also suggest this conclusion. Viscosity data by Allan and Reif (3) also indicate that the point of zero charge on the PEI molecule occurs approximately around pH 11.

If pH 10.8 is taken as the point of zero degree of protonation, the degree of protonation as a function of solution pH can be computed from the titration data. This is shown in Fig. 5.

The maximum occurring in Fig. 4 at pH 4.7 corresponds to a degree of protonation of 62.6%. If the amino groups on the PEI are considered as separate species, a pK_b value of 9.1 is obtained at 50% protonation, the neutralization point at which pK_b values are normally taken for monoprotic molecules. This value is slightly less than the pK_b of 11 suggested by Sarkanen, et al. (65). The presence of 0.1N NaCl may enhance protonation slightly by a stabilizing effect (66).

The maximum occurring at pH 7 corresponds to the neutralization of the strong base NaOH with a strong acid. Sodium hydroxide was originally present at 4.25×10^{-5}N.

Attention should be focused on the fact that only 74% of the amino groups on the PEI macromolecule are protonated at pH 3.0. This result was expected,

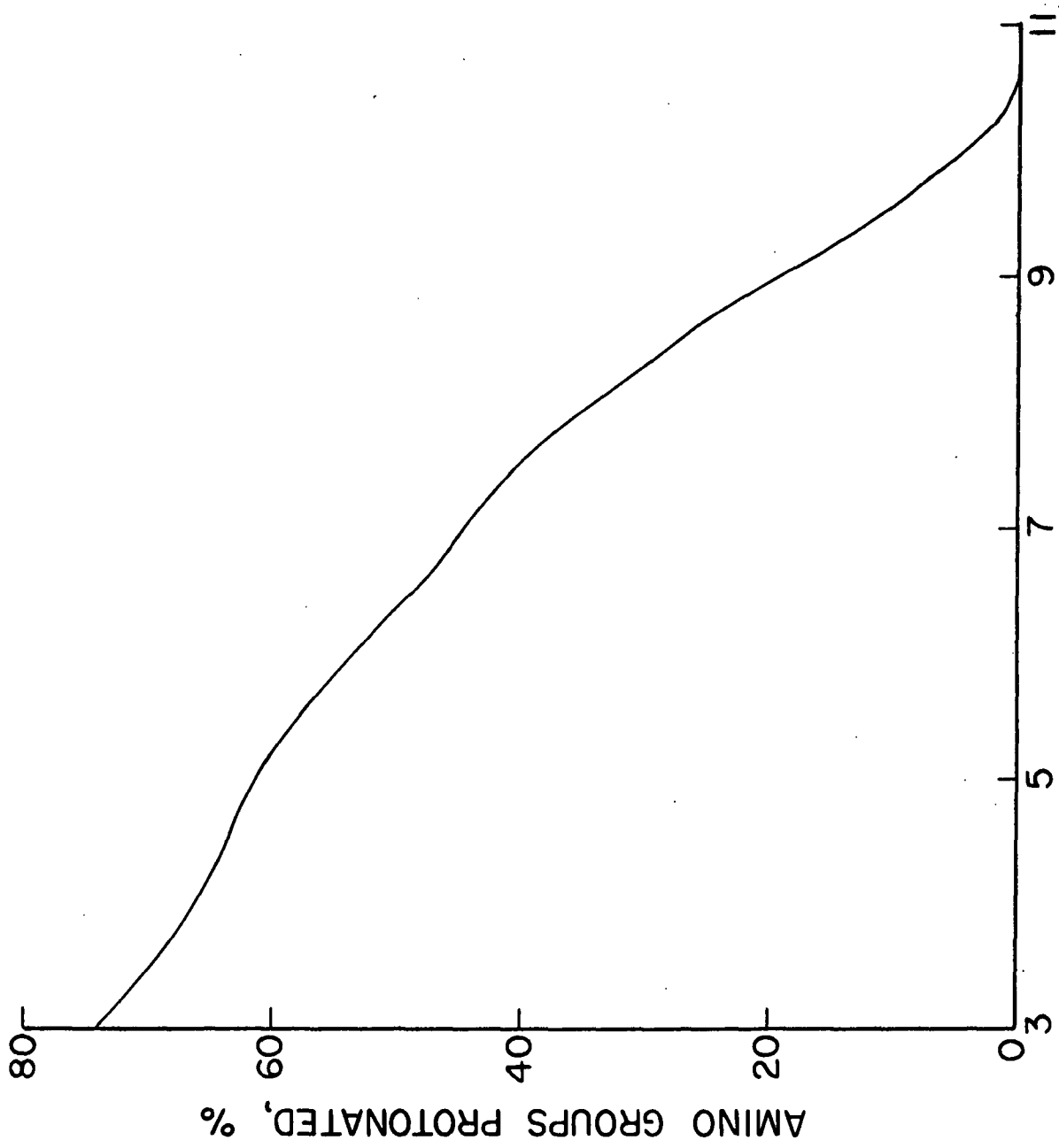

Figure 5. Percentage of Amino Groups Protonated as a Function of pH

since nontitratable amino groups are found for many polyaziridines in nonaqueous titrations (37). The reduced basicity of specific amino groups as adjacent amino groups are protonated is apparently the reason for the nontitratable amino groups. For the PEI macromolecule, that is highly branched and spherically shaped, a limiting molecular charge density probably occurs as the polymer becomes highly protonated. Light-scattering data presented later indicate that intramolecular electrostatic interactions among protonated sites on the PEI macromolecule lead to molecular expansion. As the PEI becomes highly protonated a limiting charge density may be reached where the basicity of unprotonated amines is reduced to such a level that they have negligible affinity for H ions.

ELECTROPHORETIC MOBILITY

When an isolated particle of charge q in an insulating medium is subjected to an electric field of strength E, a force qE acts upon the particle. At steady-state the velocity of the particle is

$$u = qE/f$$

where f is the frictional coefficient. The electrophoretic mobility v is defined as u divided by E. Therefore, the v is directly proportional to the charge on the molecule and inversely proportional to the frictional coefficient.

$$v = q/f$$

The frictional coefficient of a particle is directly related to its size and shape. Thus, the electrophoretic mobility reflects the charge to size and shape ratio.

The electrophoretic mobility of the PEI macromolecule as a function of solution pH is shown in Fig. 6. The ascending and descending boundaries show fair agreement at pH 4.0, 7.0, and 10.1. The descending boundary at pH 13.0 was not observed due to an experimental difficulty.

The results show that the mobility of the PEI macromolecule increases very rapidly from about pH 11 to about pH 8. This corresponds to an increase in the degree of protonation from 0 to about 34%. Very little mobility increase is noted from pH 8.0 to 4.0 which corresponds to an additional 32% increase in protonation. Counterion binding studies for PEI are of interest in the examination of the mobility data.

Lawrence and Conway (67) have investigated the binding of chloride ions to PEI as a function of molecular weight, degree of protonation, and PEI concentration. These authors determined the extent of Cl ion association to PEI by radioactive tracer diffusion measurements according to the method described by Huizenga, et al. (68). From their results the amount of Cl ions directly associated to PEI at the concentration, molecular weight, and degree of protonation at which electrophoresis experiments were done can be estimated. For PEI at a molecular weight of 10,000 and a solution concentration of 0.2%, Table II shows the fraction of Cl ions associated with PEI at four degrees of protonation.

TABLE II

FRACTION OF CHLORIDE IONS BOUND TO POLYETHYLENIMINE CATIONS

	Degree of Protonation, %			
	70	50	30	20
Fraction Cl ion bound	0.60	0.60	0.54	0.46

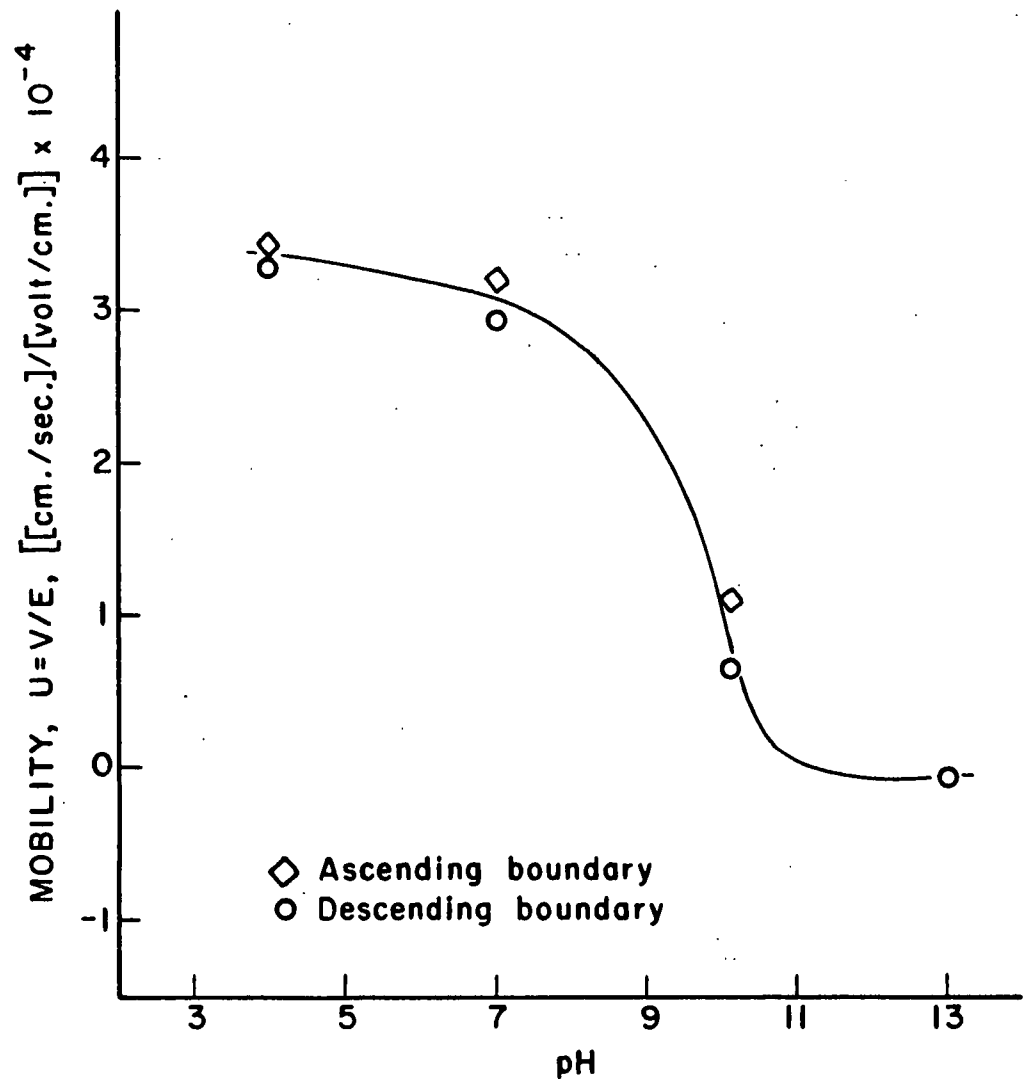

Figure 6. Mobility of PEI F-5 ($\underline{M}_{\underline{w}}$ = 10,400) in 0.109$\underline{N}$ NaCl as a Function of pH

The fraction of amino groups with Cl ions bound increases rapidly up to about 30% protonation. Little increase is noted above this point. From the titration data, 30% protonation is seen to occur at about pH 8.3 where the rate of increase in mobility as noted above has started to sharply decrease. It should be noted that the fraction of Cl ions bound at about 70% protonation is in fair agreement with the value of 0.54 reported by Lanpanje, et al. (69). The counterion studies indicate that the small increase in mobility below pH 8.0 is apparently not directly related to a decrease in the net charge of the PEI molecule resulting from increased counterion association.

Apparently, other factors such as change of coil size with protonation and binding of water molecules may cause the resulting small increase v with 32% increase in protonation. Increased molecular size was confirmed as shown later by significant increases in light-scattering ability of solutions of PEI as the pH is lowered. Increased hydration of the PEI molecule at the higher degrees of protonation may considerably increase the frictional coefficient.

Another interesting behavior is seen to occur at a very high pH of 13.0. A very slight negative mobility was found. Since PEI contains no functional group that could give it an anionic charge, this result appears as an anomaly. The apparent net negative charge may occur due to the association of hydroxyl or chloride ions to PEI. Current water structure theories (70) suggest that molecules having considerable hydrophobic character are water structure enforcing. Diamond (71) suggests that water minimizes the repulsive solvent-solute interactions by forcing solute molecules to associate into "common solvent cavities" instead of remaining free and fully solvated. This suggests that poorly hydrated anions on a localized scale (chain segments within a molecule) are forced into solvent cavities with the poorly hydrated PEI molecule

which contains substantial hydrophobic character. Intramolecular segmental association and the presence of unhydrated negative ions in common solvent cavities could result in an apparent negative mobility.

On a macroscopic scale it is well known that molecules containing hydrophilic and lipophilic parts may form emulsions in water when intra- and intermolecular attraction between lipophilic groups predominates over the solvation forces of the hydrophilic groups (72). It is generally observed that emulsion spheres take on a negative charge by the preferential adsorption of anions.

Experimentally an aqueous PEI emulsion was observed for a 1.5% PEI solution in 2N NaOH. The emulsion is easily destroyed or restored by merely adding acid or base. This result suggests that the common solvent cavity hypothesis by Diamond may explain the slight negative mobility observed.

The electrophoretic effect offers an alternate explanation. A net flow of solvent in the direction of negative mobility is predicted by conservation of mass considerations. This is expected since the highly hydrated sodium ion has a positive mobility and the poorly hydrated chloride ion has a negative mobility. The boundary observed in electrophoresis measurements, in this case, would indicate an apparent negative mobility due to the shift in its position because net bulk solvent flow occurs in the direction of negative mobility.

DIFFUSION COEFFICIENTS AS A FUNCTION OF MOLECULAR WEIGHT

The diffusion coefficients of Fractions 1, 3, 4, 5, 7, and 9 were determined as a function of time and concentration. The apparent diffusion coefficients (D) at infinite time were obtained by a linear extrapolation of the diffusion coefficient *versus* the reciprocal of time. The limiting diffusion coefficient (D_o) was obtained by a linear extrapolation of D versus concentration.

The least squares method was used for the extrapolation. Appendix III lists the D at various concentrations expressed as interference fringe number J.[2] The limiting diffusion coefficients at infinite dilution are given in Table III.

TABLE III

LIMITING DIFFUSION COEFFICIENTS

Fraction	$D_o \times 10^6$, cm.^{2}/sec.
1	0.601
3	0.947
4	0.843
5	1.060
7	1.344
9	1.829

The effect of concentration on the D depends on the reciprocal of the frictional coefficient (f) and on the thermodynamic nonideality occurring. An expression for the diffusion coefficient (73) is

$$D = kT\,(1 + d \ln y/d \ln C)/f \qquad (4)$$

where y is the activity coefficient of the solute and the other symbols have their usual meaning. In general, the thermodynamic factor ($d \ln y/d \ln C$) reflecting nonideality causes an increase in D with concentration. The hydrodynamic factor, $1/f$, is thought to cause a decrease in the D with concentration.

Figure 7 shows that little diffusion coefficient-concentration dependence exists in standard aqueous solvent. The data suggest that perhaps the hydrodynamic factor predominates slightly under these conditions. This diffusion coefficient-concentration dependence is in sharp contrast to that found by

---

[2]The fringe number is directly proportional to solute concentration: $J = na'C/\lambda$ where n is the specific refractive increment, a' is the cell length, C is the solution concentration, and λ is the wavelength of light. This relationship was shown to hold for the PEI system (1).

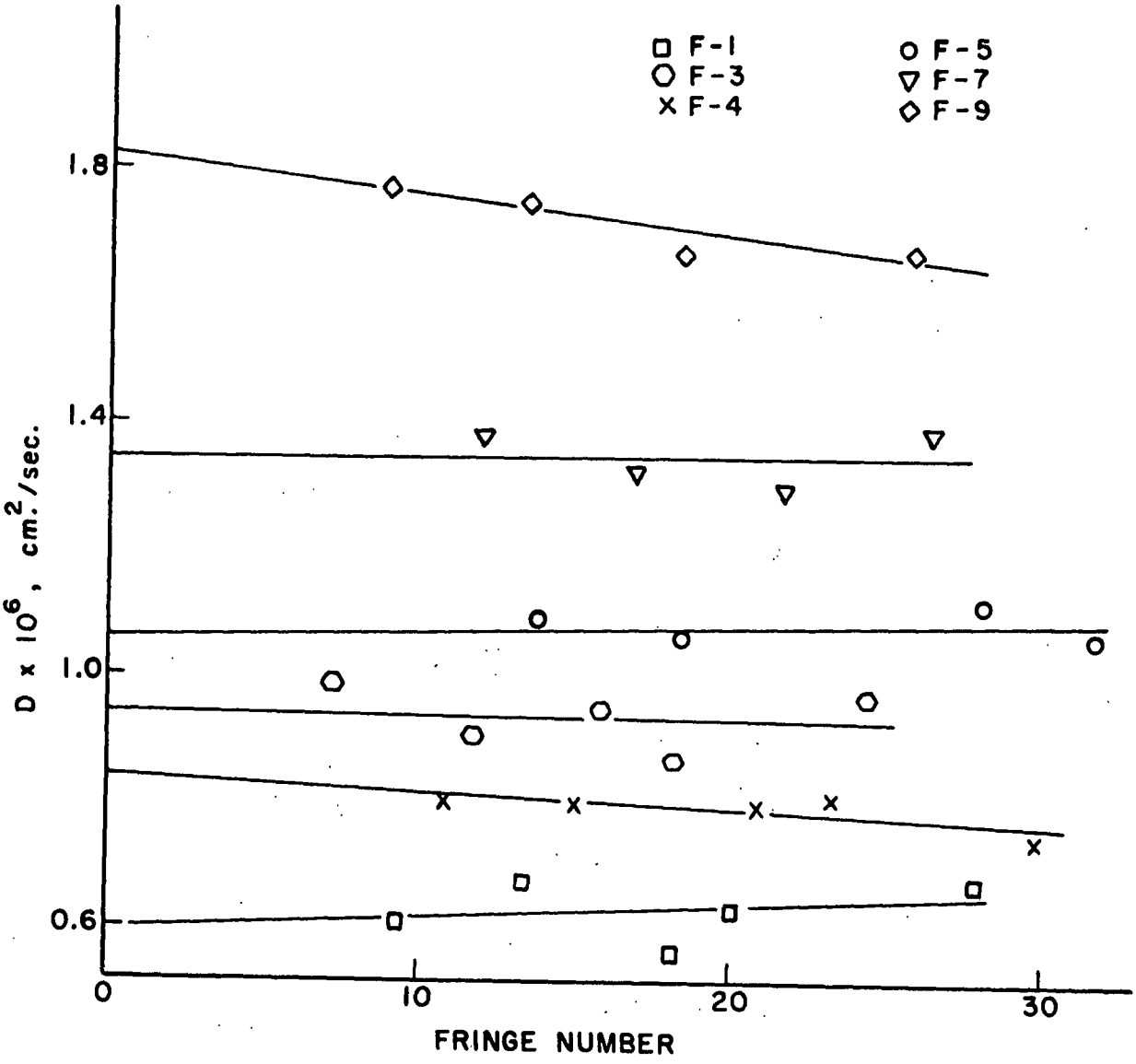

Figure 7. Diffusion Coefficients of PEI Fractions as a Function of Concentration Expressed as Fringe Number

Kindler (1) at lower ionic strength. He found that PEI at a molecular weight of 8,000 has limiting diffusion coefficients of 2.1, 1.7, and 1.2 x 10^{-6} cm.^{2}/sec. in the solvent containing no NaCl, 2 x 10^{-3}N NaCl, and 5 x 10^{-3}N NaCl, respectively. A positive diffusion coefficient-concentration dependence was noted under those conditions and the slope of D versus C plots were shown to increase with increase in ionic strength.

The data displayed graphically in Fig. 7, on the other hand, supports the conclusion that little diffusion coefficient-concentration dependence occurs when 0.109N NaCl is present.

The diffusion coefficient-molecular weight dependence reflected by the D_o is easily assessed and is harmonious with the trend found previously. Kindler (1) has demonstrated that the logarithm of D_o shows a linear relationship with the logarithm of the molecular weight. This relationship was also found to hold for the poly-L-lysine molecule (74). This relationship for PEI is shown in Fig. 8 for the data in Table III. The least squares method of fit gave the following regression equation with 95% confidence limits (75).

$$\log D = [-0.491 \pm 0.067] \log M_w - [4.072 \pm 0.260] \qquad (5)$$

The highly branched and solvated PEI molecule which shows considerable counterion binding even at low degrees of protonation probably acts as an impermeable sphere in solution. Therefore, the concept of the hydrodynamic equivalent sphere is convenient and probably closely approximates the actual molecular dimension of the external boundaries of the molecule in solution. The Stokes equation which relates the limiting diffusion coefficient to the radius of solid spheres can be used to calculate the radius (R_e) of a hydrodynamic equivalent sphere. The Stokes equation (76) may be expressed as

$$R_e = kT/6\pi \eta_o D_o \qquad (6)$$

where k is the Boltzmann constant, T is the absolute temperature, and η_o is the solvent viscosity. In theory, the R_e is thought to be directly proportional to the radius of gyration (R_g) of a polymer. In turn the R_g is thought to be proportional to the molecular weight, effective segmental length, and the interaction between segments. For flexible polymers that are approximately spherical in solution, in theory the D_o depends on $M_w^{-0.5}$ in poor solvent and on $M_w^{-0.55}$ in a good solvent (77). This has been demonstrated for a number of systems.

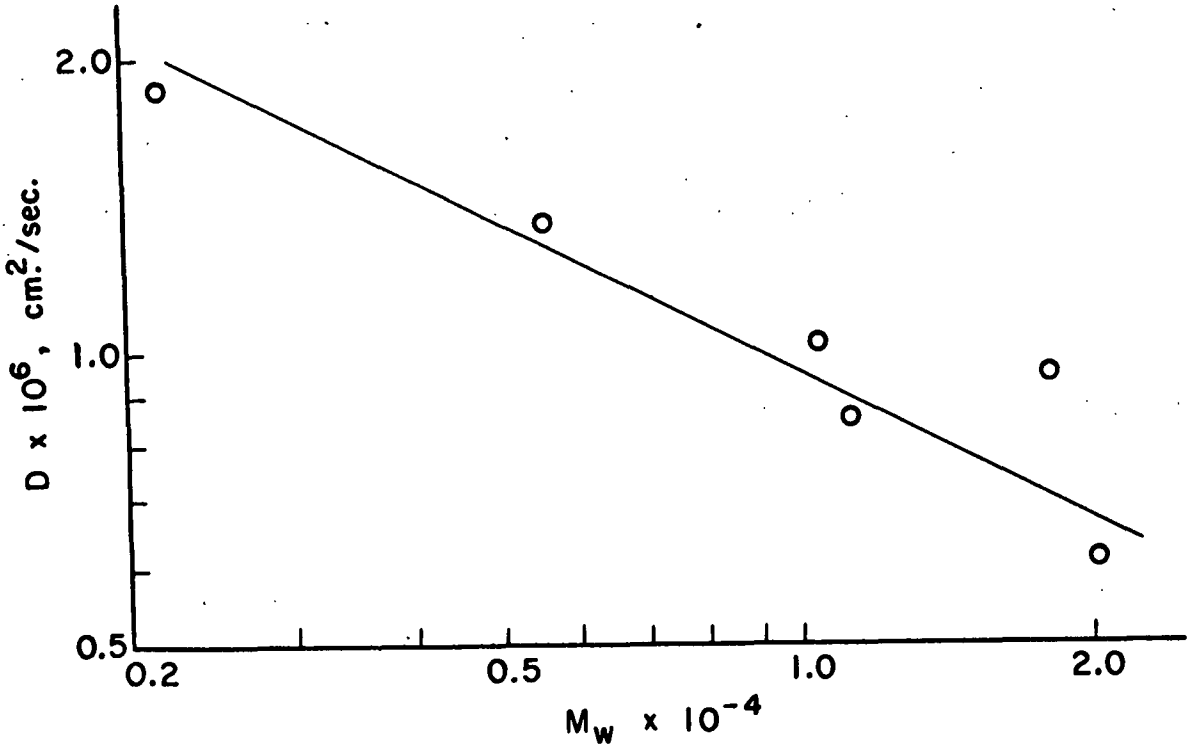

Figure 8. Effect of Molecular Weight on the Diffusion Coefficient

The value obtained for PEI, $\underline{D}_o$ proportional to $\underline{M}_w^{-0.49}$, is consistent with the idea that PEI is a spherical shaped molecule. The Stokes diameters calculated from $\underline{M}_w$ values and the regression line of log $\underline{D}_o$ versus log $\underline{M}_w$ are shown in Table IV.

TABLE IV

STOKES DIAMETER

Fraction	Diameter, A.
1	74
3	69
4	55
5	53
7	38
9	25

DIFFUSION COEFFICIENT AS A FUNCTION OF pH

The diffusion coefficients on F-5 PEI were determined on the same solutions used for electrophoretic mobility studies earlier cited. The apparent diffusion coefficient of 0.2% solutions as a function of pH is shown in Fig. 9. As the cationic charge increases with lowering of the pH from 13.0 to 7.0 a large decrease in the $\underline{D}$ was found. At about pH 7.0, however, a marked change was noted; the diffusion coefficient begins to increase.

Recognized authors of diffusional theory (78, 79) conclude on theoretical grounds that three factors influence the observed diffusion coefficients for polyelectrolytes: (1) changes in molecular configuration resulting from intramolecular electrostatic repulsions, (2) electrophoretic effects resulting from interactions between polyions, counterions, by-ions, and solvent, and (3) changes in the osmotic or second virial coefficients.

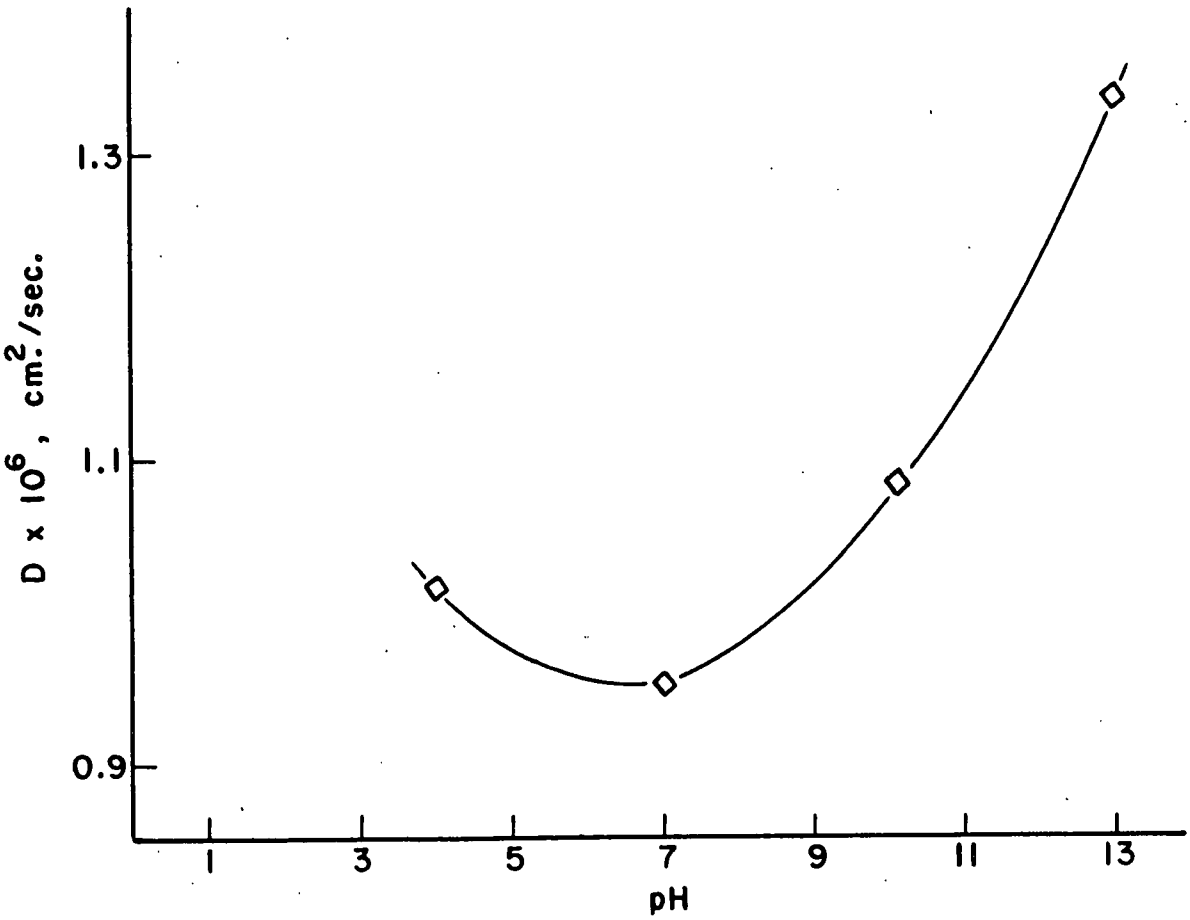

Figure 9. Apparent Diffusion Coefficient of PEI F-5 ($\underline{M}_w$ = 10,400) at 0.2% Concentration in 0.109$\underline{N}$ NaCl as a Function of pH

Molecular expansion resulting from intramolecular electrostatic repulsion of cationic sites on the PEI molecule can explain the observed decrease in $\underline{D}$ with decrease in pH from pH 13.0 to 7.0. The increase of the $\underline{D}$ with further decrease in pH must be attributed to either electrophoretic effects or changes in the second virial coefficients.

Morawetz (80) supports theoretical considerations with experimental data and shows that the second virial coefficient is directly proportional to the square of the polyelectrolyte charge and inversely proportional to the added simple electrolyte concentration. At constant molecular weight and ionic

strength the second virial coefficient is found to increase with increased polyelectrolyte charge. An increase in the second virial coefficient can be related to the diffusion coefficient through application of thermodynamic theory (73). The diffusion coefficient theoretically is directly proportional to the second virial coefficient. Experimentally the dependence has been found to be somewhat less than predicted although relative agreement has been found. An increase in the second virial coefficient apparently explains the increased D at low pH.

It is unlikely that appreciable electrophoretic effects occur in 0.109N NaCl as the pH is lowered. The salt concentration does not change as the pH is lowered beyond the amount of HCl added to control pH.

It is interesting to note that application of the Stokes equation to the above data suggests that the size of the PEI macromolecule decreases 21% when the pH is raised from pH 10.1 to pH 13.0. The data also suggest that the relative size of the PEI macromolecule increases 13.5% when the pH is lowered from pH 10.1 to pH 7.0.

VISCOSITY

The viscosity data are given in Appendix IV. The reduced specific viscosity, η_{sp}/C, and PEI concentration are listed. The intrinsic viscosity, $[\eta]$, at infinite dilution is taken as the intercept of the regression line of the η_{sp}/C versus C plot by the method of least squares.

Few equations are available that relate the viscosity and molecular weight of branched polymers to their molecular dimensions in solution. Seely (81) derived a relationship by applying Darcy's law to the fluid flow within a hypothetical porous molecule and the equations of motion to the flow of fluid outside

the molecule. The equation has been applied to data for a number of branched and/or cross-linked molecules and has shown good correlation. The equation was applied to the PEI viscosity and molecular weight data. The molecular diameters calculated for Fractions 1, 3, 4, 5, 7, and 9 are shown in Table V. Since it was reasoned that hydrodynamic equivalent sphere concepts may properly describe the actual dimensions of PEI, the combined Einstein-Stokes equation

$$[\eta] = 2.5N \frac{4}{3} \pi R_e^3 / M_w \qquad (7)$$

where N is Avogadro's number, was also used to calculate molecular diameters.

TABLE V

MOLECULAR DIAMETER OF POLYETHYLENIMINE

Fraction	Seely, A.	Einstein-Stokes, A.
1	69	66
3	66	62
4	57	52
5	55	51
7	43	40
9	33	28

The intrinsic viscosity values based on 95% confidence limits have an average error of about ± 2.8%. The molecular weight values have an average error of about ± 4%. Details of the application of the Seely equation to $[\eta]$ and molecular weight data are given in Appendix V. A regression coefficient of 0.97 was obtained for the $[\eta]$ and M_w data fitted to the Seely equation.

The molecular diameters calculated by the Einstein-Stokes equation on the average are about 7% less than the values calculated using the Seely equation. However, for the experimental error involved, the agreement is very good. The Seely treatment is for a porous sphere of radius a, which is considered to have a porosity of ε and a permeability K. The Einstein-Stokes equation, on the

other hand, is for impermeable solid spheres. For a highly branched polymer, with very limited permeability, the Seely model should give theoretically slightly larger diameter values than the Einstein-Stokes model.

The Seely equation predicts a curved relationship between the log [η] and log $\underline{M}_w$. Figure 40 in Appendix V shows this is the case for PEI [η] and $\underline{M}_w$ data.

LIGHT SCATTERING

The absolute Rayleigh scattering ratio of 90° ($\underline{R}_{90}$) of a solution of PEI and the solvent alone as a function of pH are shown in Fig. 10. The $\underline{R}_{90}$ of the solvent at the same addition levels of acid or base was subtracted from the $\underline{R}_{90}$ of the PEI solution. The absolute $\underline{R}_{90}$ of the solvent at a given acid or base addition level is plotted as a function of the pH of the PEI solution when the same amount of acid or base is added.

The nearly constant value of solvent scattering throughout the acid and base addition range indicates no extraneous materials are present in the solvent which cause an increase in scattered light. This result suggests that the absolute $\underline{R}_{90}$ values obtained for the PEI macromolecule are highly significant and indicative of molecular size changes.

The light-scattering measurements of polyelectrolyte solutions with simple electrolyte present parallel the behavior of uncharged polymers. This is in sharp contrast to the light-scattering behavior of polyelectrolyte solutions not containing added simple electrolyte. Charge interactions decrease the randomness of a system and impose order which results in a decrease in the observed scattering (51). On the other hand, when sufficient simple electrolyte is present, intermolecular charge interactions are suppressed and random concentration fluctuations through the solution are maintained. Thus, as the charge

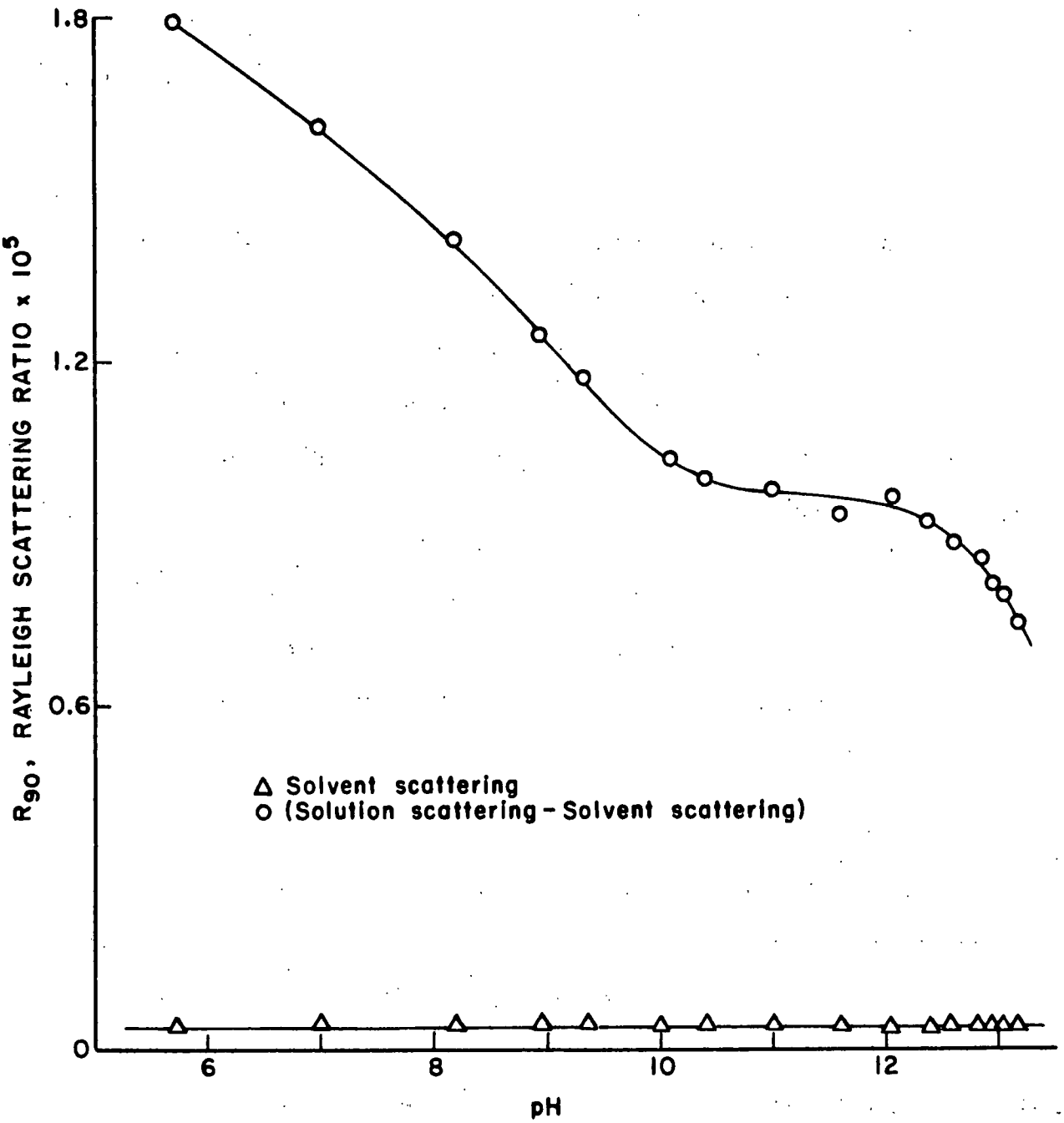

Figure 10. Rayleigh Scattering Ratio of PEI F-3 at 0.167% Concentration in 0.109N NaCl as a Function of Solution pH

on a polyelectrolyte molecule is increased, increased scattering is observed which reflects the expansion of the macromolecule. For example, expansion of the polymethacrylic acid was found to occur with increased ionization even when 0.8N NaCl was present (50, 51). Data on cellulose xanthate, carboxymethyl cellulose, arabic acid, and bovine serum albumin are also available (51). Little size changes are noted for isoionic dilutions with concentration changes. However, the size of polyions are found to change greatly with the ionic strength of the solution and polyion charge.

The interpretation of PEI light-scattering data are based on the literature (51) for the light scattering of polyelectrolytes with simple electrolyte present. The R_{90} of the PEI solution increases rapidly from pH 10.0 to 5.7 and only slightly from pH 10.8 to 10.0. An inflection point occurs in the regions of pH 10.8 and 11.8. Nearly constant scattering occurs from pH 10.8 to 11.8 with subsequent decrease at higher pH.

As the solution pH is lowered, H ion associates with amino groups. The increased PEI molecular charge leads to increased repulsive forces and causes an expansion of the molecule.

The inflection point at about pH 10.8 above which no expansion is indicated, probably corresponds to the point of nearly zero charge on the PEI molecule. At values greater than pH 11.8, the decreasing $R_{90}°$ suggests a further decrease in the molecular size of the PEI molecule. As the pH is increased the solvent becomes poorer. A change in the molecular configuration to a more compact structure, perhaps by the association of lipophilic hydrocarbon parts within the PEI molecule is suggested. The coiling of uncharged polymers in poor solvents and intramolecular hydrophobic association through Van der Waals forces are commonly known. The light-scattering data for PEI in 0.109N NaCl

solvent suggest that as the pH is increased above pH 11.8, the solvent becomes poorer and the uncharged PEI molecule coils into a tight compact structure. Intermolecular association does not occur since light-scattering increases would result.

Some of the current thinking concerning water structure also suggests the above phenomenon. Diamond (71) has referred to this as water structure enforced association, whereby hydrophobic ions are forced to associate into common solvent cavities rather than remaining free and fully solvated. This association is thought to minimize the water-hydrocarbon interaction. For example, association between nonpolar side chains of amino acids are often observed in aqueous solutions (82). Intramolecular association is postulated since intermolecular association leads to increased R_{90} values. However, the decreased light-scattering at very high pH may result from the slight concentration decreases occurring when the pH was changed by addition of 1N sodium hydroxide.

Dissymmetry measurements were also taken. They are presented in Fig. 41 of Appendix VI. Interpretations of dissymmetry determinations for polyelectrolytes are obscure. They generally show dissymmetry values less than unity, which are thought to result due to internal and external scattering interference (65).

DIFFUSION THROUGH A MEMBRANE

In an attempt to further characterize the effective apparent size of the PEI molecule in solution, simple diffusion experiments through dialysis membrane were done. Regenerated cellulose dialysis membrane reported to have a nominal pore diameter of 48 A. was used (83). The amounts of PEI in Fractions 1, 3, 4, 5, 7, and 9 diffusing through the membrane are given in Table VI. A membrane completely permeable to a given fraction would have a value of 50% on this basis.

TABLE VI

POLYETHYLENIMINE DIFFUSING THROUGH DIALYSIS MEMBRANE

Fraction	Molecular Weight	PEI Passing Through Membrane, %
1	20,000	2.0
3	18,000	1.3
4	11,100	1.6
5	10,400	5.6
7	5,350	15.6
9	2,140	45.7

The data are presented to show which fractions can easily diffuse into and through pores of the membrane. The low percentage of PEI diffusing through the membrane for F-1, 3, 4, and 5 apparently reflects low molecular weight PEI present in the fractions or the presence of pores larger than the nominal pore size stated by the manufacturer. The data clearly indicate F-9 diffuses readily into and through the pores of the membrane. Fraction 7 also apparently has an appreciable number of PEI molecules able to diffuse through the membrane.

It is generally found that the molecular size of the solute relative to the characteristic membrane pore size is the controlling factor determining whether passage of solute through the membrane occurs. The charge of the species is found to play a less significant role (84).

Determination of the pore size of membranes is complicated by their gel-like nature. Pore size estimates are subject to the errors of the method of measurement; stresses imposed on a membrane, along with hydration changes markedly affect the effective membrane pore size. The 48 A. membrane pore size stated by the manufacturer thus must be viewed with much reservation. If the 48 A. figure is considered a valid estimate, then the polyethylenimine diffusion data presented above indicate PEI of 5,000 mol. wt. and less have effective molecular sizes less than 48 A. Previous study at lower ionic strength showed

that PEI of 8,000 mol. wt. was the lower limit of the solute retained by the membrane. It may be concluded, with some reservation, that PEI Fractions 1, 3, 4, and 5 have molecular size greater than 48 A. and F-7 and 9 have a considerable number of molecules with molecular sizes less than 48 A.

CHARACTERIZATION OF SILICA GEL

DESCRIPTION OF PARTICLES

The silica beads of Porasil A, B, and C were observed under the light microscope and found to be spherically shaped. Some beads have nearly perfect spherical geometry. Many of the beads, at slightly higher magnification using the scanning electron microscope, exhibit appreciable surface imperfections such as cracks, fissures, gouges, and protruding surface build-ups. The ultrastructures of the spherical beads were observed at high magnification using the SEM and TEM.

SEM and TEM micrographs of Porasil C revealed the same structure as has been previously described by Beau, et al. (24). A three-dimensional network composed of randomly packed elemental particles was observed. TEM micrographs of Porasil A also were of this type structure. TEM micrographs of Porasil B indicated a slightly different ultrastructure. Fusion between adjacent elemental particles resulting in loss of individual elemental particle identity was observed. A somewhat more closed structure as compared to Porasil C was indicated. The elemental particles for Porasil A were found to be much smaller than Porasil B and C. The elementary particles that form the spherical beads of Porasil A or C are not of uniform size or shape. They can be described as roughly spherical with a considerable size range.

The Porasil bead ultrastructure described above was seen by viewing direct carbon replicas of the surface of the Porasil particles. Representative TEM

micrographs of Porasil A, B, and C are shown in Fig. 42 of Appendix VII. Beau, et al., on the other hand, viewed crushed particles and observed what they concluded to be the basic internal structure of the Porasil beads. Beau, et al. found that the average size of the pores is comparable to that of the elementary particles composing the beads and concluded from electron micrographs that the straight cylindrical capillary pore model, generally assumed for analysis of porosimetry and gas adsorption isotherm data, was perhaps a poor choice. They found the average pore diameter calculated from the pore volume and BET surface area was larger than the average pore diameter calculated from porosimetry data. These results were taken by Beau as evidence that the average pore aperture is less than the diameter of the interior of the pore. He found that instead of the factor of 2 in the expression for the average pore radius,

$$\bar{r} = 2(\text{Porous Volume})/(\text{Surface Area}) \qquad (8)$$

most Porasil types showed this factor to vary between 1.3 and 1.6.

PORE SIZE DISTRIBUTIONS

Although conventional techniques for determining pore size distributions such as mercury intrusion porosimetry and nitrogen gas adsorption-desorption isotherms are in wide use, both methods are still viewed skeptically with regard to absolute pore size values. Routine porosimetry data, consisting of the volume of mercury intruded as a function of absolute pressure, are generally obtained on one of the commercial instruments available. Pore size distributions are then calculated using the Washburn form of the Laplace equation. For straight cylindrical capillaries open at one end the Washburn form has the factor 2 in its numerator as shown below:

$$P = 2\gamma \cos \theta / R_a \qquad (9)$$

where P is pressure applied, γ is the surface tension of mercury, θ is the contact angle, and R_a is the radius of a straight cylindrical capillary. For a parallel plate model for pores the numerical factor is 1. The numerical factor may range between 1 and 2 depending on the model chosen. It is generally felt that the cylindrical capillary model represents the physical situation for the forcing of liquid having an obtuse contact angle through and into the interconnecting canals and pores within a three-dimensional rigid porous material. In this respect, the term "equivalent pore size" (EPD) which refers to the diameter of a straight cylindrical capillary is commonly used for assignment of pore size diameters from porosimetry data.

Table VII is a summary of the calculated results obtained from mercury intrusion porosimetry (MIP) and nitrogen gas adsorption isotherm (NAI) data. The total pore volumes over the pressure ranges investigated are shown. The cumulative pore surface area, average pore diameter and maxima in the distribution functions [$D(R_a) = dV/dR_a$] (59) versus equivalent pore diameter are given. The distribution functions as a function of equivalent pore diameter (EPD) for Porasil A, B, and C that were calculated from MIP and NAI data are shown in Fig. 11, 12, and 13, respectively. The MIP volume frequency plots of Porasil A, B, and C versus log P, to enable the comparison of their distributions are given in Fig. 14.

Porasil A

The results of the pore size analysis for Porasil A show good agreement with the characteristics generally found for other silica gels. The total pore volume for pores having EPD between 40 and 600 A. was 0.93 cc./g. and 0.90 cc./g. for MIP and NAI determinations, respectively. Porasil A has an extremely narrow pore size distribution. Both MIP and NAI data show pores between 40 A. and 300 A. The MIP $D(R_a)$ is significantly shifted to smaller

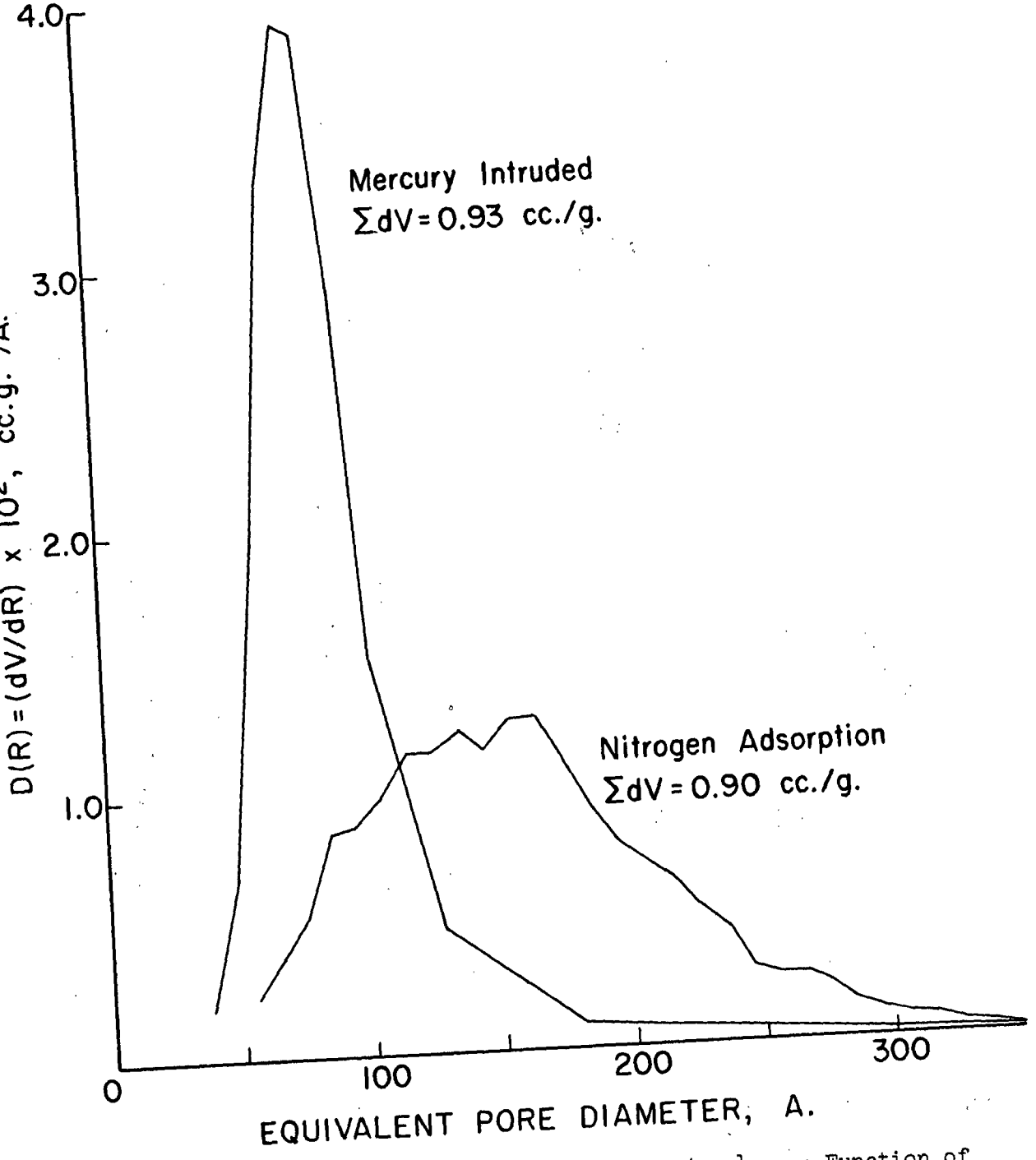

Figure 11. Distribution Function [$D(R_a) = dV/dR_a$] as a Function of Equivalent Pore Diameter for Porasil A

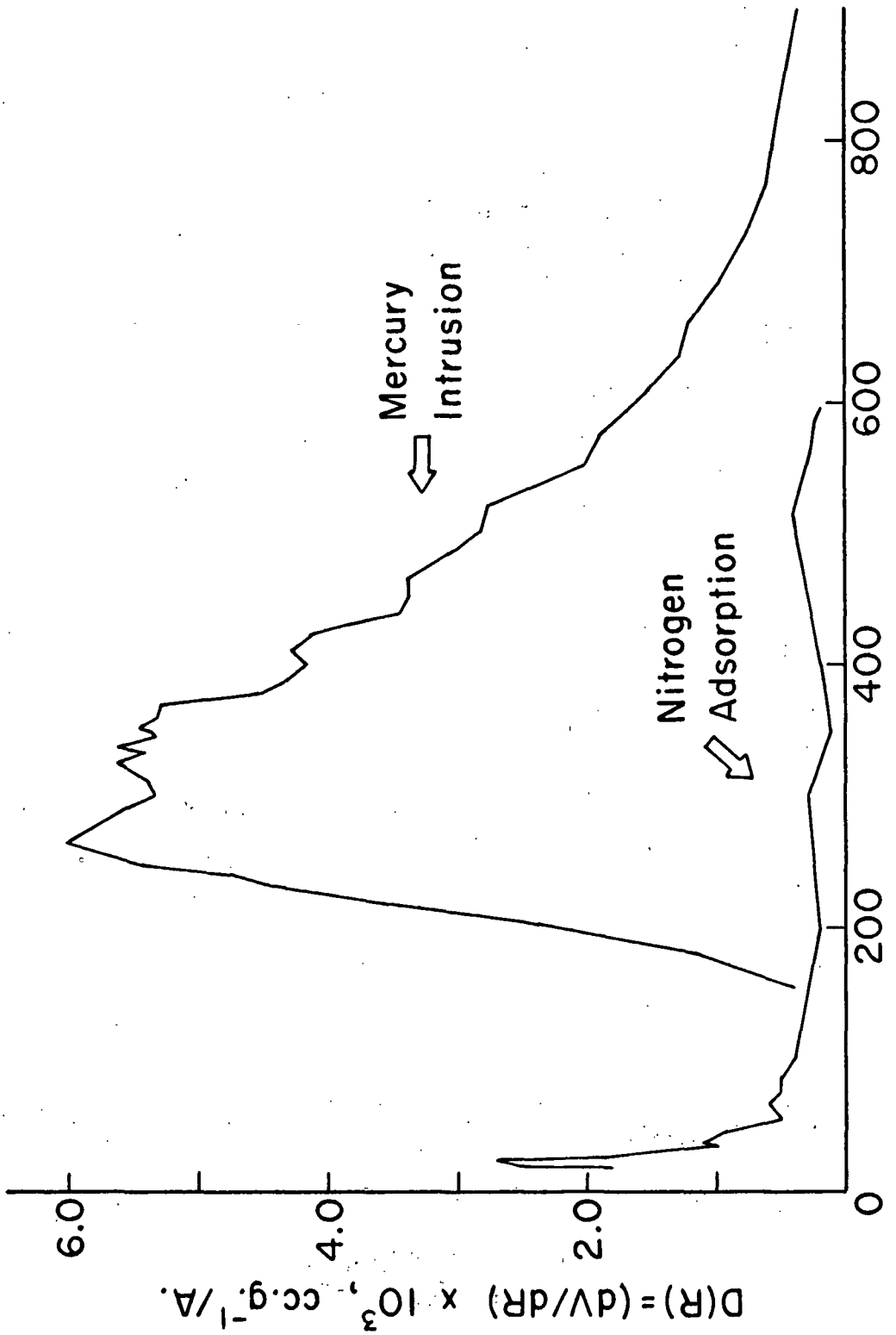

Figure 12. Distribution Function [$\underline{D}(\underline{R}_a) = d\underline{V}/d\underline{R}_a$] as a Function of Equivalent Pore Diameter for Porasil B

TABLE VII

SUMMARY OF MERCURY INTRUSION POROSIMETRY AND NITROGEN ADSORPTION

PORE SIZE ANALYSIS

	Nitrogen Gas Adsorption Porasil			Mercury Intrusion Porosimetry Porasil		
	A	B	C	A	B	C
Total pore volume, cc./g.	0.90[a]	0.10[a]	0.24[a]	0.93[d]	0.915[b]	0.708[c]
BET surface area, $m.^2/g.$	282	60	76	--	--	--
Cumulative pore surface area, $m.^2/g.$	257	54	60	350	103	125
Average pore diameter, A. $4V/BET\ SA$	128[a]	67[a]	127[a]	132[a]	610[b]	377[c]
Maxima in pore size in the distribution	165	22	22	76	265	155
Plot of dV/dR_a versus EPD, A.		300 510	385 550			255

[a]Includes equivalent pore sizes from 14 to 600 A.
[b]Includes equivalent pore sizes from 150 to 900 A.
[c]Includes equivalent pore sizes from 150 to 600 A.
[d]Includes equivalent pore sizes from 30 to 600 A.

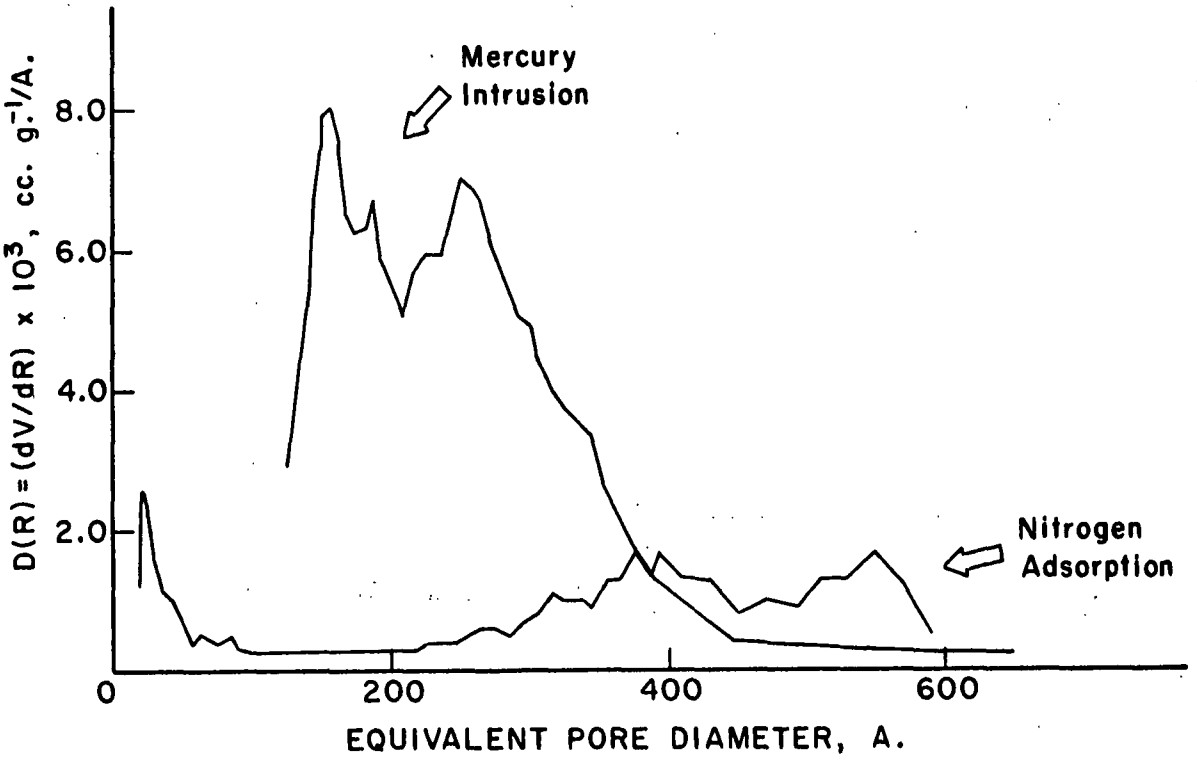

Figure 13. Distribution Function $[D(R_a) = dV/dR_a]$ as a Function of Equivalent Pore Diameter for Porasil C

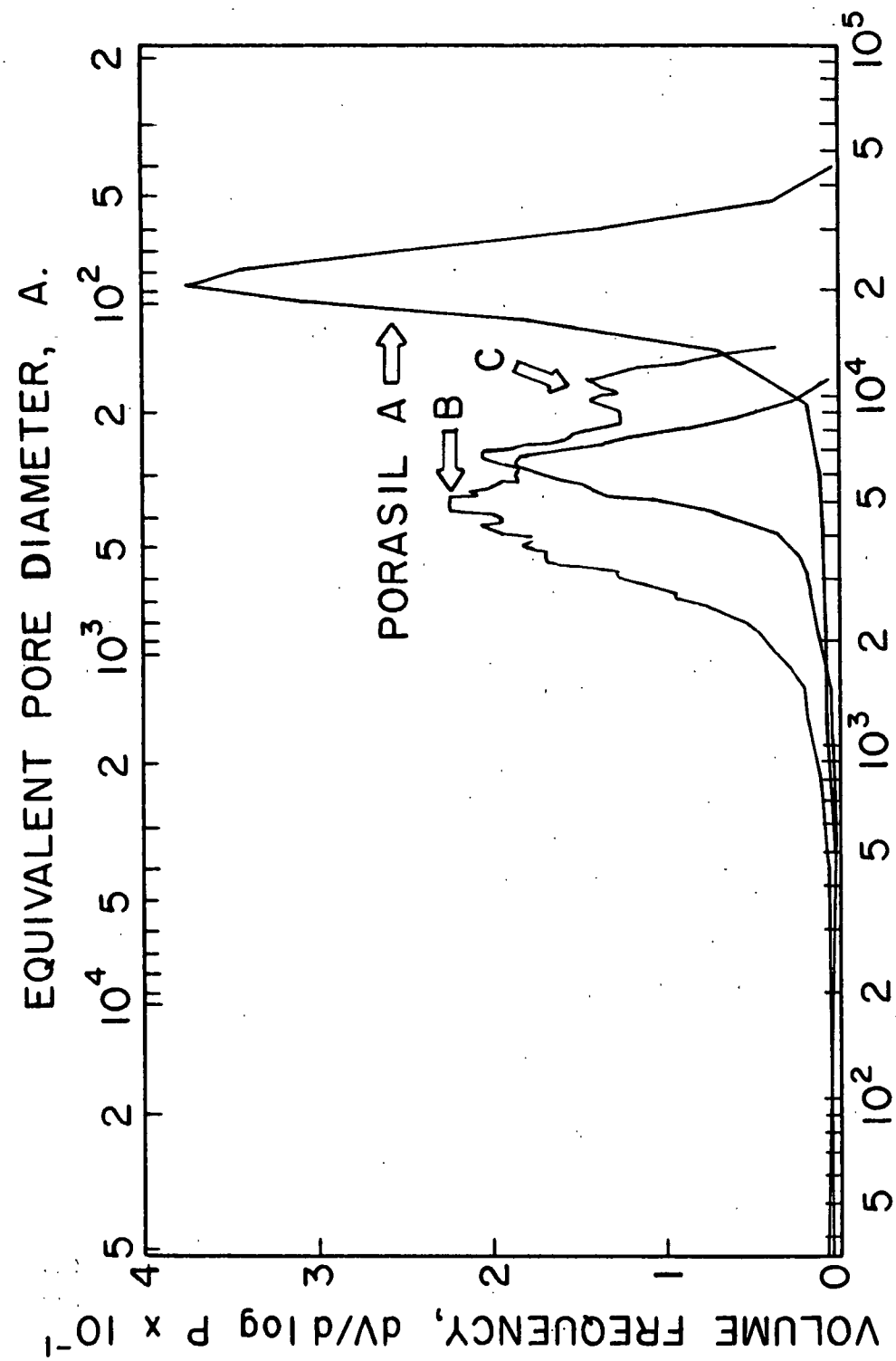

Figure 14. Mercury Intruded Volume Frequency as a Function of Absolute Pressure for Porasil A, B, and C

pore diameters and sharpened compared to the NAI $\underline{D}(\underline{R}_a)$. The MIP $\underline{D}(\underline{R}_a)$ has the characteristic shape of the nitrogen gas desorption isotherm commonly found for silica gel. The shifting of the pore size distribution is commonly observed with pore analyses done separately on adsorption and desorption gas isotherms. Shifting of the distribution function is often attributed to "ink bottle pores" (19) as well as other causes, such as hysteresis of the contact angle (85) and delayed meniscus formation (86). The term "ink bottle pore" is representative of any pore that is accessible through apertures small in comparison to the major dimensions of the interior cavity of the pore.

During the nitrogen adsorption process, pore filling by the condensation of nitrogen is based on the Kelvin equation (87). For a wetting liquid the vapor pressure is reduced across the meniscus formed. The radii of curvature of the meniscus determine the driving force for further nitrogen condensation. Three meniscus shapes occur which lead to further condensation of nitrogen to fill pores. The meniscus formed may have a spherical, elliptical, or cylindrical curvature.

For ink bottle pores having very small necks, filling of the neck will occur first followed by its larger cavity at higher partial pressure. However, during the desorption process large volumes of nitrogen contained within the large cavity of the ink bottle pore escapes only when the relative pressure has been reduced to the value corresponding to the diameter of the small neck or aperture leading into the pore cavity. The gross result is that inflated volume changes are noted to occur which correspond to small EPD for the cylindrical capillary model. This behavior is easily detected by comparing the cumulative pore surface area (CPSA) from the distribution function to the BET surface area. deBoer and Lippins (88) found that when ink bottle-type pores prevail the CPSA

calculated from desorption isotherms is as much as 30 to 40% greater than the BET surface area.

The data presented in Table VII clearly show the above behavior. The CPSA calculated from MIP data is 350 $m.^2/g$. This surface area is 24% greater than the BET SA of 282 $m.^2/g$. and 37% higher than the CPSA of 257 $m.^2/g$. calculated from the NAI.

A comment here is important when considering the use of pore size distributions for relating the adsorption behavior of polymers from solution onto a porous structure. A polymer molecule must diffuse to the surface region of the adsorbent before being adsorbed. The surface area contained within a pore either of the straight cylindrical or "ink bottle pore type" is available for adsorption only if the polymer molecule can diffuse through the interconnecting canals and apertures which lead into the pore cavity. The distribution function $\underline{D}(\underline{R}_a)$ determined by MIP parallels the above situation. The smallest aperture in a canal leading to a pore cavity is the controlling factor determining the $\underline{P}$ versus $\underline{V}$ intruded curve obtained. However, the surface area that is seen by the polymer macromolecule parallels the nitrogen adsorption isotherm. From these considerations it is apparent that pore entry criteria for rigid spherical macromolecules in solution are probably best established on the pore size $\underline{D}(\underline{R}_a)$ from MIP. On the other hand, available surface area criteria once the polymer macromolecule enters the pore are perhaps more accurate if based on the nitrogen adsorption isotherms. In light of this reasoning a minimum accessible surface area as a function of pore aperture may be calculated using both the MIP and NAI data. The calculation may be performed in the following way. The pore aperture is taken from MIP data. The volume of mercury intruded corresponding to a given pore aperture size and smaller is known from the $\underline{P}$ versus $\underline{V}$ intrusion

curve. The volume intruded in this case strongly reflects the filling of the cavity of an ink bottle-type pore. However, cumulative pore surface area calculations based on the cylindrical capillary model are excessively high since the large volume intruded is mistakenly associated with the small radius of aperture of the pore.

On the other hand, the actual porous volume of a given pore size and smaller is given by nitrogen gas adsorption. The volume of mercury intruded and nitrogen gas condensed for given size pores and smaller are compared. Because ink bottle pores prevail, the volume of mercury intruded is greater than the nitrogen gas condensed corresponding to a given EPD. The volume difference at an EPD for MIP and NAI must be associated with pores having diameters much larger. Applying a minimum surface area model in which the volume difference is associated with the largest pores known present, the minimum accessible surface areas for a rigid spherical molecule may be calculated. Table VIII gives the specific surface area of Porasil A accessible to a rigid molecule assuming that it can diffuse into pores having an EPD of its same size and larger pores. A typical calculation is outlined in Appendix VIII. The main function that Table VIII serves is to evaluate polymer adsorption data discussed later. A few comments are in order about this table. Table VIII predicts that if a molecule of 40 A. can diffuse into a pore having a 40 A. EPD then it has access to 99.6% of the BET surface area determined for Porasil A. It also indicates that 46.2% of the BET surface area is accessible to molecules of 90 A. It is interesting to note that approximately 61% of the total specific surface area is characterized by pore apertures between 60 and 100 A. diameter.

TABLE VIII

SPECIFIC SURFACE AREA OF POROSIL A ACCESSIBLE TO GIVEN SIZE RIGID SPHERE

Rigid Sphere Diameter Equal to Equivalent Pore Aperture, A.	Specific Surface Area Accessible, $m.^2/g.$	%
40	281	99.6
50	268	95.3
60	257	91.3
70	202	71.9
80	169	59.8
90	130	46.2
100	84	29.9
120	56	19.8
140	45	15.8
160	32	11.5
180	26	9.3
200	13	4.6
300	10	3.5

Porasil B

The cumulative volume distributions for Porasil B from MIP and NAI are not directly comparable. They are shown in Fig. 12 and listed in Table XXIII of Appendix IX. Equivalent pore diameters outside the useful range of inspection of each method are presented: EPD > 600 A. for the NAI case, and < 120 A. for the MIP. With this in mind, examination of the total pore volume from the NAI shows only 0.10 cc./g. pore volume for EPD between 14 and 600 A. In contrast, MIP shows a total pore volume of 0.915 for EPD between about 150 and 900 A. The MIP total pore volume in conjunction with the NAI data indicates that a pore volume of 0.815 cc./g. (0.915 - 0.10 = 0.815 cc./g.) is indicative of pore cavities having EPD larger than 600 A. The MIP $\underline{D}(\underline{R}_a)$ shows that the majority of the porous volume is characterized by EPD from 200 to 500 A. with the most frequent pore size being at 265 A.

The MIP volume frequency distributions as a function of log $\underline{P}$ and log EPD are shown in Fig. 14. Porasil B and C distributions are seen to differ greatly from that of Porasil A.

The CPSA calculated from MIP is 103 $m.^2/g.$ compared to 54 $m.^2/g.$ for the NAI. The NAI CPSA compares favorably with the BET surface area of 60 $m.^2/g.$ The MIP CPSA is 88% greater than the BET surface area.

The NAI $\underline{D}(\underline{R}_a)$ shown in Fig. 13 indicates that 20.6% of the pore volume and 62.8% (see Table XXIII, Appendix IX) of the CPSA is associated with EPD < 40 A. This result is not congruent with the findings by other investigators (24, 89). There are two reasonable explanations for the observed result. The Barrett, et al. (55) method of pore analysis is considered reasonably accurate down to about 60 A. EPD. The curvature factor is assigned a constant value over a small pore size range. However, for pores of small diameter the curvature factor changes too rapidly to be assigned a constant value even over a narrow pore size range.

A second possibility, which is consistent with polymer adsorption data presented later, is that the sharp $\underline{D}(\underline{R}_a)$ peak at 22 A. for NAI data for Porasil B corresponds to the condensation of nitrogen about the periphery of the points of contact of two elemental particles that compose the silica beads. Barrer, et al. (90) have presented a mathematical description of this situation of the condensation of nitrogen gas in the toroidal space between touching solid spheres. For a given pair of spheres the toroidal volume condensed increases with sphere size at a given partial pressure. Since the elemental particles are somewhat irregularly shaped as shown in electron micrographs, meaningful calculations cannot be obtained.

Porasil C

The pore surface area and volume distributions for Porasil C determined from the MIP and NAI data are listed in Table XXIV. The differences between the MIP and NAI volume distributions for Porasil C are similar to the differences in the distributions earlier shown for Porasil A. Except for the anomalous

maximum at 22 A. EPD bimodal distributions were obtained by MIP and NAI methods. The shifting of the MIP distribution to smaller EPD as noted for Porasil A is also evident in Fig. 13 for Porasil C. The bimodal shape of the $\underline{D}(\underline{R}_a)$ for NAI data showing a maximum at about 400 and 550 A. EPD suggest that this region may correspond to the bimodal shape of the $\underline{D}(\underline{R}_a)$ determined from MIP data showing maxima at about 150 and 250 A. EPD. In contrast, the distribution functions for Porasil B show no apparent similarities.

Porasil C, like Porasil B, has a high percentage of surface area attributable to pores having EPD < 40 A. The same rationale applied to Porasil B concerning this region of the NAI is thought to also apply here (90).

Comparison of the MIP and NAI total pore volumes corresponding to pores of less than 600 A. EPD indicates that 0.468 cc./g. (0.708 - 0.24 = 0.468 cc./g.) pore volume must be associated with pore cavities larger than 600 A. EPD. The majority of the pore apertures according to the MIP data have EPD between 130 and 340 A.

Figure 14 shows that the volume frequency distribution for Porasil C does not contain appreciable porous volume in the EPD range associated with Porasil A. However, the EPD ranges for Porasil B and C are seen to overlap substantially.

POLYMER ADSORPTION EXPERIMENTS

TIME TO REACH EQUILIBRIUM

The adsorption of polymers from solution is indeed interesting and very complex in nature. Although for practical purposes equilibrium adsorption may occur within a few hours with many systems, a slow upward drift may occur for days or months.

The polyethylenimine-water-silica gel system under consideration at various experimental conditions was found, for all practical purposes, to be at equilibrium adsorption within 36 hours. To ensure the establishment of equilibrium, all adsorption isotherms obtained were taken at 72 hr. and at longer adsorption times as noted. Two sets of data, listed in Table XXVI of Appendix X and shown in Fig. 15 and 16, illustrate that little significant change in adsorption occurs at times longer than 72 hours up to 720 hours.

Figure 15 shows the specific adsorption (Γ_w) of DUPEI[3] onto Porasil A, B, and C from distilled water as a function of the PEI equilibrium concentration (C_e). Negligible adsorption changes occur between adsorption times of 3 and 10 days for all three silica gels. These data indicate that sufficient time was allowed for the system to establish mass equilibrium. Apparently, the penetration of PEI into the porous structure of the silica gels and other possible molecular reshuffling effects are complete after three days.

Figure 16 further supports that negligible adsorption changes occur after three days. Little adsorption changes are shown to occur between 3 and 30 days for the adsorption of F-10[4] PEI onto Porasil B from standard aqueous solvent. These data also suggest that the dissolution and possible precipitation of silica gel does not occur over long adsorption periods to appreciably affect the amount of adsorption.

---

[3]Dialyzed unfractionated polyethylenimine (DUPEI) whole sample has an approximate M_w of 13,100. The original PEI sample was dialyzed 16 hr. against constantly fresh distilled water. Dialysis studies have shown that PEI below about 8000 mol.wt. diffuses readily through the cellulose acetate dialysis membrane. A weight average molecular weight was calculated from the concentration *versus* elution volume and elution volume *versus* molecular weight curves previously shown.

[4]Molecular weight estimated from the elution volume-molecular weight relation established experimentally.

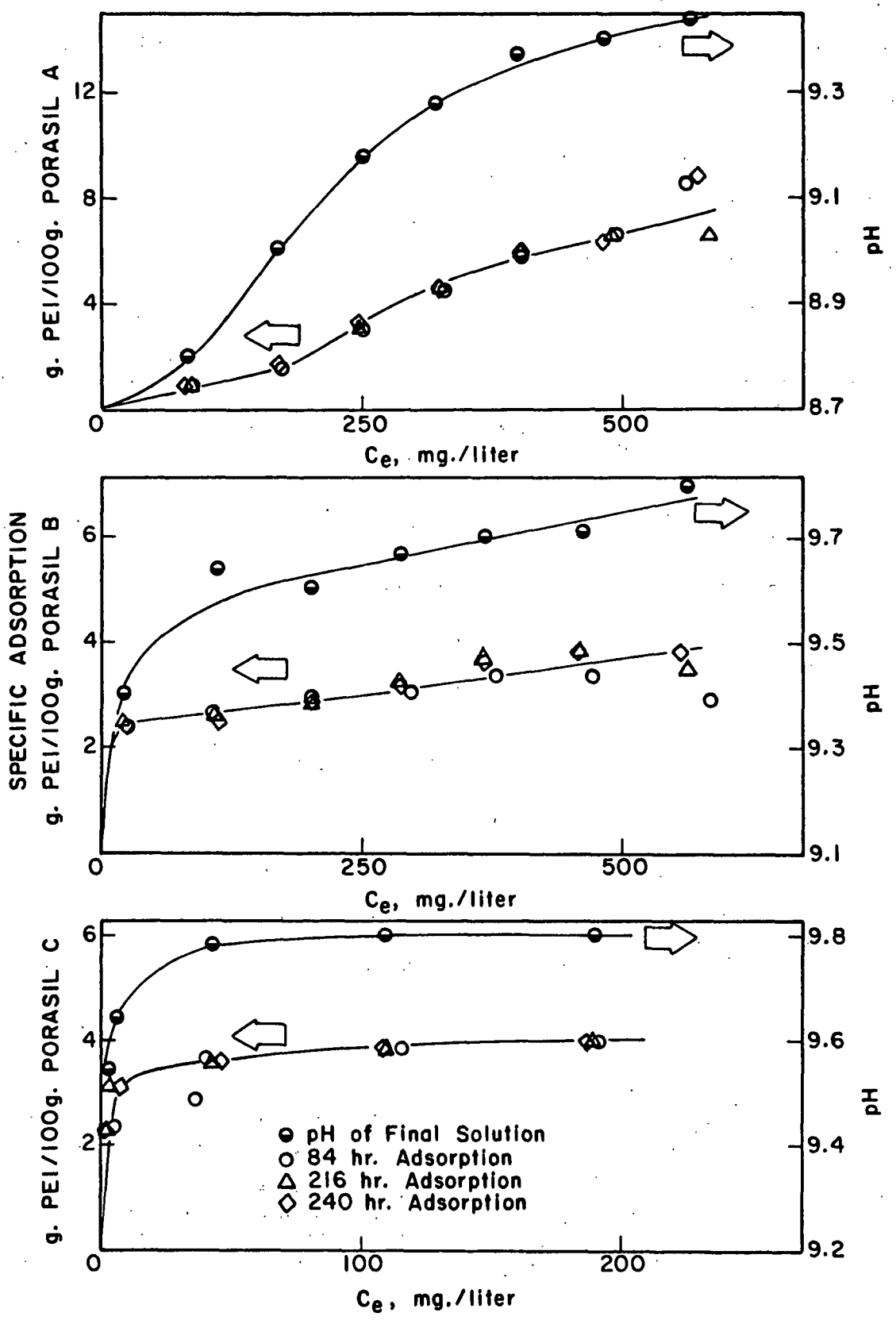

Figure 15. Equilibrium Adsorption Isotherm for DUPEI from Water

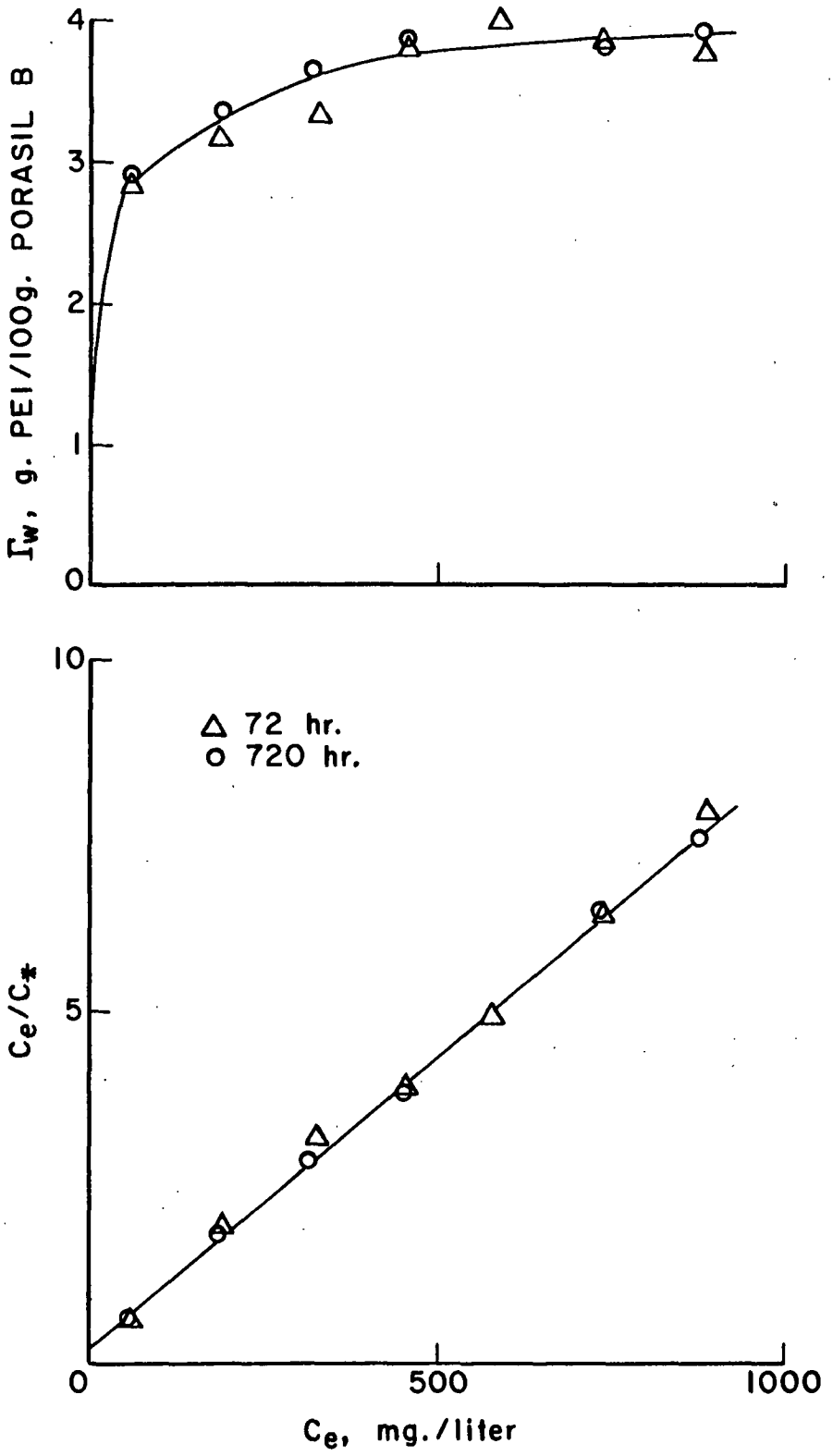

Figure 16. Equilibrium Isotherm for F-10 ($\underline{M}_w$ = 1,500) Adsorbed on Porasil B from 0.109$\underline{N}$ NaCl Containing 4.25 x $10^{-5}\underline{N}$ NaOH

EFFECT OF pH

The effect of pH on the adsorption of PEI on silica gel was investigated over a range from pH 4.3 to 13.1. The initial adsorption solution concentration was 107.4 mg./liter. One hundred milligrams of Porasil A were present in 40.0 ml. of adsorption solution. DUPEI was used as the adsorbate. The results are shown in Fig. 17. The data are given in Table XXVII of Appendix X.

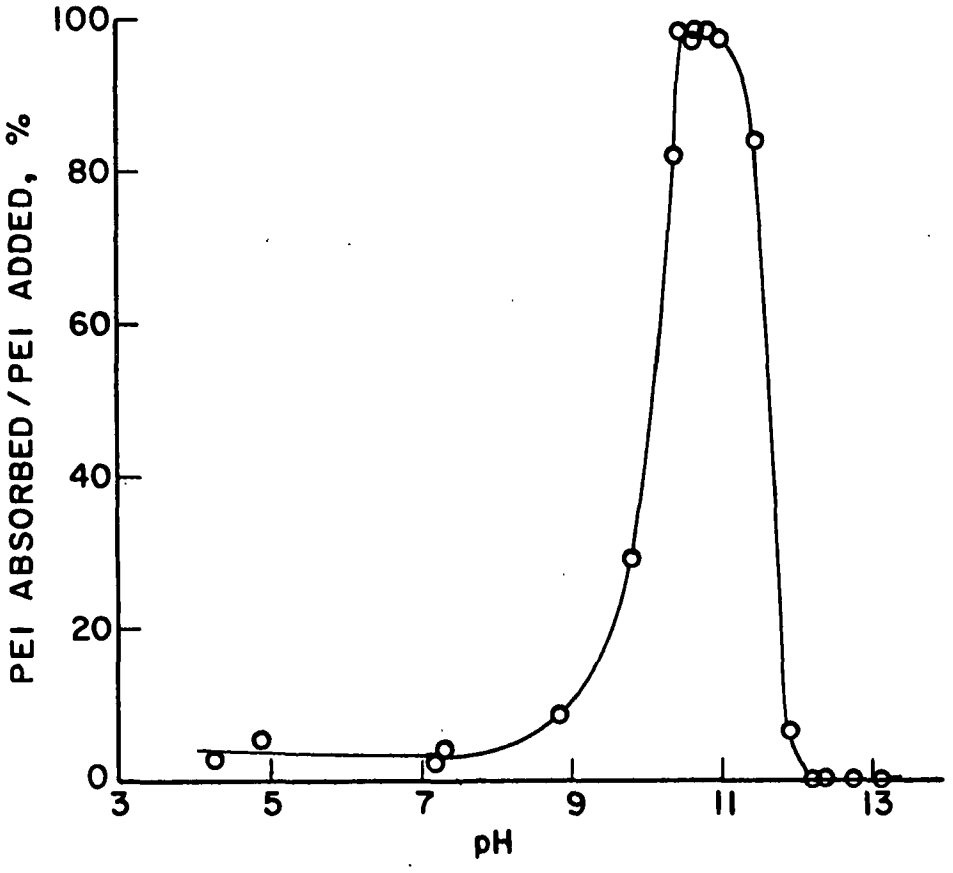

Figure 17. Effect of pH on Adsorption — DUPEI Adsorption on Porasil A from Water

Maximum adsorption occurs from pH 10.5 to 11.0 where the PEI molecule has a small size and low charge. Its small size allows it to diffuse into the small porous structure. The low charge minimizes repulsive forces between adsorbed PEI molecules and those approaching the surface.

Little adsorption occurs from pH 4.3 to 8.0 where molecular exclusion and repulsive forces between adsorbed PEI molecules may predominate. The sharp adsorption increase from pH 9.5 to 10.5 probably results from a decrease in repulsive forces between PEI molecules and a decrease in molecular exclusion. The decreased adsorption above pH 11.5 may result because silica gel is dissolving or the charge of the PEI molecule is anionic.

The pH of maximum adsorption parallels the results reported by Kindler (1) and Allan and Reif (3) for the adsorption of PEI on cellulose fibers. This result suggests that adsorption of PEI on silica gel may be very similar to the nature of the adsorption of PEI on cellulose fibers. The ionization constant for cellulose is estimated at two orders of magnitude less than that taken for silica gel, i.e., silica acid. Thus, at the same pH and molar concentration of ionizable cellulose hydroxyl groups and silanol groups on the silica gel, about two orders of magnitude more anionic sites are present on silica gel than cellulose. The characteristic maximum adsorption of the PEI-cellulose or silica gel system apparently does not depend on the number of anionic sites present on the absorbent. The point of maximum adsorption reflects a condition of the PEI molecule under which it is easily adsorbed. Light scattering, mobility, and hydrogen ion association data presented earlier suggest that the PEI molecule has nearly a zero charge at the pH corresponding to maximum adsorption. This suggests that if the adsorption is purely electrostatic involving the PEI cation and an anionic ionized silanol group, then very few protonated amine sites are

required to initiate attachment of the PEI molecule on the silica surface. However, it may be expected that once an acid-base reaction between a protonated amino group and the conjugate base of the silanol group takes place, Van der Waals forces become operative. The small size of the PEI macromolecule and low charge would allow it to diffuse to the surface of silica gel rapidly and permit its access to the internal pore structure. This is reasonable since the anionic sites on silica gel increase with pH. The small size and the low charge of the PEI molecule should allow it to assume a close packed arrangement on the surface of silica gel.

At lower pH the PEI molecule has a considerable charge which leads to an increased molecular size and increased lateral interactions between adjacently adsorbed PEI molecules. These factors together with the lower surface charge of silica gel and inaccessible porous surface area probably contribute to the lower adsorption observed.

EFFECT OF CONCENTRATION

Since PEI is a polybase, the pH of the resulting equilibrium adsorption solution is controlled in part by the PEI equilibrium concentration when other H^+ or OH^- producing chemicals are not added. Initially, sodium hydroxide was added to adsorption runs in varying amounts so the resulting pH at equilibrium adsorption would be in the maximum adsorption region between about pH 10.5 and 11.0. In general, decreasing amounts of sodium hydroxide were added with increasing initial PEI concentration. The resulting adsorption solutions contained from 5×10^{-3} to 1.4×10^{-2} N NaOH. The equilibrium adsorption isotherm (EAI) for DUPEI adsorbed on Porasil C is shown in Fig. 18. The specific adsorption (Γ_w) g. PEI per 100 g. of Porasil C as a function of the equilibrium concentration (C_e) is given at the top of the figure. The data are given in

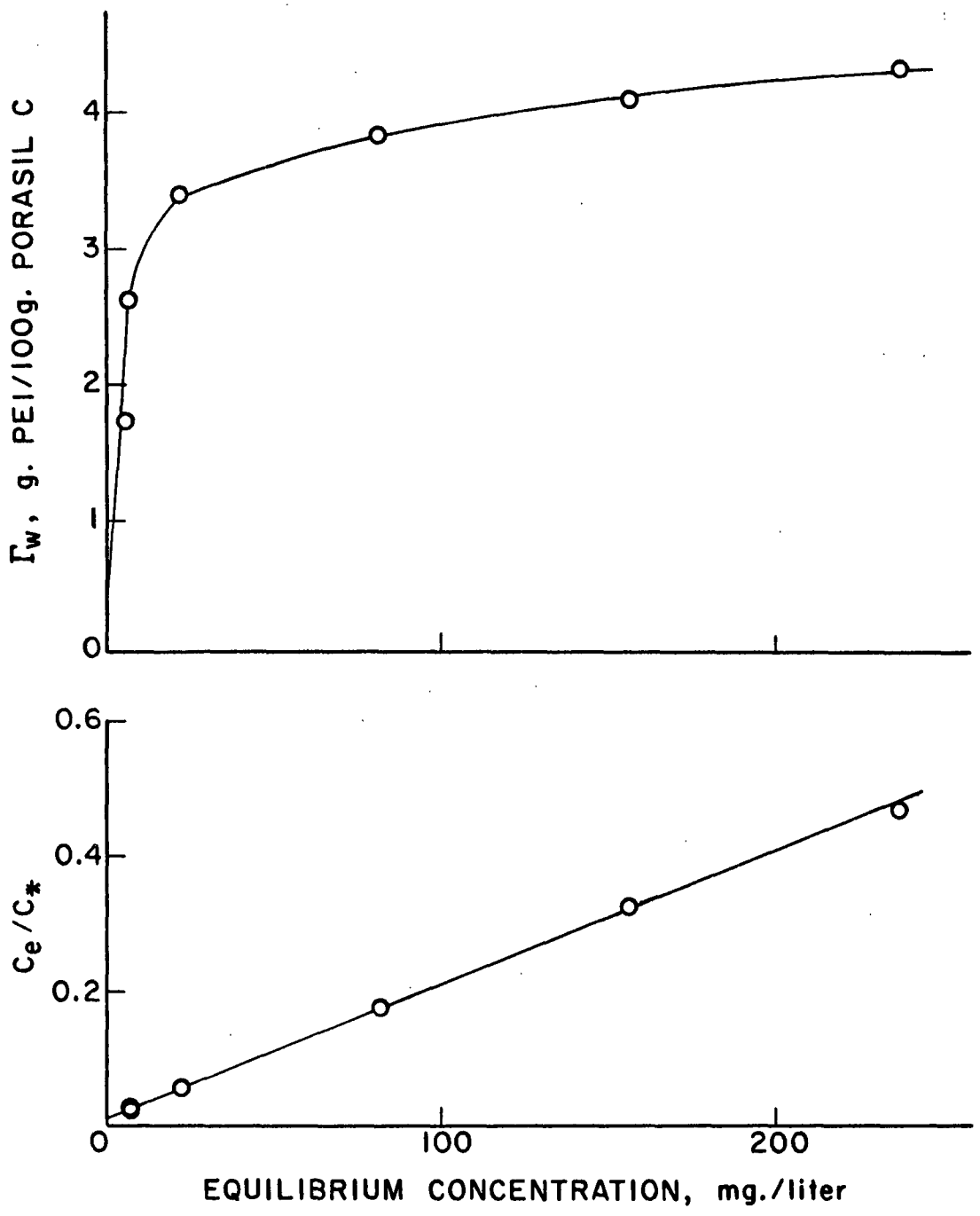

Figure 18. Equilibrium Adsorption Isotherm-DUPEI Adsorption on Porasil C Sodium Hydroxide Added to Give Final pH of ≅ 10.8

Table XXVIII of Appendix X. The specific adsorption increases rapidly with concentration initially but asymptotically approaches a limiting adsorption level. This type isotherm is commonly referred to as the Langmuir type (91). Its form was originally derived for the adsorption of gases on solids. The same equation may be derived for the adsorption of polymers from solution. The assumptions made in the development are often viewed with reservation as to whether the model is really applicable to polymer adsorption. Silberberg (9) has shown theoretically that the Langmuir form should fit most polymer adsorption systems. The basic assumptions made are that the adsorbent surface is homogeneous having a given number of adsorption sites and that the adsorbed species interact only with a site and not with each other. Adsorption is limited to a monolayer. The Langmuir form is given below.

$$\Gamma = K \Gamma_M C_e/(1 + KC_e) \qquad (10)$$

where Γ is the specific adsorption at equilibrium concentration (C_e), K is the Langmuir constant, and Γ_M is the specific adsorption at surface saturation. Since adsorption isotherms are usually constructed from data on the change in bulk solution concentration, the Langmuir form is easily expressed in terms of solution concentration as follows:

$$\frac{C_e}{C_*} = \frac{1}{C_m K} + \frac{C_e}{C_m} \qquad (11)$$

where C_* is the loss in solution concentration at C_e and C_m is the change in solution concentration when the adsorbent is saturated with adsorbate. If the Langmuir equation describes the adsorption behavior then a plot of C_e/C_* versus C_e is linear with slope $1/C_m$ and intercept $1/C_m K$. The specific adsorption at surface saturation is then calculated directly from the reciprocal of the slope. The Langmuir constant (K), which reflects the affinity or intensity of adsorptions, is given by the slope divided by the intercept.

For the adsorption data being considered, compliance to the Langmuir form was found to be very good. The plot of C_e/C_* versus C_e is given at the bottom of Fig. 18. The Langmuir constant and Γ_M are 0.152 liter/mg. and 4.2 g. PEI/100 g. Porasil C, respectively.

EFFECT OF PORE SIZE

Equilibrium adsorption isotherms were established for DUPEI on Porasil A, B, and C. One set of experiments was done with addition of NaOH (5×10^{-3} to 1.4×10^{-2}N) to control pH to the region where maximum adsorption occurs. Another set of experiments was conducted in which the resulting equilibrium solution pH was controlled by the amount of PEI added and adsorbed and also silica gel present. The equilibrium adsorption isotherms (EAI) for both sets of data are shown in Fig. 19, 20, and 21. The data are given in Tables XXVI and XXVIII of Appendix X. The final pH of the solutions at equilibrium concentrations (C_e) for a given set of data are shown as pH ranges on the figures and listed separately in data tables.

The EAI for Porasil A, B, and C when NaOH is added to obtain maximum adsorption are described by the Langmuir form. Linear plots of C_e/C_* versus C_e were obtained in the three cases as shown at the bottom of Fig. 19, 20, and 21.

The EAI for Porasil B and C when the final pH is determined by the amount of PEI and silica gel present comply to the simple Langmuir form. The EAI for Porasil C, with or without NaOH added to control pH, are about the same. However, in the case of Porasil B, the specific adsorption without NaOH added is significantly less than the Γ_w at the maximum adsorption pH.

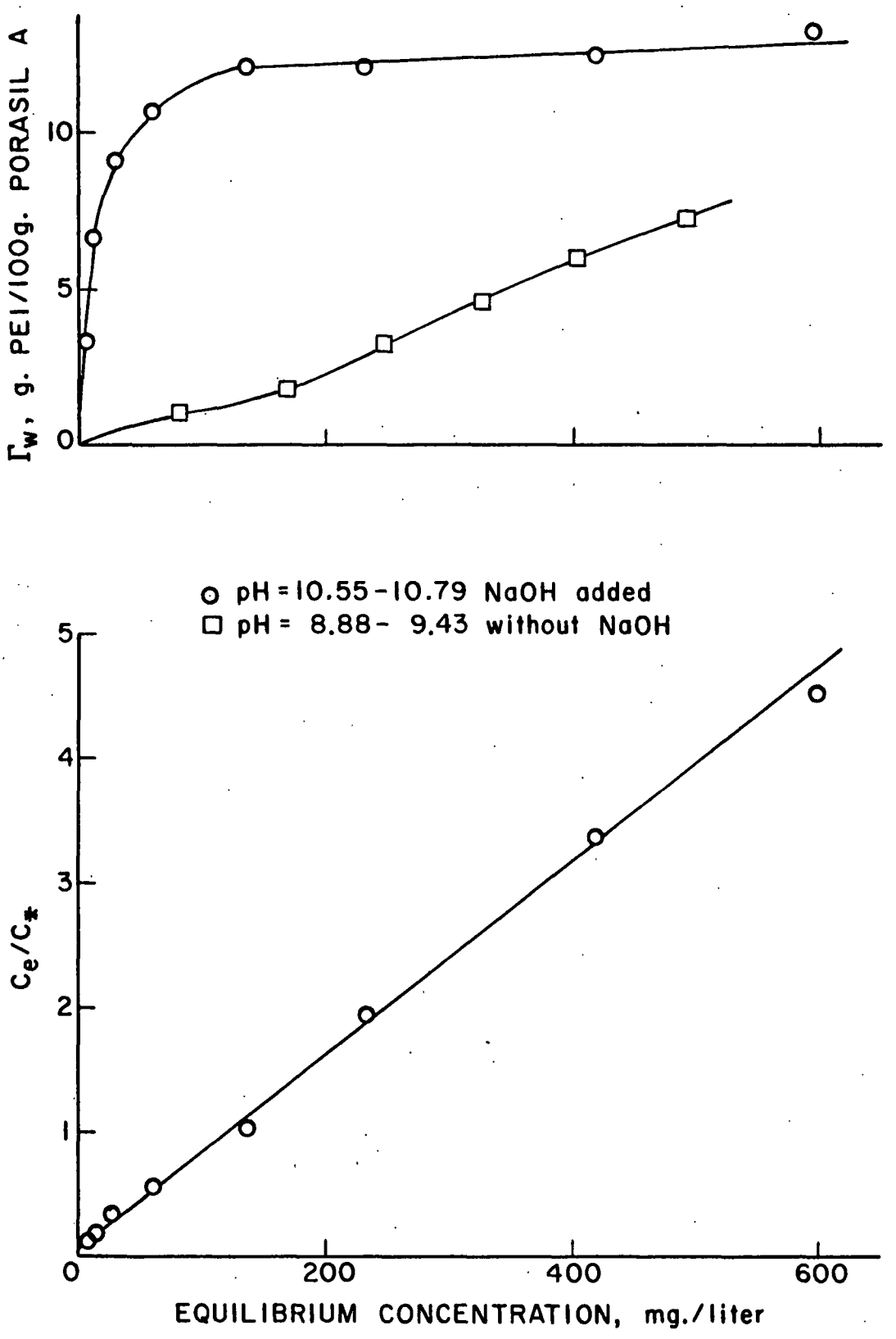

Figure 19. Equilibrium Adsorption Isotherms-DUPEI Adsorption on Porasil A from Water With and Without NaOH Added

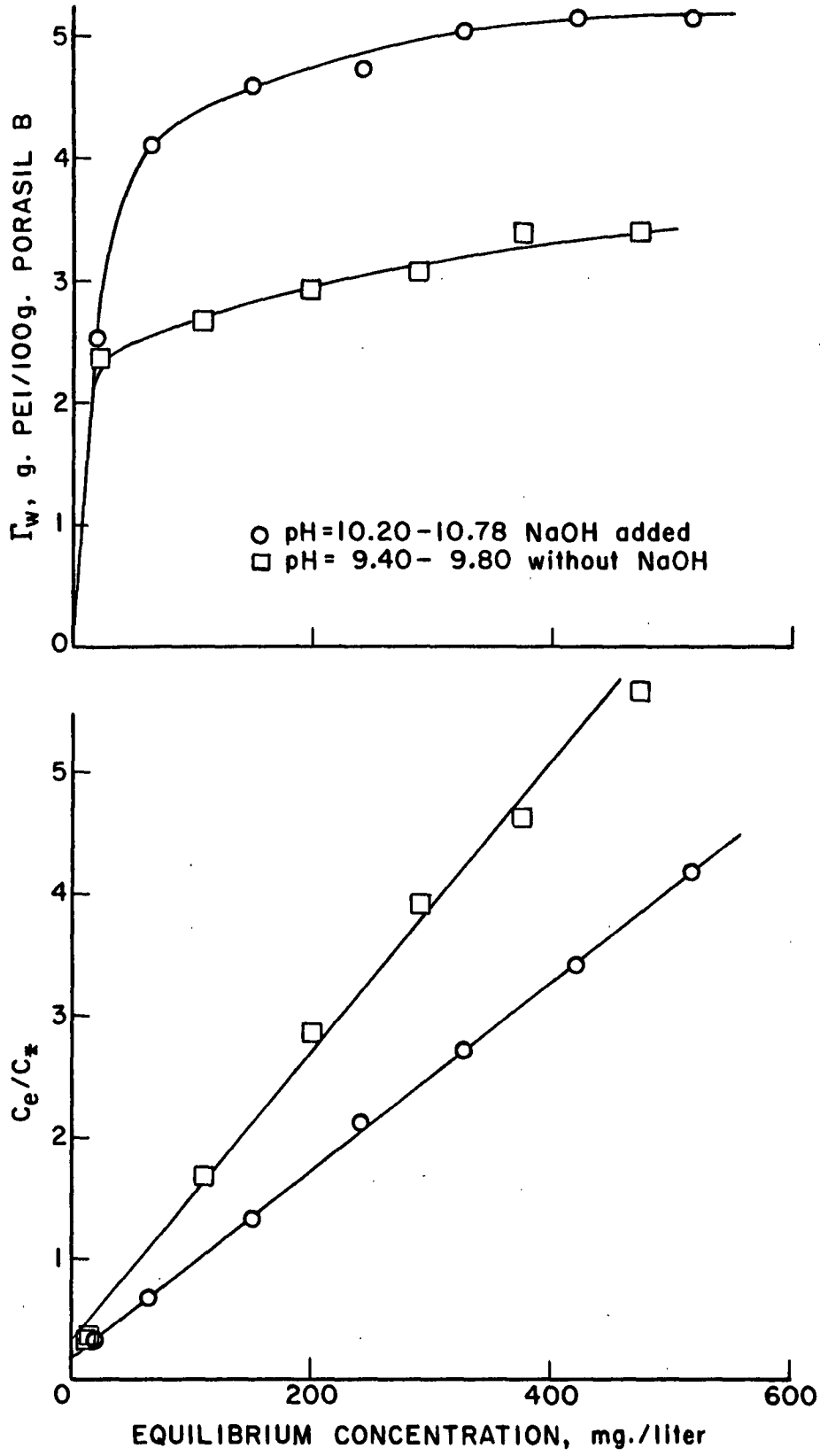

Figure 20. Equilibrium Adsorption Isotherms-DUPEI Adsorption on Porasil B from Water With and Without NaOH Added

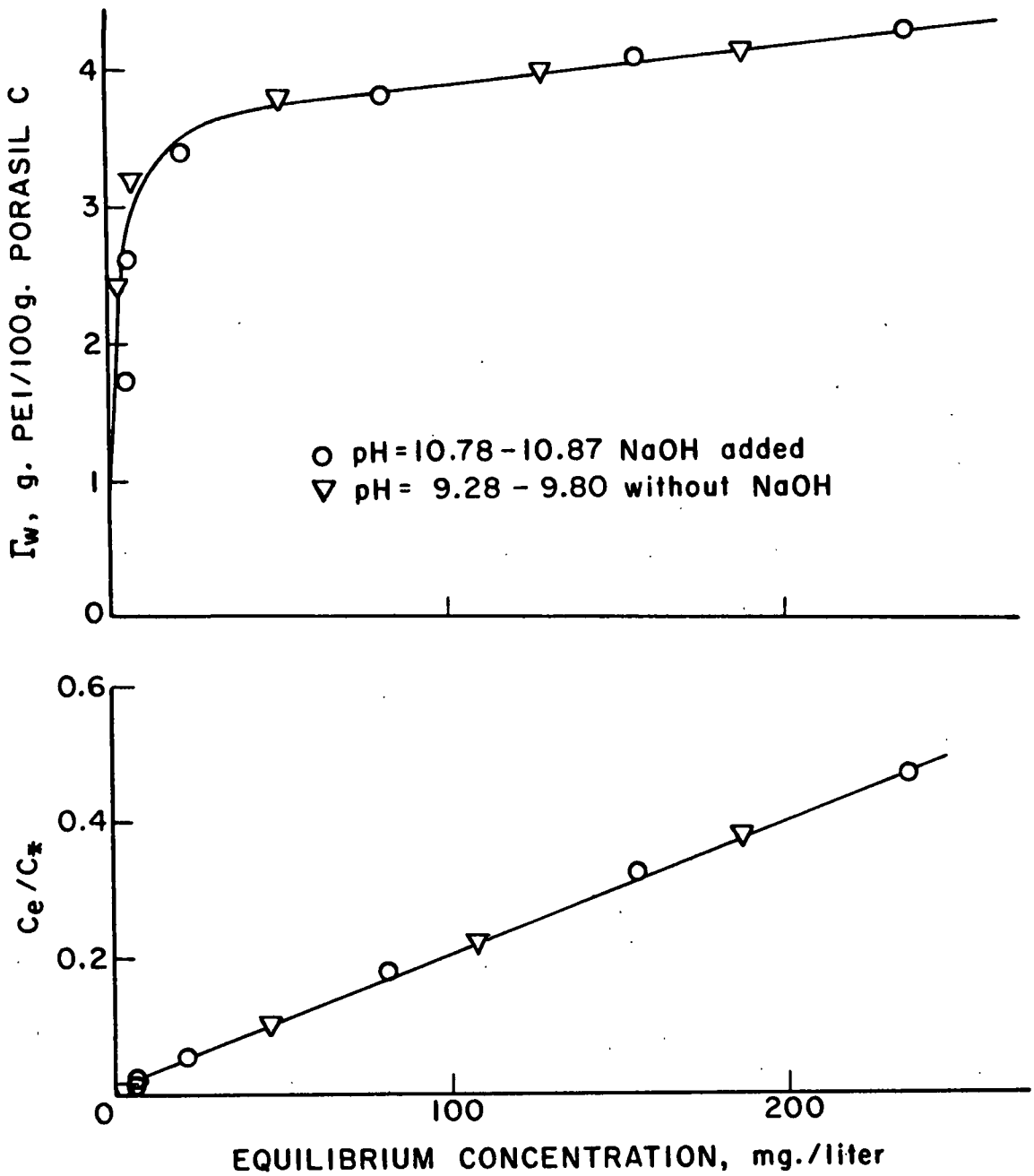

Figure 21. Equilibrium Adsorption Isotherms-DUPEI Adsorption on Porasil C from Water With and Without NaOH Added

The EAI for Porasil A when the pH is not controlled by addition of base does not show compliance with the Langmuir form. It does, however, fit the Freundlich adsorption isotherm equation (92). The Freundlich form is obtained from the Langmuir form by assuming that the adsorbent surface is heterogeneous and that the heat of adsorption has an exponential form instead of being constant. Unlike the Langmuir isotherm, the Freundlich isotherm shows no saturation point for adsorption of species from dilute solution. The agreement of experimental data with the Freundlich form is sometimes used as an indication of surface heterogeneity (72). However, little justification is available to confirm this assertion. Figure 22 gives a plot of log C_* versus log C_e. The nearly linear plot suggests the Freundlich isotherm fits the data.

Porasil A, B, and C are chemically the same. Feitl and Smolkova (93) have shown that the number of hydroxyl groups per unit surface area is constant and does not vary with increase in the total surface area with the various Porasil types. Since the adsorption experiments were done under similar conditions, the differences in the EAI for Porasil A, B, and C apparently result from physical differences in the porous silica gels.

Table IX is helpful in examining the adsorption behavior. The specific adsorption on a unit surface area basis (Γ_A) at C_e values of 100 and 200 mg./liter and the final solution pH are given. Table IX was constructed from the data in Fig. 16. It is interesting to note that the equilibrium adsorption isotherms for Porasil A, B, and C are described qualitatively by the shape of a plot of the final solution pH versus C_e.

Table IX shows that at equal values of C_e the pH of the resulting solution is significantly lower with Porasil A adsorbent than with either Porasil B or C. At an equilibrium concentration of 200 mg./liter Porasil B has approximately

7 times the amount PEI adsorbed per unit surface area compared to Porasil A. Porasil C has approximately 8 times the amount adsorbed per unit surface area compared to Porasil A.

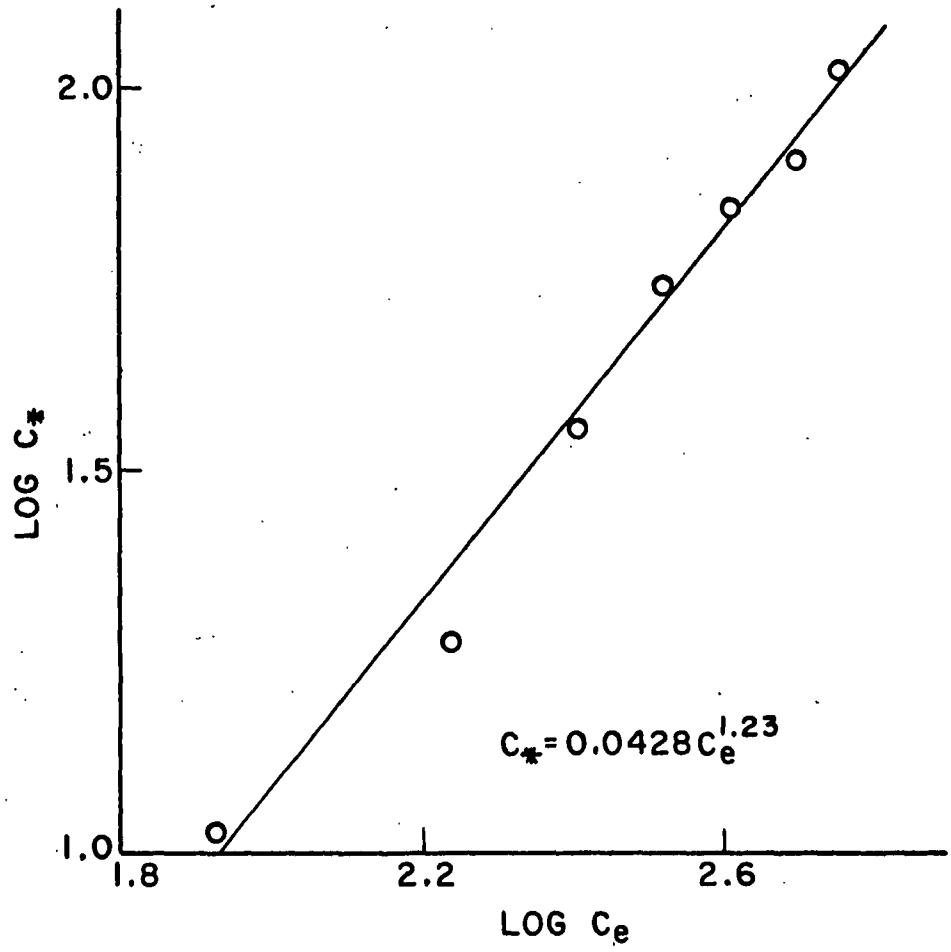

Figure 22. Freundlich Isotherm for Adsorption of DUPEI on Porasil A from Water Without NaOH Added

Using a figure of 4.6 OH^-/100 $A.^2$ (19, 20) of silica gel surface area, the slurry concentrations of surface hydroxyl groups for adsorption experiments using Porasil A, B, and C are 3.4, 1.4, and 6.6 meq./liter or a ratio of approximately 2:1:4, respectively. Figure 16 shows that the pH of the resulting

TABLE IX

SPECIFIC ADSORPTION OF PEI PER UNIT SURFACE AREA

C_e, mg./liter	Porasil	Γ_A, mg. PEI/m.^{2} [a]	pH
100	A	0.03	8.8
100	B	0.42	9.6
100	C	0.54	9.8
200	A	0.07	9.1
200	B	0.48	9.6
200	C	0.58	9.8

[a]The BET surface areas were used in the calculations.

equilibrium adsorption solution is directly related to C_e values. However, the absolute value of the pH is also influenced by the amount of OH^- groups on silica gel present and amount of PEI adsorbed. Table IX also illustrates this point. At an C_e of 200 mg./liter the resulting solution pH values of 9.1, 9.6, and 9.8 were obtained for Porasil A, B, and C, respectively. The lower final solution pH for Porasil A probably results from the ionization of the H ion from the silanol groups coupled with the inability of PEI to enter most of the pores present in Porasil A. This behavior is apparently true since twice the amount of silanol groups are present in adsorption experiments on Porasil C which at a given equilibrium PEI concentration has the highest pH. This result suggests that adsorption of PEI strongly reduces the tendency of the ionization of surface hydroxyl groups or that a substantial number of surface hydroxyl groups participate in electrostatic bonds with PEI making them unavailable as possible H ion producing groups contributing to the bulk solution pH. It is interesting to note that the adsorption experiment with Porasil B contained the lowest concentration of surface hydroxyl groups and has only a slightly lower Γ_A compared to Porasil C. This further supports the observation that the number of H ions ionized and contributing to the final solution pH is largely determined

by the PEI adsorbed. The adsorption is greatly affected by the accessibility of pores in the adsorbent to the adsorbate molecule. Addition of NaOH to control pH to the point at which a maximum adsorption occurs increases the Γ_A for Porasil A up to 0.46 mg./m.^{2} This is of the same order of magnitude as the Γ_A of Porasil C at 0.58 mg. PEI/m.^{2} However, it still indicates molecular exclusion is occurring even under these conditions with Porasil A.

The fact that the maximum adsorption on cellulose and porous silica gel occurs at the same pH (approximately pH 10.8) rules out the possibility that ionization of surface hydroxyl groups is the controlling factor. The dissociation constant for H ion of the silanol groups is estimated at two orders of magnitude greater than for cellulose.

An explanation suggesting that the maximum adsorption of PEI on porous adsorbents occurs as a result of the small molecular size of the PEI, which allows it to penetrate into the smaller pores of the adsorbent is favored. Since the adsorption of PEI on Porasil C, with or without NaOH added, is approximately the same, molecular exclusion of the PEI molecule from the pores present in Porasil C apparently is not influencing adsorption. On the other hand, molecular exclusion apparently plays a dominant role in the adsorption of PEI on Porasil A and Porasil B when NaOH is not added. This is easily seen by the very low Γ_A for Porasil A compared with Porasil C and the slightly lower Γ_A found for Porasil B.

It should be noted that the lower pH of the equilibrium adsorption solution for Porasil A and B should also contribute to molecular exclusion since the PEI molecule expands with decrease in pH.

EFFECT OF IONIC STRENGTH

The effect of ionic strength on adsorption was investigated with respect to polyelectrolyte concentration, pH, pore size, and molecular weight. The specific adsorption of DUPEI on Porasil A as a function of PEI concentration was determined at three ionic strengths by addition of 0.0, 0.054, and 0.109N NaCl in the pH region of maximum adsorption. The specific adsorption of F-7 on Porasil A, B, and C as a function of ionic strength was also investigated at pH values controlled by the amount of silica gel and PEI concentration at adsorption equilibrium.

The EAI obtained for DUPEI at three ionic strengths are shown in Fig. 23. The data points are given in Tables XXVIII and XXIX in Appendix X. The final pH of the adsorption solutions are listed as ranges for a given set of data on Fig. 23 and are listed separately in Tables XXVIII and XXIX. Agreement with the Langmuir form is apparent at all ionic strength levels as clearly shown by the linear C_e/C_* versus C_e plots at the bottom of Fig. 23. The Γ_A and Langmuir constants are shown in Table X. These values were calculated based on the method of least squares fit of the data.

TABLE X

SPECIFIC ADSORPTION AND LANGMUIR CONSTANTS FOR DUPEI ADSORBED ONTO PORASIL A

NaCl, N	Γ_A, mg. PEI/m.^{2a}	$K \times 10^2$ liter/mg.
0.000	0.473	6.25
0.054	0.516	4.24
0.109	0.521	2.89

[a]The BET SA from NAI was used as the surface area.

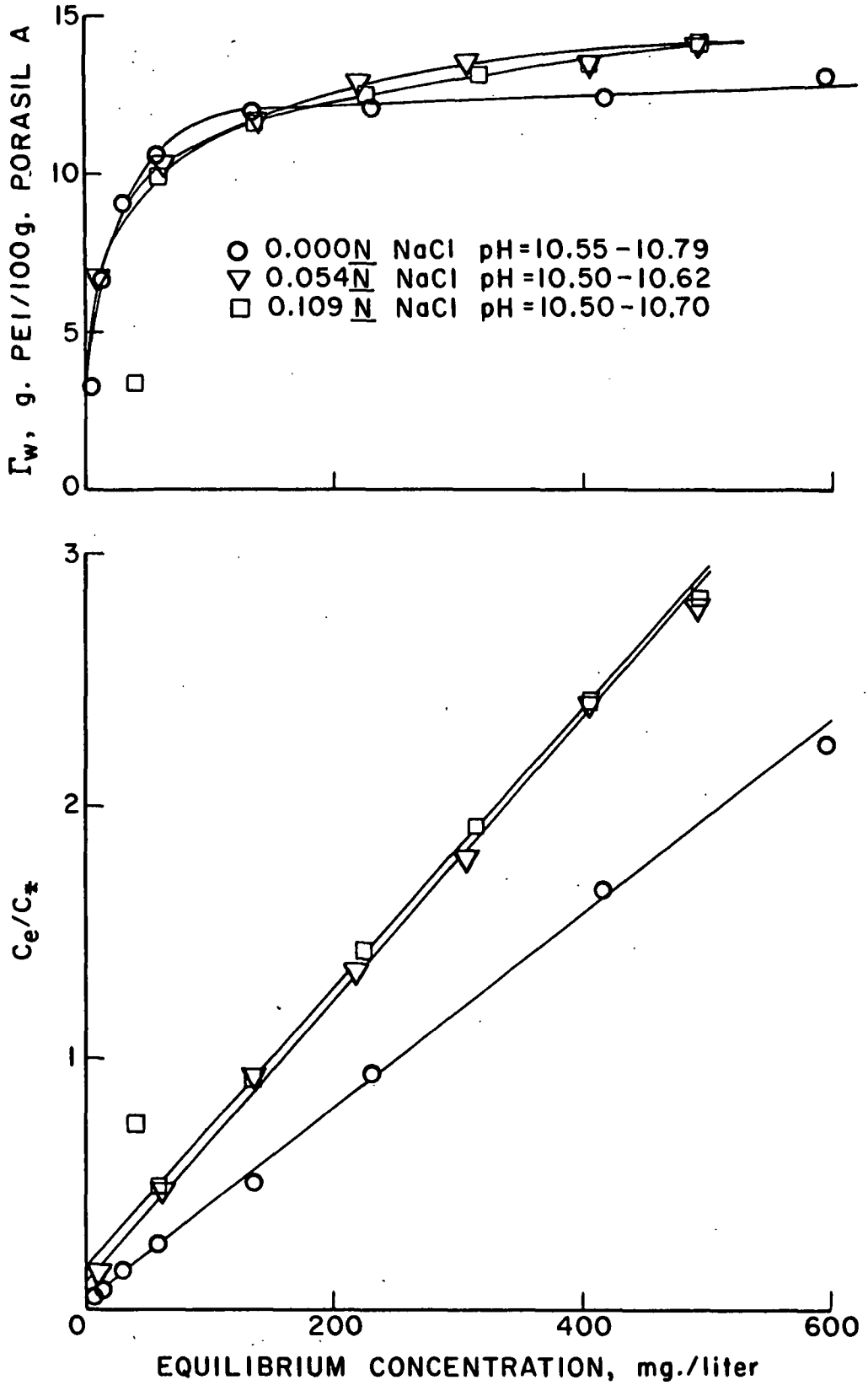

Figure 23. Equilibrium Adsorption Isotherms — Effect of Ionic Strength, NaOH Added

The effect of ionic strength with NaOH added to control pH to the point of maximum adsorption is significant between the addition levels of 0.0N NaCl and 0.054N NaCl. The Γ_A increased about 9% when 0.054N NaCl was present; however, negligible increase occurred when the NaCl concentration was doubled.

The Langmuir constant, which is often referred to as a measure of the intensity of adsorption, decreases with increased ionic strength. The simple electrolyte apparently decreases the intensity of electrostatic interaction between cationic PEI and anionic silica gel.

Configurational changes are generally noted for polyelectrolytes when the ionic strength is increased. In general, viscosity and light-scattering measurements indicate that the molecular size of polyelectrolytes decreases rapidly with increase in ionic strength at extremely low ionic strength levels. At higher ionic strengths less molecular size reduction is noted. This effect is generally found to be smaller with branched and cross-linked polyelectrolytes compared with linear polyelectrolytes (50, 51, 94). At a given degree of ionization addition of simple electrolyte is thought to decrease the intra- and intermolecular repulsive forces.

For the Langmuir model, polyelectrolyte adsorption would be expected to increase as the ionic strength is increased. The reduced molecular size and decreased intermolecular interactions facilitate adsorption of an increased number of molecules per unit surface area. From viscosity data it is well established that intermolecular and a portion of the intramolecular repulsive forces are easily suppressed with low concentrations of added simple electrolytes. However, intramolecular repulsive forces are found to cause considerable molecular expansion even at 0.8N NaCl for the moderately charged linear polyelectrolyte,

polymethacrylic acid (95). It is highly likely that the 9% increase in Γ_A from 0.0 to 0.054N NaCl addition levels results from the decreased molecular size and intermolecular forces between PEI molecules.

There are also two other possible explanations for the adsorption behavior, the "salting out effect" and the decrease in the double layer thickness on the porous surface of silica gel. As a general rule, organic molecules, polymers, and polyelectrolytes are adsorbed to a greater extent from poor solvents than from good solvents (96-98). When simple electrolyte is added to PEI solutions it requires water of hydration. Less solvent is available to the PEI molecule to maintain its degree of hydration. This in turn facilitates increased adsorption. This behavior has also been shown by Greene (99) for another polyelectrolyte. The second consideration will be discussed later.

Since a major effect of adsorption on Porasil A was noted earlier with NaOH present, adsorption runs without NaOH addition were done on Porasil A, B, and C at constant initial PEI concentration to evaluate the effect of pore size in conjunction with ionic strength changes. Polyethylenimine F-7 having a M_w of 5350 and M_w/M_n value of 1.01 was used in adsorption runs at 194 mg./liter. The ionic strength was varied using NaCl concentrations between 6.85×10^{-3}N and 0.214N. The specific adsorption as a function of NaCl concentration is given at the top of Fig. 24 for Porasil A, B, and C. The data are shown in Table XXX of Appendix X.

The Γ_w on Porasil B and C increases only slightly with increase in ionic strength. A pronounced effect, however, occurs for Porasil A. As the ionic strength increases the Γ_w increases rapidly at a declining rate. This behavior apparently reflects the change in the effective size of the PEI molecule in solution relative to the pores characteristic of Porasil A.

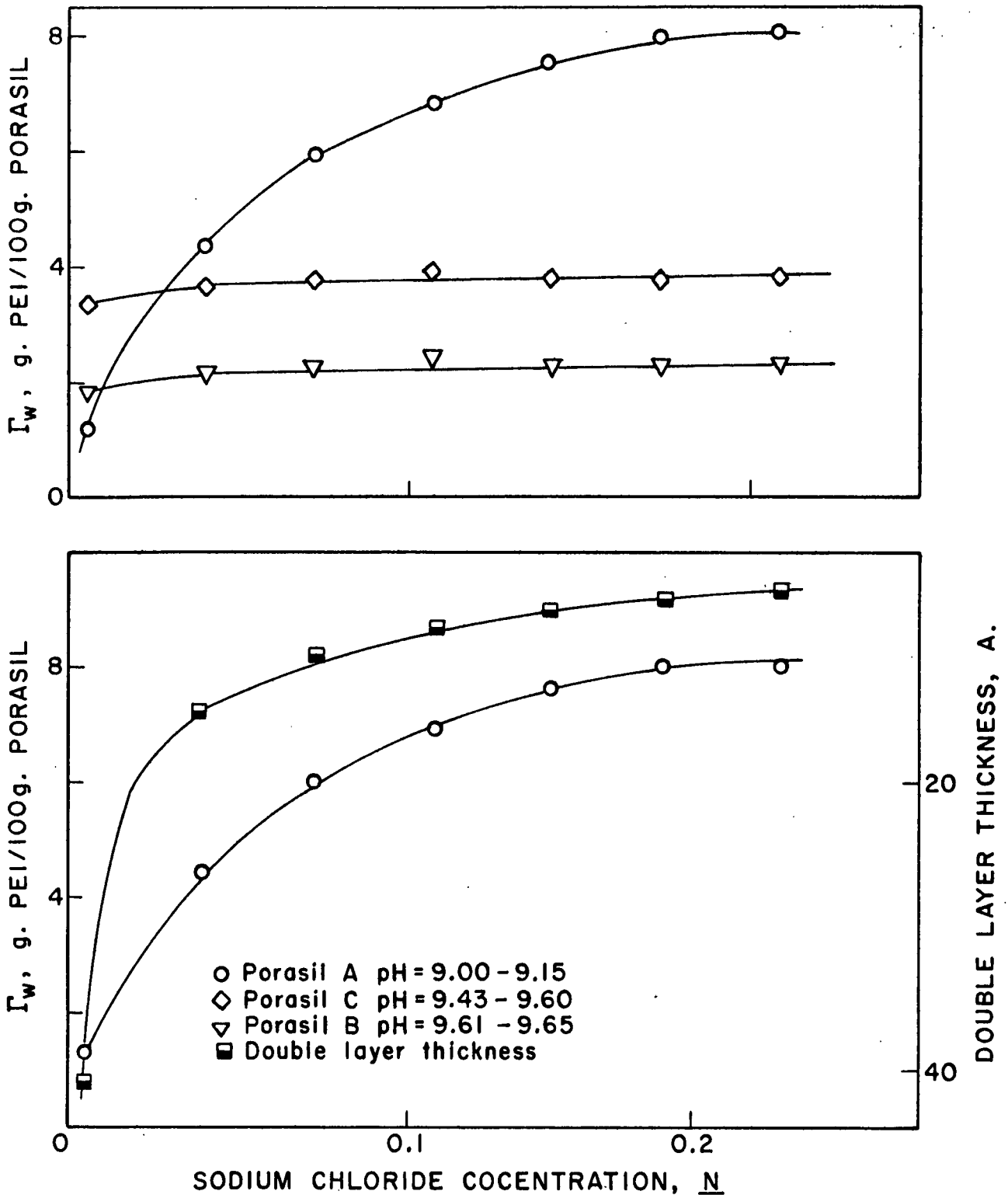

Figure 24. Equilibrium Adsorption Isotherms — F-7 ($\underline{M}_w$ = 5,350) Adsorption on Porasil A, B, and C as a Function of Ionic Strength

The slight increase in adsorption with increase in ionic strength for Porasil B and C probably reflects the slight decrease in molecular size and decreased interaction between adjacently adsorbed PEI molecules. The "salting out" effect is discounted since only a slight adsorption increase occurs on Porasil B and C compared to Porasil A. The large increase in the adsorption of F-7 on Porasil A apparently is adequately explained by the decrease in the molecular size and intermolecular interactions of the PEI molecules. However, it is interesting to note the close correlation between the increase in the $\Gamma_{\underline{w}}$ on Porasil A and the calculated double layer thickness extending from the silica gel surface as shown at the bottom of Fig. 24. This calculation is based on the simplest qualitative treatment of the diffuse part of the double layer given by Gouy (100) and Chapman (101).

The electric double layer holds an important place in the field of physical chemistry. The interaction of electric double layers is used to explain colloidal stability as well as many other phenomena. It is of interest to qualitatively apply the concept to evaluate the space potential and counterion and coion distributions in the central volume element of a small capillary pore with an equal volume element of solvent extending from a flat surface.

In the absence of added simple electrolyte the double layer thickness extends a considerable distance from the solid surface. For the parallel plate model the double layer thickness is approximately equal to the reciprocal of the Debye length or the distance from the surface at which the potential falls by an exponential factor. For an uni-univalent electrolyte the double layer thickness is about 100 A. for a $10^{-3}\underline{M}$ solution and about 10 A. for a $10^{-1}\underline{M}$ solution at 25°C. It may be reasoned that at low ionic strength the central volume element of small pores (EPD $\leq$ 100 A.) will have a considerably higher

potential than a volume element at a given distance from a flat surface due to the large surface area charge to volume element ratio in the pore. This would enhance the attraction of counterions. For the system under consideration, the Na ion concentration in the central volume element of a pore by the above appraisal should be higher the smaller the pore. Since Na ions are water structure promoting, a greater ordering of water structure should prevail within the smaller pores. At low ionic strength the potential and counterion concentration differences between equal volume elements of small pores and a flat surface are expected to be very great. However, as the ionic strength is increased and the double layer moves closer to the surface the differences become less. This effect, in addition to the smaller PEI molecular size, may account for the large increase in adsorption on Porasil A with increase in ionic strength.

EFFECT OF MOLECULAR WEIGHT

The effect of molecular weight on adsorption of PEI on silica gel was investigated under various experimental conditions. Equilibrium adsorption isotherms were obtained on Porasil A and C using Fractions 1, 3, 5, 7, and 9 and on F-4 only using Porasil A. The adsorption runs were done in standard aqueous solvent.

Porasil A was used as a representative adsorbent which contains a considerable porous volume characterized by EPD of approximately the same diameter as PEI of 20,000 mol. wt. On the other hand, Porasil C was picked as representative of adsorbent having most of its porous volume with pore apertures much larger than the adsorbing molecule.

The EAI for the adsorption of PEI fractions on Porasil A and C are shown in Fig. 25 and 26, respectively. The resulting solution pH at the various

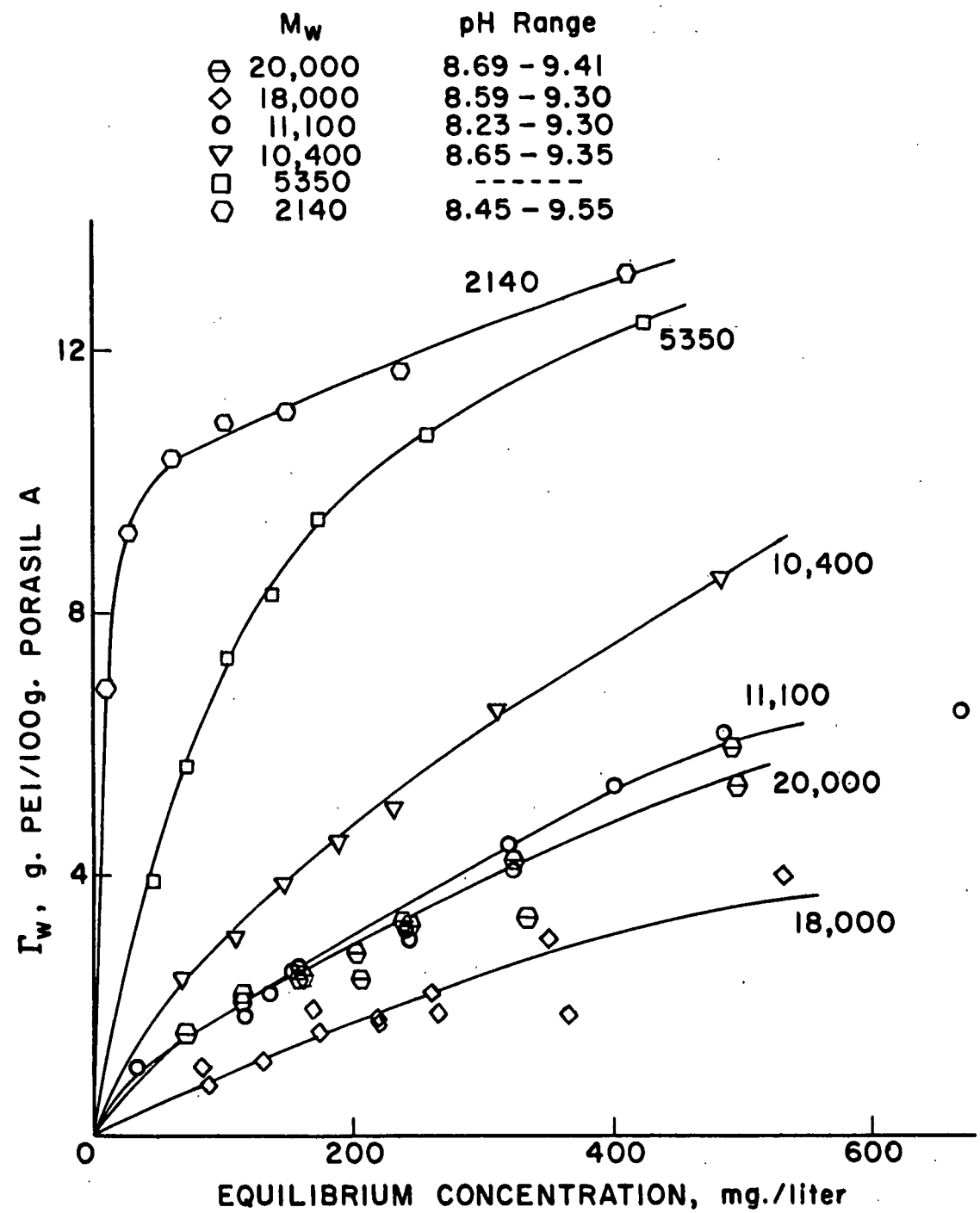

Figure 25. Equilibrium Adsorption Isotherms — Effect of Molecular Weight Adsorption from Aqueous 0.109N NaCl Containing 4.25×10^{-5}N NaOH on Porasil A

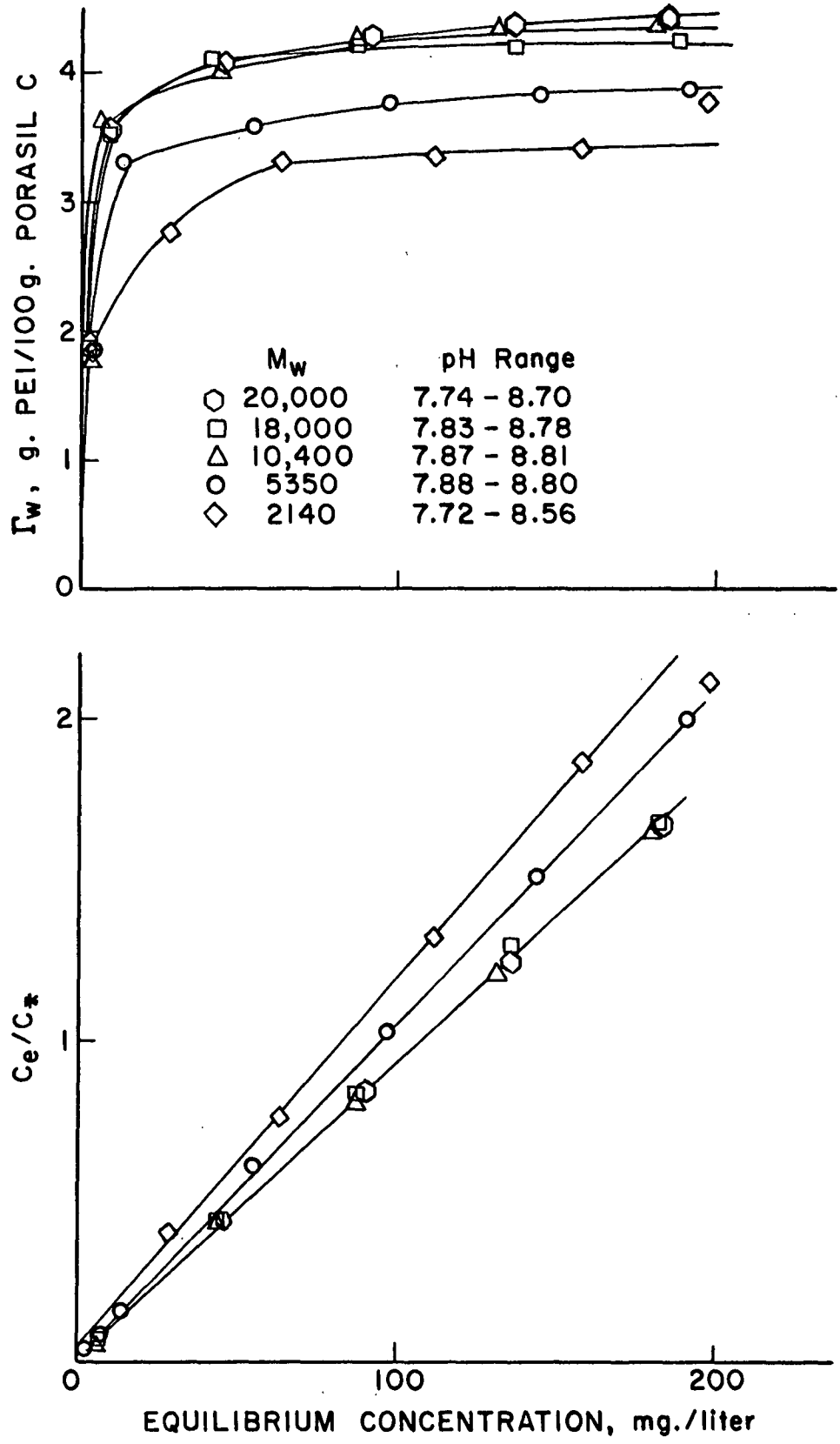

Figure 26. Equilibrium Adsorption Isotherms — Effect of Molecular Weight Adsorption from Aqueous 0.109N NaCl Containing 4.25×10^{-5}N NaOH on Porasil C

equilibrium concentrations are listed as ranges on the figures. The data are given in Tables XXXI and XXXII of Appendix X.

The general trend, with the exception of F-1, is that the adsorption of PEI on Porasil A increases with decrease in molecular weight. In contrast to this behavior, the adsorption on Porasil C increases with molecular weight up to a molecular weight of about 10,000. Above this point the adsorption increased very little with increased molecular weight up to 20,000.

The Langmuir form fits the adsorption data obtained for all molecular weights adsorbed on Porasil C. This is clearly seen by the linear C_e/C_* versus C_e plots shown at the bottom of Fig. 26. The regression coefficients for these plots are all greater than 0.998.

The decrease in adsorption on Porasil A with increased molecular weight is easily explained in terms of the inaccessible surface area, unavailable for adsorption, resulting from the exclusion of PEI from small pores. On the other hand, the increased adsorption with molecular weight on Porasil C is also easily explained from thermodynamic considerations. Two anomalies, however, are apparently present: (1) the near independence of adsorption above 10,000 mol. wt. on Porasil C and (2) the apparent increase in adsorption on Porasil A when going from 18,000 to 20,000 molecular weight. It should be pointed out that similar behavior has been reported for other systems (33, 99, 102).

The independence of adsorption with increased molecular weight has been shown for the adsorption of the linear polyelectrolyte, sodium poly (2-sulfoethylmethacrylate) (NPSEM) onto nonporous polyethylene particles from an aqueous 0.8N NaCl solvent (99). The amount of NPSEM adsorbed was the same at molecular weights of 3×10^4, 5×10^5, and 2×10^6. Greene (99) concluded that

in the 0.8N NaCl, NPSEM assumes a compact randomly coiled configuration and upon adsorption, a constant segment density of attachment occurs, so that the affinity per molecule increases with molecular weight, while the total amount adsorbed is constant.

Felter and Ray (102) have found that adsorption increases with molecular weight up to about 10,000 and then becomes independent thereafter for the adsorption of polyvinyl chloride on nonporous pigment $CaCO_3$ from dilute chlorobenzene solution. They suggest that the number of attachment points per molecule increases up to a limiting value. At the limiting value, a negative entropy effect ($-T\Delta S$) associated with the unfolding of an additional polymer segment is thought to equal the heat liberated ($-\Delta H$) in attaching the additional segment. Thus, the change in free energy ($\Delta F = 0$) is zero and no additional adsorption results.

Howard and McConnell (33) give evidence to the second anomaly. They found that the adsorption of polyethylene oxide onto porous powdered nylon decreases with increased molecular weight up to a point at which adsorption increases with subsequent increase in molecular weight. They concluded that the reversal in the trend corresponds approximately to the point at which polyethylene oxide is excluded from the majority of the pores present in the nylon powder.

The explanation of adsorption behavior of polymers on porous adsorbents is complicated by the accessibility of the surface area in small pores. The data presented here suggest the following generalization. For macromolecules small in comparison to the pores of the adsorbent, the amount adsorbed increases with molecular weight up to a point corresponding to the maximum density in segmental attachments as suggested by Felter and Ray (102). When the size of the macromolecule is of the same order of magnitude as the pores present, the

amount of polymer adsorbed decreases with increased molecular weight up to a point where molecular exclusion predominates. Subsequent molecular weight increases lead to increased adsorption up to a point where the maximum segment density of attachment occurs.

The specific adsorption and Langmuir constants for the adsorption of F-1, 3, 5, 7, and 9 on Porasil C give some support to the above generalization. They are given in Table XI. The Γ_A and Langmuir constant increase with molecular weight up to a point. At the higher molecular weights the Γ_A is approximately constant as the Langmuir constant shows an increase.

TABLE XI

PORASIL C SPECIFIC ADSORPTION AND LANGMUIR CONSTANT

Fraction	M_w	Γ_A, mg./m.^{2}	K, liter/mg.
1	20,000	0.587	0.331
3	18,000	0.564	0.472
5	10,400	0.585	0.303
7	5,350	0.512	0.325
9	2,140	0.457	0.252

On the other hand, from the adsorption data shown in Fig. 25 for Porasil A it is not apparent that the Langmuir form roughly describes the adsorption behavior for most fractions up to equilibrium concentrations of 250 mg./liter. Reasonably linear C_e/C_* versus C_e plots are shown in Fig. 27. The specific adsorption and Langmuir constants shown in Table XII were calculated from the visually estimated lines through the data. It is quite clear, that the Γ_A on Porasil C is much greater than that for Porasil A at all molecular weights, with the exception of F-7. The large Γ_A value for F-7 adsorbed on Porasil A results on account of the extrapolation. It is quite clear from Fig. 25 that the adsorption of F-9 is greater at all C_e values than that of F-7.

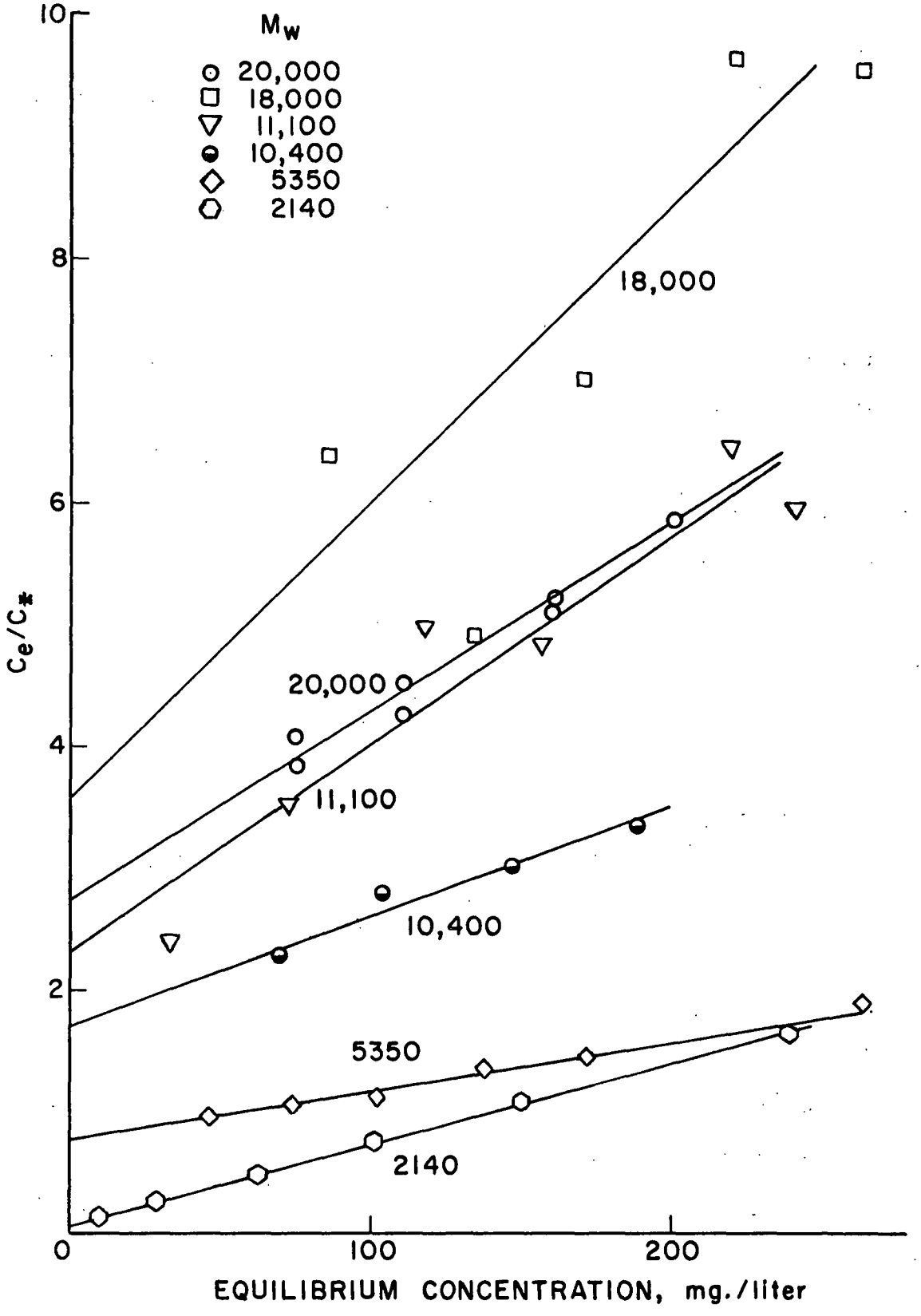

Figure 27. Langmuir Isotherm Fit-Effect of Molecular Weight Adsorption on Porasil A

TABLE XII

PORASIL A SPECIFIC ADSORPTION AND LANGMUIR CONSTANTS

Fraction	$\underline{M}_w$	$\Gamma_{\underline{A}}$, mg./m.^{2}	$\underline{K}$, liter/mg. x 10^2
1	20,000	0.185	0.558
3	18,000	0.117	0.671
4	11,100	0.116	0.741
5	10,400	0.314	0.524
7	5,350	0.718	0.506
9	2,140	0.422	11.400

These results indicate that the $\Gamma_{\underline{A}}$ for the two adsorbents approach each other with decrease in molecular weight. This behavior is expected, since molecular exclusion would decrease with decrease in molecular weight. The Langmuir constants for Porasil A for all fractions, except F-9, are approximately two orders of magnitude less than those typical of Porasil C. The Langmuir constants for F-9 are of the same order of magnitude for both adsorbents. The lower affinity of Porasil A for PEI apparently results as a consequence of its small pore sizes. Figure 28 is a bar graph depicting the actual porous volume present during adsorption experiments on Porasil A and C. The volumes shown are taken from nitrogen gas adsorption isotherms and show the total volume of pores corresponding to increments of 20 A. in EPD.

The average $\Gamma_{\underline{A}}$ of F-1, 3, 5, and DUPEI on Porasil C is 0.58 mg./m.^{2} The specific adsorptions for F-7 and F-9 are 0.512 mg./m.^{2} and 0.457 mg./m.^{2}, respectively, on Porasil C. If the pores contained in Porasil C are assumed to be accessible to all PEI fractions, then a rough calculation can be made of the amount of surface area accessible to PEI adsorbed on Porasil A. For example, the $\Gamma_{\underline{A}}$ of F-3 on Porasil A is 0.117 mg./m.^{2} If all the surface area within the pores of Porasil A were accessible then the $\Gamma_{\underline{A}}$ would be approximately 0.58 mg./m.^{2} or that of Porasil C. These figures indicate that only 30% [(0.117/0.58) 100%] of the surface area in Porasil A is accessible to PEI F-3 compared to Porasil

C. On this basis a percentage of surface area accessible in Porasil A for F-1, 3, 5, 7, and 9 may be calculated. These results are shown in Table XIII. The percentage of surface area of Porasil A accessible calculated in this manner may then be related to the EPD associated with a given percentage of accessible surface area for Porasil A calculated previously from mercury intrusion porosimetry and nitrogen gas adsorption data and shown in Table VIII. The approximate EPD corresponding to the accessible surface area calculated from the PEI adsorption data are also shown in Table XIII.

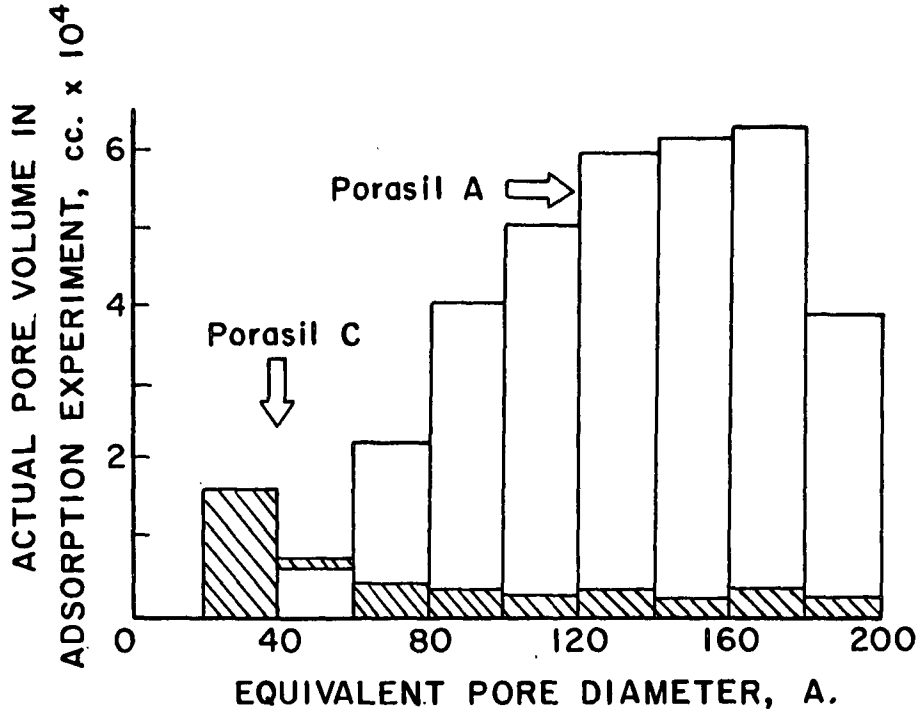

Figure 28. Pore Volumes[a] as a Function of Pore Diameter — Pore Volume of Porasil A and C Present During Adsorption Experiments for the Effect of Molecular Weight

[a] Nitrogen gas adsorption data.

TABLE XIII

APPARENT PERCENTAGE OF SURFACE AREA ACCESSIBLE TO GIVE FRACTION AND CORRESPONDING ESTIMATION OF EXCLUDING EQUIVALENT PORE DIAMETER

Fraction	Surface Area Accessible, %	Corresponding EPD from Table VIII, A.
1	32	100
3	30	100
5	54	80
7	140	--
9	92	50

The percentage of surface area accessible figures all seem reasonable except the value calculated for F-7 which appears as an anomaly.

It is of interest to compare the Stokes diameters calculated for the fractions to the corresponding estimation excluding EPD shown in Table XIII. This comparison is made in Table XIV. On the average the Stokes diameters are about 25 to 30 A. less than the calculated excluding EPD. Since these calculations possess rather high uncertainty, their absolute value and reliability must be viewed with reservation. In view of this difficulty, the apparent difference in the size of PEI molecular and excluding EPD may result by (1) an underestimation of the molecular size of the PEI, (2) a decrease in the effective pore size in solution because of an electric double layer, (3) an overestimation of the EPD, or (4) the fact that rigid spheres of a given dimension may not be able to diffuse into EPD of the same size. Any or all of these could be contributing factors.

TABLE XIV

ESTIMATED EXCLUDING EPD AND STOKES DIAMETER OF EXCLUDED FRACTION

Fraction	(a) Excluding EPD, A.	(b) Stokes Diameter, A.	Difference (a-b), A.
1	100	74	26
3	100	69	31
5	80	53	30
7	--	38	--
9	50	25	25

ADSORPTION REVERSIBILITY

The reversibility of adsorption with respect to pH, concentration, ionic strength, and molecular weight was briefly investigated to learn more about the nature of attachment between PEI and silica gel.

EFFECT OF CONCENTRATION

After the equilibrium adsorption experiment was completed for the adsorption of F-1 onto Porasil A from standard aqueous solvent, the bulk solution was decanted. Forty milliliters of deionized and distilled water having pH = 7 were placed in the adsorption tubes with the 50 mg. of Porasil A. The Porasil was allowed to settle out and another exchange of solvent was made. The water was exchanged in the tubes 10 times over the next 5-day period in which the desorption experiment was carried out at constant temperature with agitation. The amount of PEI still adsorbed was then determined by an organic nitrogen analysis on Porasil A. The EAI and desorption isotherm resulting after elution with water are shown in Fig. 29. The data are given in Table XXXIII of Appendix XI. Recall the data presented in Fig. 17; little adsorption was shown to occur at pH 7.

The EAI resulting after elution with water is within the experimental error of being the same as the original EAI. For the most part the desorption isotherm

has a slightly lower specific adsorption. However, it must be concluded that the isotherms are apparently the same and that PEI is not easily eluded from silica gel with water. It should be noted that the elution solvent has a pH = 7 compared to adsorption solutions which ranged at equilibrium from pH 8.69 to 9.41.

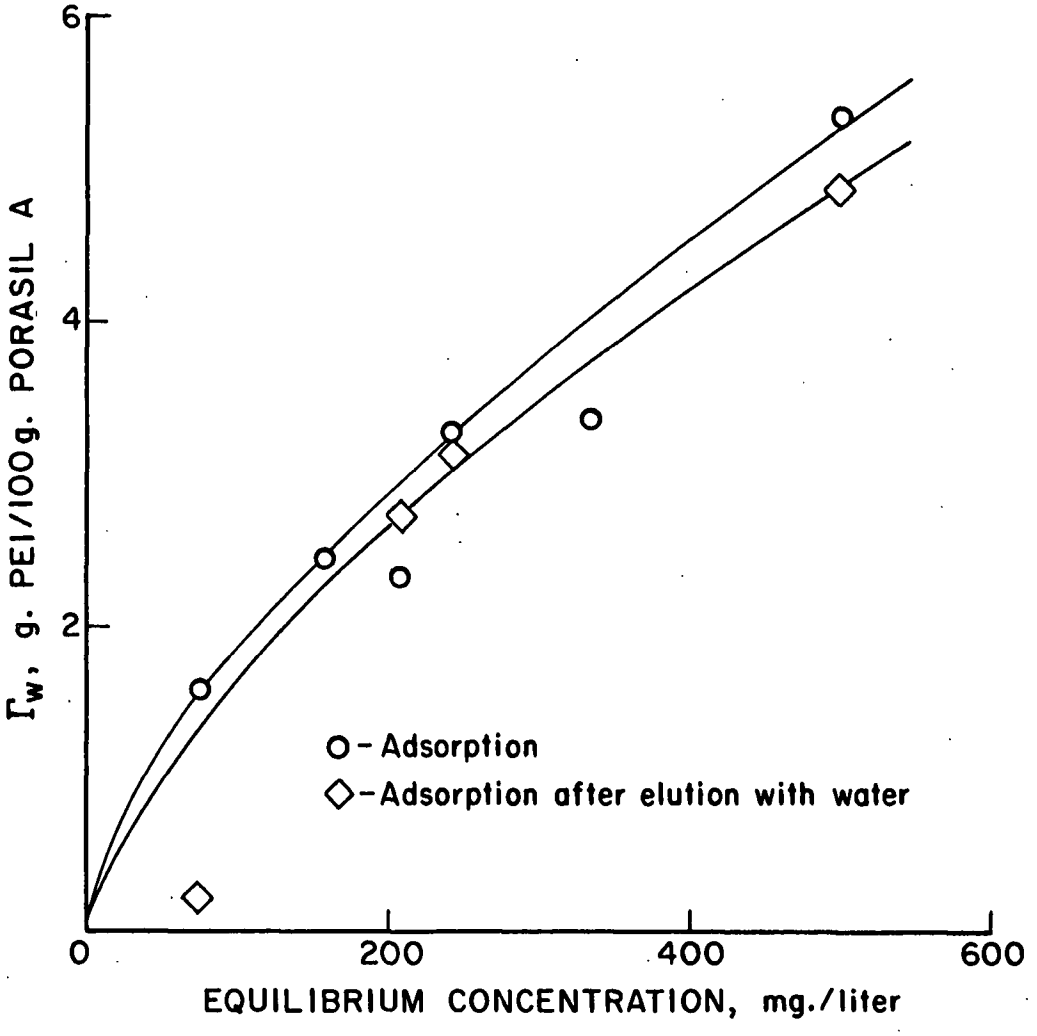

Figure 29. Reversibility of Adsorption — Adsorption of F-1 ($\underline{M}_w$ = 20,000) on Porasil A from Aqueous 0.109$\underline{N}$ NaCl Containing $4.25 \times 10^{-5}\underline{N}$ NaOH, Desorption in Distilled Water

EFFECT OF IONIC STRENGTH

The irreversibility occurring when water is used as an elutriator is thought by Allan and Reif (3) to result from the "Jack in the Box Effect." Viscosity and light-scattering studies indicate a decrease in the molecular size of polyelectrolytes with increase in ionic strength. The EAI presented earlier for the effect of ionic strength also indicated an apparent decrease in the molecular size of the PEI molecule. If physical entrapment of PEI in pores because the molecule expands is the cause of the irreversibility then elution with water having a higher ionic strength than the adsorption solution should facilitate desorption of PEI.

A similar experiment to that described in the previous section was performed with the exceptions that the elutriate used was 0.218N NaCl and a lower molecular weight PEI (F-4) was used as the adsorbate. Figure 30 shows the adsorption and desorption isotherms. The data are given in Table XXXIII of Appendix XI. The desorption isotherm has a slightly lower Γ_w than the adsorption isotherms. The data clearly show that little desorption takes place. It should be emphasized that the data points originate from two different analytical methods. The EAI is determined by a spectrophotometric method. The desorption isotherm is determined by organic nitrogen determination. The actual amount of PEI adsorbed on 50 mg. of Porasil A ranges from 0.43 to 2.05 mg. The amount of PEI was calculated on the basis of the theoretical nitrogen content of 32.53% by weight. The final titration of the ammonia distilled over was made using a 5.0×10^{-3}N HCl to a brom cresol green end point.

EFFECT OF pH

Desorption isotherms in a 0.109N NaCl solution having pH = 12 were obtained for F-10 adsorbed onto Porasil B. Fraction 10 was adsorbed onto Porasil B from

standard aqueous solvent. The desorption was carried out over 120 hr. at 25.0°C. with agitation. Seven exchanges of solvent were made. The results of the adsorption and desorption isotherms are shown in Fig. 31. The data are given in Table XXXIII of Appendix XI.

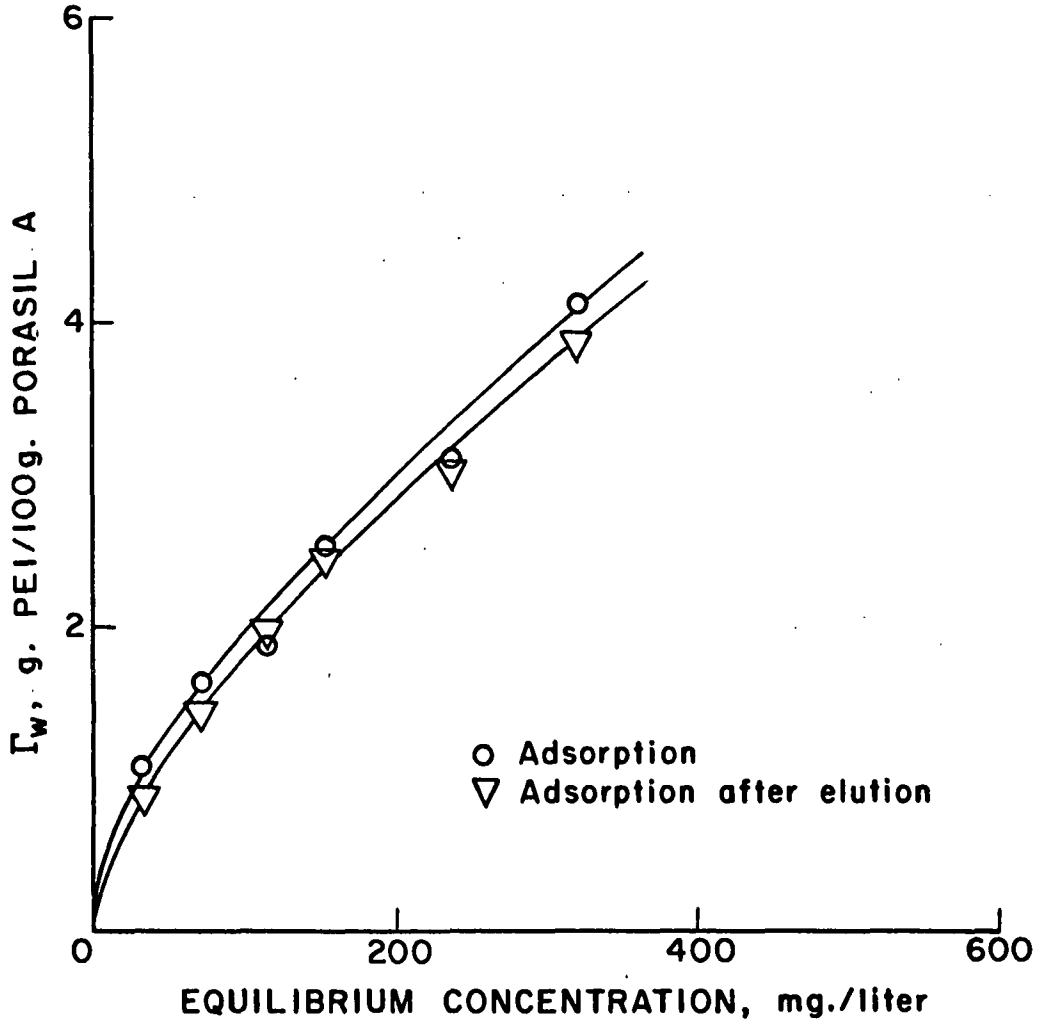

Figure 30. Reversibility of Adsorption — Adsorption of F-4 ($\underline{M}_w$ = 11,100) on Porasil A from Aqueous 0.109$\underline{N}$ NaCl Containing $4.25 \times 10^{-5}\underline{N}$ NaOH, Desorption in 0.218$\underline{N}$ NaCl

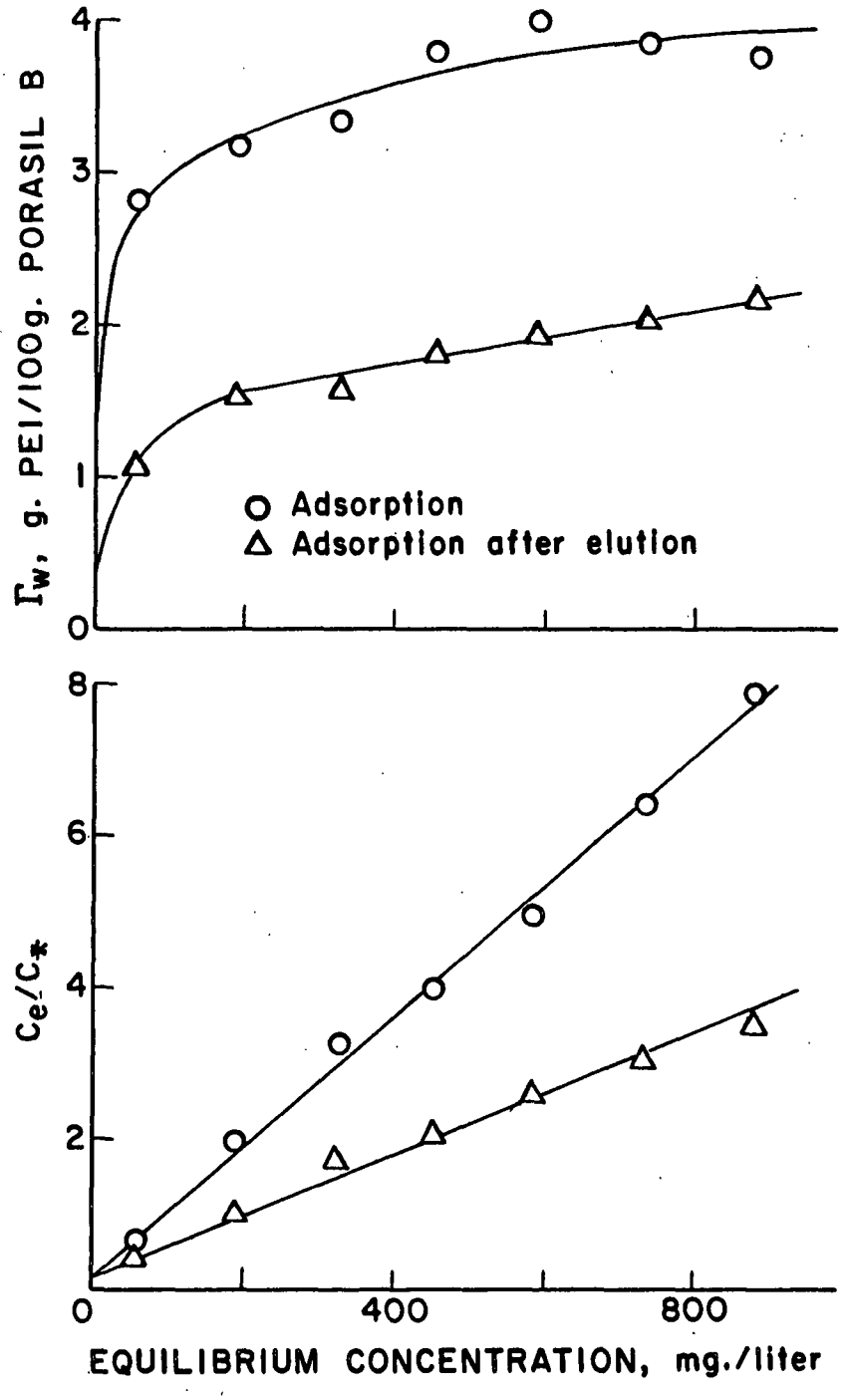

Figure 31. Reversibility of Adsorption — Adsorption F-10 ($\underline{M}_w$ = 1,500) on Porasil B from 0.109$\underline{N}$ NaCl Containing 4.25 x $10^{-5}\underline{N}$ NaOH, Desorption in 0.109$\underline{N}$ NaCl Solution Adjusted to pH 12.00 with NaOH

The EAI complies to the Langmuir form. The desorption isotherm shows compliance with the Langmuir form when plotted against the EAI C_e values. The average amount of PEI desorbed for the seven concentration levels is 44% of the specific adsorption at surface saturation as calculated from the Langmuir fit of the EAI. The similar shapes of the adsorption and desorption isotherms show that approximately equal amounts of PEI are desorbed at each C_e. This suggests that the amount desorbed is independent of the surface coverage, i.e., the amount of PEI adsorbed. The rate-controlling step and resulting chemical equilibrium thus depends solely on the solvent conditions. It should be emphasized that physical entrapment should play little part in the apparent exceedingly slow reversibility noted here. The adsorbing molecules (F-10) are very small compared to the pores of the adsorbent (Porasil B).

EFFECT OF pH AND IONIC STRENGTH

The effect of low pH on the reversibility of adsorption was investigated by lowering the pH of the slurry after adsorption equilibrium was obtained at the pH of maximum adsorption. The system was again allowed to come to equilibrium at 25°C. with constant agitation. The final pH and C_e were determined. The solution pH was lowered by adding various amounts of HCl to each centrifuge tube.

Reversibility runs were done on DUPEI adsorbed on Porasil A from aqueous solvents containing 0.0, 0.054, and 0.109N NaCl. The EAI established at high pH (10.5-10.8) have been shown previously in Fig. 23. The desorption isotherms or reestablished equilibrium isotherms for the three ionic strengths are given in Fig. 32 with the original adsorption data. The resulting pH ranges for the reestablished EAI are also shown. The data are given in Table XXXIV of Appendix XI.

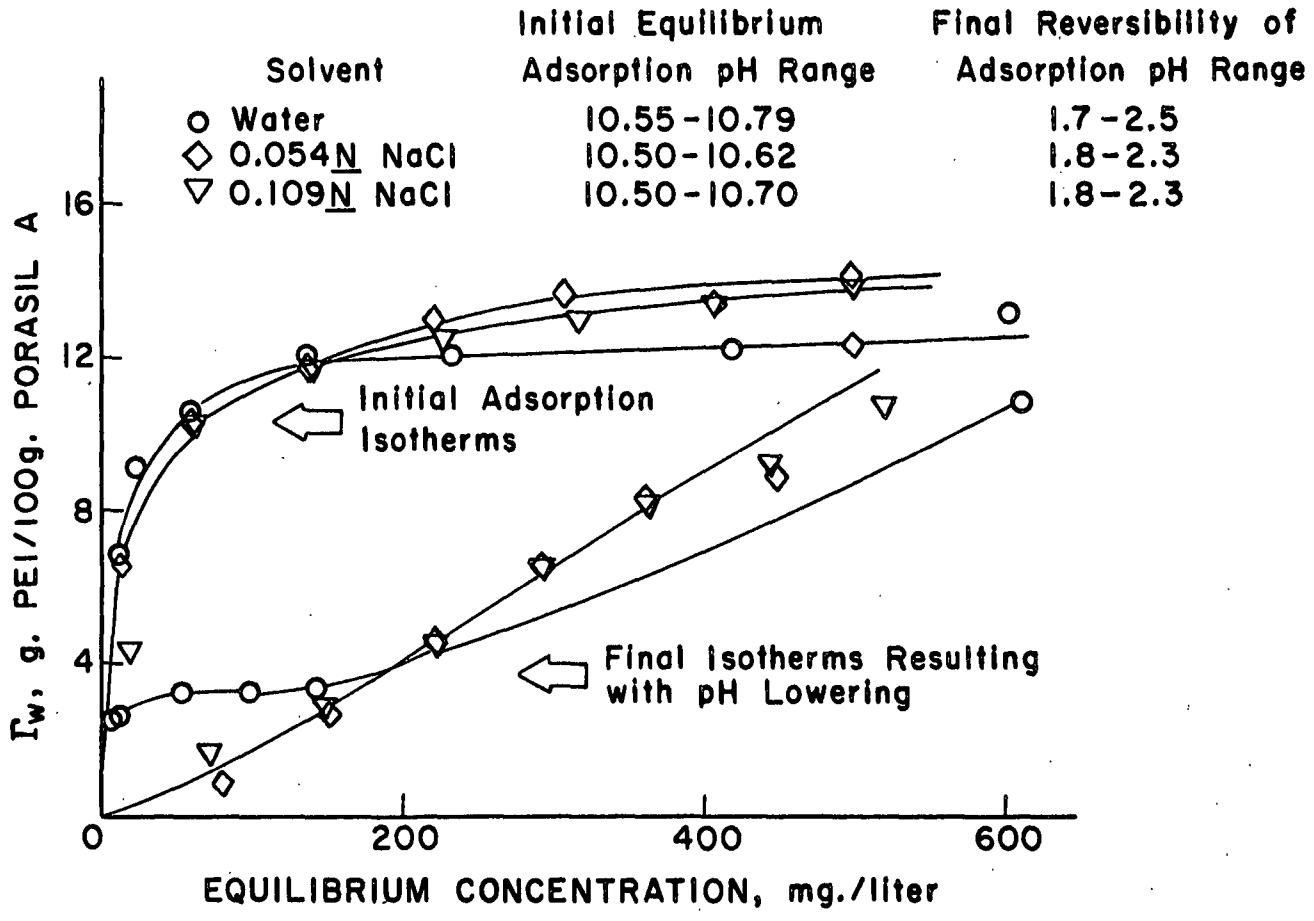

Figure 32. Reversibility of Adsorption of DUPEI Adsorbed onto Porasil A with Respect to pH and Ionic Strength

The reestablished EAI with the absence of NaCl obeys the Langmuir equation up to C_e 150 mg./liter. The Γ_A and K for the EAI at high pH (10.5-10.8) are 0.473 mg. PEI/m.^{2} and 0.0625 liter/mg., respectively. The constants for the reestablished low pH EAI are 0.124 mg. PEI/m.^{2} and 0.230 liter/mg. In the region where the Langmuir equation was obeyed about 74% reversibility occurs. Although the Γ_A decreases with pH the intensity of adsorption increases fourfold. The highly charged and expanded PEI molecule probably accounts for the larger Langmuir constant. The reestablished EAI for the solution containing NaCl substantiate

this conclusion. The added simple electrolyte apparently shields the highly charged molecule thus decreasing adsorption. This is evident at low C_e from the EAI for 0.054 and 0.109N NaCl solvents. No apparent Langmuir region was observed. The data show reasonable agreement with the Freundlich isotherm. This is shown in Fig. 33.

Another approach was tried to investigate reversibility with respect to pH. An experiment was designed to illustrate the "Jack in the Box Effect" (JBE) (3) if operative. Fraction 1, 0.109N NaCl solution, and Porasil A were used as the adsorbate, solvent, and adsorbent system. EAI were obtained on separate runs at low and high pH. The reversibility of the runs with respect to pH was then checked. Sodium hydroxide was added to the equilibrium adsorption run at low pH without removing excess polymer in order to raise the pH to the pH where maximum adsorption occurs. The pH of the equilibrium adsorption run done at high pH was lowered by addition of HCl acid. The resulting isotherms thus should show any irreversibility occurring between the given pH values. If the JBE is operative, then the high pH isotherms should be similar but the low pH isotherms should be quite different. The EAI resulting at a low pH from the adsorption run originally conducted at a high pH should exhibit a greater Γ_A than the EAI resulting from the adsorption run initially conducted at low pH.

Figure 34 shows the resulting equilibrium adsorption isotherms. The pH range for the seven adsorption solutions resulting at equilibrium adsorption for the high and low pH regions are listed on the figure. The data are given in Table XXXV of Appendix XI. The isotherms clearly indicate the JBE. The Γ_w at low pH for Run 2 is about twice that of Run 1 at low pH. Run 2 experienced the high-low pH sequence, whereas Run 1 was initially conducted at low pH.

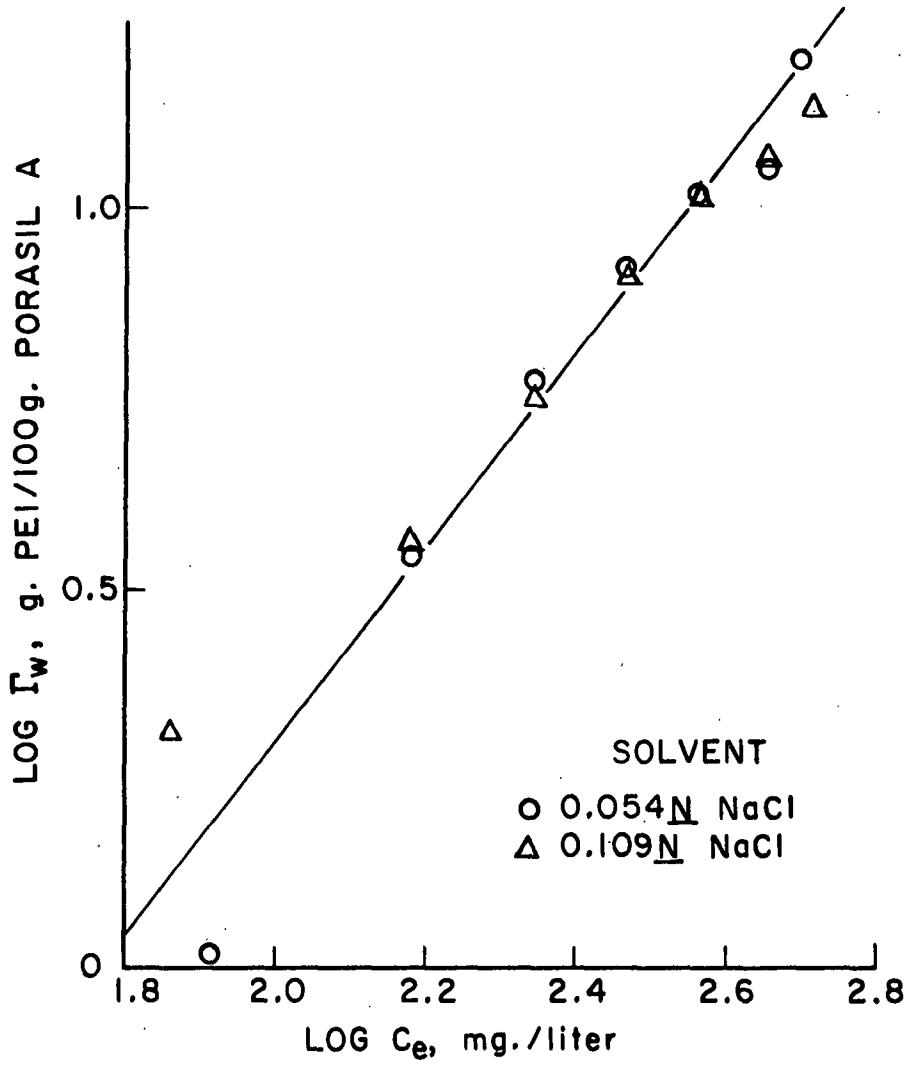

Figure 33. Freundlich Isotherm for Reversibility of Adsorption of DUPEI at Low pH

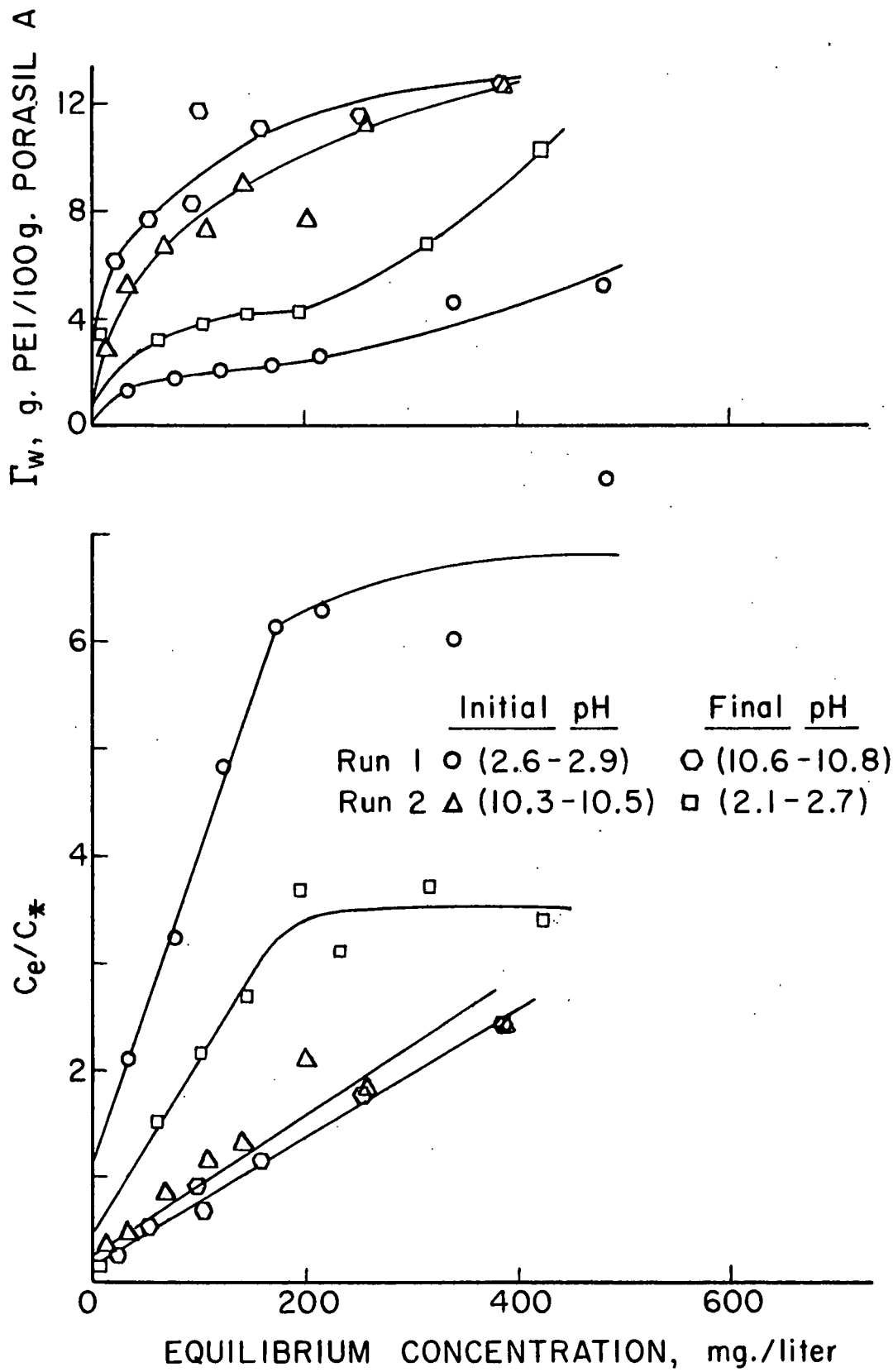

Figure 34. Reversibility of Adsorption with Respect to pH Adsorption of F-1 ($\underline{M}_{\underline{w}}$ = 20,000) on Porasil in 0.109$\underline{N}$ NaCl

The EAI at high pH are in reasonably good agreement. At the high C_e the data points are nearly the same. The lower Γ_w for Run 2 compared to Run 1 at low C_e results from the slightly lower pH values for Run 2 than Run 1. For Run 1 the range was from pH 10.60 to 10.85. For Run 2 the range was from pH 10.30 to 10.50. The amount of PEI adsorbed on Porasil A is strongly dependent on pH near the pH region where maximum adsorption takes place (see Fig. 17). About a 16% increase in PEI adsorption was shown to result between pH 10.30 and 10.50. Thus, if the Γ_w values of Run 2 at low C_e are inflated about 16% the agreement between the high pH isotherms of Run 1 and Run 2 is within the experimental error of this type of experiment.

EFFECT OF MOLECULAR WEIGHT

The displacement of adsorbed low molecular weight polymers by higher molecular weight polymers of the same type has been reported for uncharged polymers by Emery (103) and Farrar (104) and for an anionic polymer by Laffend (105). This effect was also tentatively reported for the PEI-cellulose fiber system (32) by viscosity determinations on the adsorption solution. Quantitative experimental evidence is presented below that also demonstrates this behavior for the PEI-silica gel adsorption system.

Fraction 10 (25 ml. at 1.2%) was dialyzed against 25 ml. of standard aqueous solvent for 6 days. The polyethylenimine diffusing through the dialysis membrane was designated DF-10 and used as low molecular weight polymer in the adsorption experiment. Dialysis experiments showed 47.1% of F-10 readily passes through the dialysis membrane in 39 hr. If the molecules were completely permeable then 50% would diffuse through the membrane.

Fraction 3 (30 ml. at 0.4%) was dialyzed 6 days under similar conditions as F-10 except the solvent (80 ml.) was exchanged three times. Dialysis experiments showed 1.28% of F-3 passes through the dialysis membrane after 10 days.

Sedimentation equilibrium and high-speed osmometry molecular weight determinations showed F-3 to be largely monodispersed with a molecular weight of about 18,000. A ratio of $\underline{M}_w : \underline{M}_n$ of 1.02 was found. A molecular weight of about 1,500 was estimated for F-10 from the gel permeation elution volume versus molecular weight of PEI relation found experimentally.

The EAI at 134 hr. for the adsorption of DF-10 on Porasil B from standard aqueous solvent was determined. At adsorption equilibrium the supernatant was decanted. The adsorbent was rinsed with 50 ml. solvent. The adsorption tubes were refilled with 50 ml. solvent and agitated 6 hr. The solvent was decanted and the tubes were refilled with F-3 PEI at the same concentration as the original initial concentration of DF-10, not the equilibrium concentration of F-10.

The isotherms were determined at 139 hr. and 260 hr. and found to be the same. The PEI concentration changes were determined spectrophotometrically. The amount of low molecular weight PEI desorbed was determined by dialyzing 5.0-ml. aliquots of supernatant from each of the 6 different concentration levels against 5.0 ml. of solvent for 124 hr. The initial and final PEI concentrations and volumes in the solvent and solution compartments of the dialysis cells were determined.

The amount of DF-10 displaced from the silica surface by F-3 was calculated from the adsorption and dialysis data shown in Table XXXVI of Appendix XI. The amount of PEI diffusing through the membrane was considered to be composed

entirely of DF-10. The amount of DF-10 remaining on the solution side of the membrane was calculated on the basis that the molarity of PEI is approximately equal on both sides of the dialysis membrane at equilibrium. Since the concentration and molecular weights of the PEI on each side of the dialysis membrane are known, a simple algebraic equation was used to calculate the actual amount of F-3 and DF-10 on the solution side of the membrane at equilibrium. The amount of PEI adsorbed by the dialysis membrane was calculated from the concentration changes resulting during dialysis and found to be insignificant at all but the lowest concentration of PEI used in the adsorption experiments.

The results of the molecular replacement experiment are shown as EAI in Fig. 35 and 36. Figure 35 shows the equilibrium adsorption isotherms for the adsorption of DF-10, for the additional PEI adsorbed when F-3 was introduced, and the total amount of F-3 and DF-10 adsorbed on Porasil B. Figure 36 shows the actual amounts of DF-10 and F-3 adsorbed at replacement equilibrium. The top of Fig. 37 is a plot of the weight percent of DF-10 replaced as a function of the $\underline{C}_{\underline{e}}$. These data are fitted to the Langmuir form as shown at the bottom of Fig. 37. The equilibrium concentration ($\underline{C}_{\underline{e}}$) of F-3 and DF-10 in solution at replacement equilibrium was used to plot the amount of additional PEI adsorbed when F-3 was introduced and to plot the total amount (F-3 and DF-10) adsorbed.

The Langmuir form adequately describes the adsorption of DF-10, F-3 and the total PEI (DF-10 plus F-3) on Porasil B. In the plateau region of the equilibrium adsorption isotherms on a weight basis, an average increase of 65.4% adsorption is found when F-3 is introduced into the system. An average of 42% of DF-10 originally adsorbed was replaced (desorbed). At equilibrium replacement, approximately 7 moles of DF-10 are adsorbed per one mole of F-3.

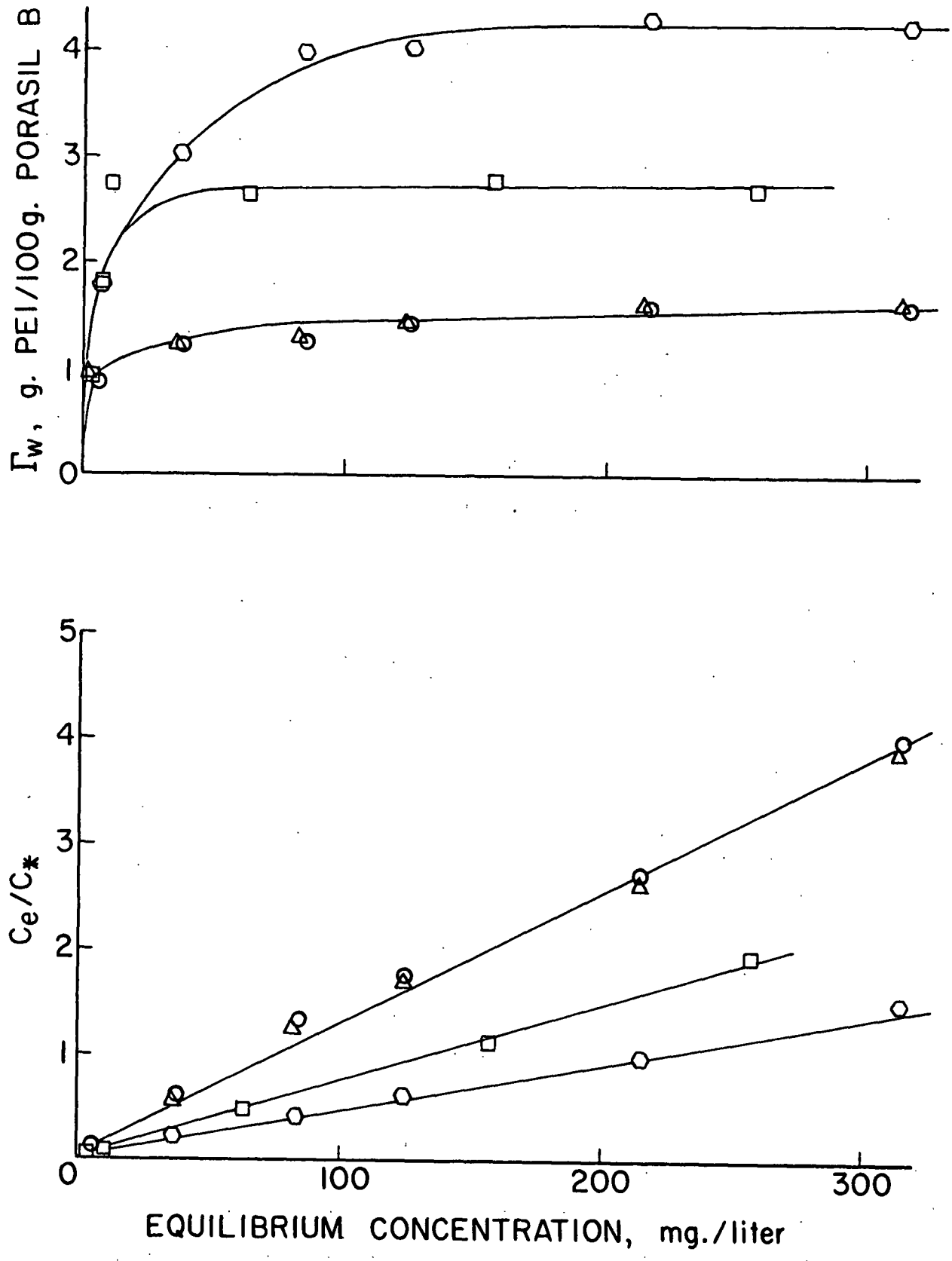

Figure 35. Reversibility of Adsorption with Respect to Molecular Weight

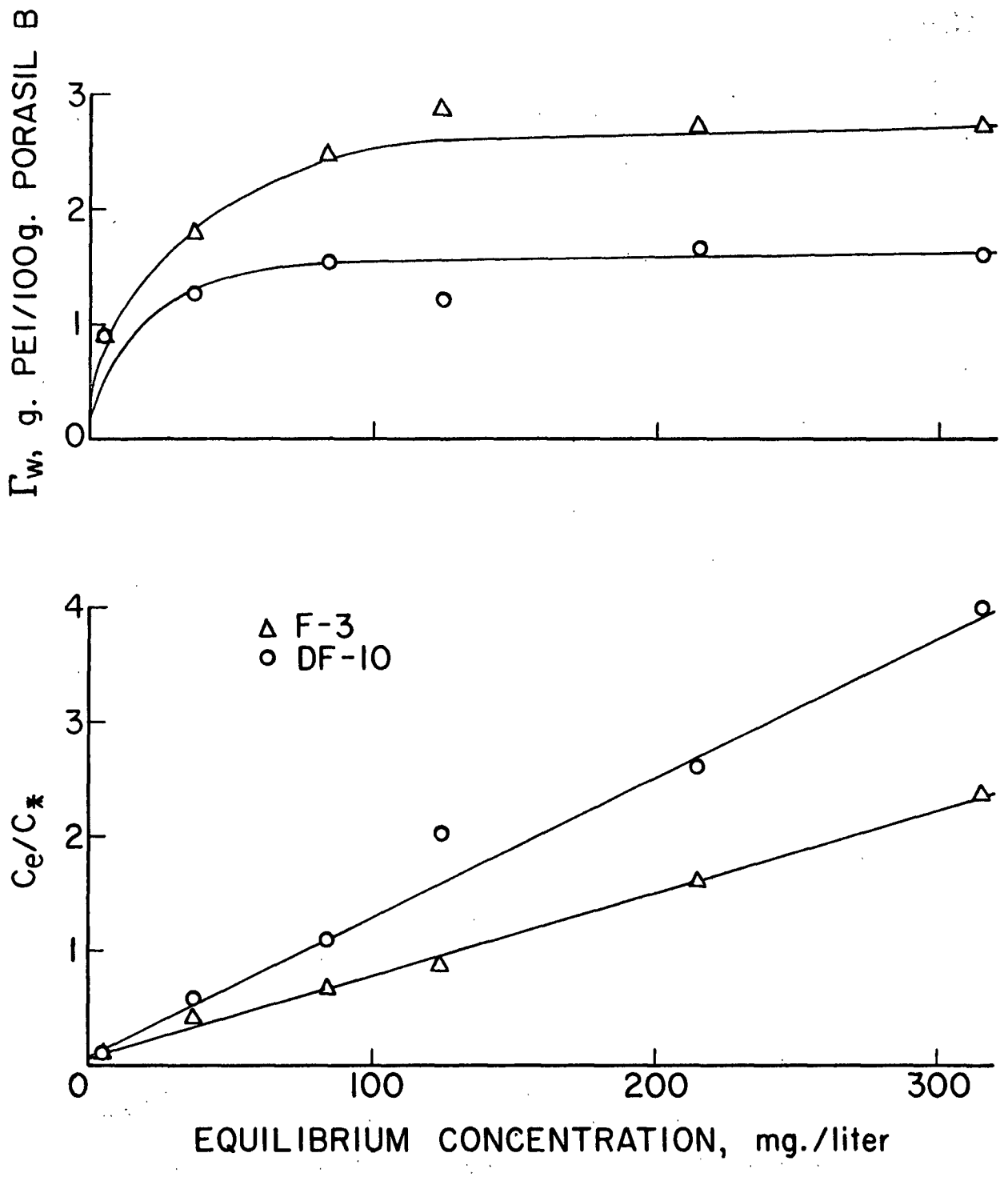

Figure 36. Equilibrium Adsorption Isotherm — Adsorption of F-3 ($\underline{M}_w$ = 18,000) and DF-10 ($\underline{M}_w$ = 1,500) at Replacement Equilibrium

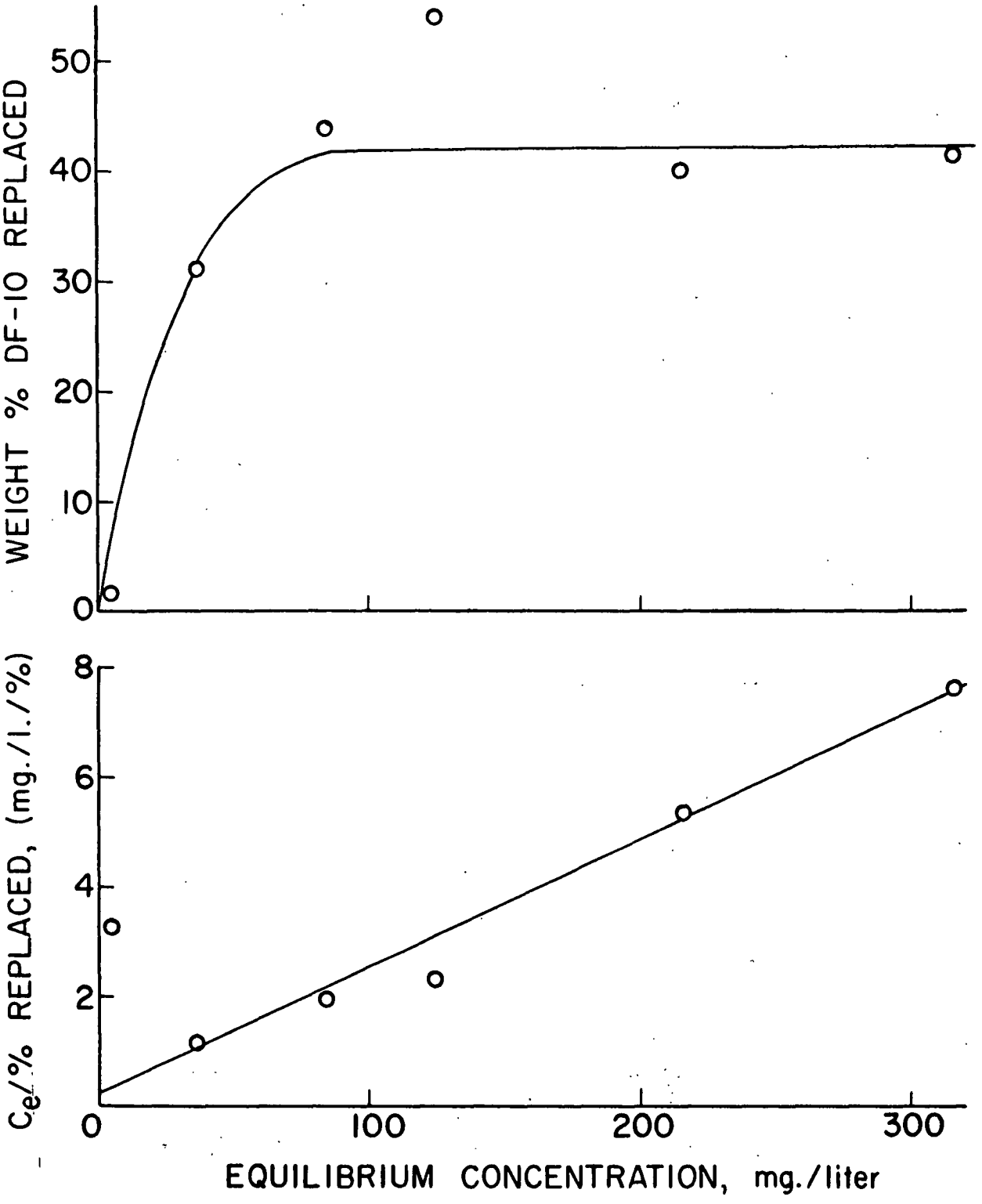

Figure 37. Replacement Adsorption Isotherm

However, on a weight basis about 3 parts DF-10 are adsorbed per 5 parts F-3. It should be emphasized that data presented previously in Fig. 20 have shown that Porasil B apparently contains some pores that are not accessible to higher molecular weight PEI. This may be part of the reason for the 42% replacement level obtained.

It is clearly evident from these findings that higher molecular weight PEI displaces adsorbed low molecular weight PEI. Compliance to the Langmuir form for the percent DF-10 replaced versus C_e clearly indicates a definite limiting replacement level, which may be synonomous with the limiting adsorption dependence as explained by Felter and Ray (102).

ANALYSIS OF RESULTS AND CONCLUSIONS

CHARACTERIZATION OF POLYETHYLENIMINE

The preparative gel permeation fractionation technique gave nearly monodispersed PEI fractions. Agreement of the number and weight average molecular weights, experimentally established this fact. A near linear relationship was found between the log of the molecular weight and the reduced elution volume of the fractions obtained by the permeation fractionation technique.

The Seely, Einstein-Stokes, and Stokes equations were used to estimate the size of the PEI molecule in standard aqueous solvent from experimental data. Intrinsic viscosity and molecular weight values were used for molecular size calculations by the Seely and Einstein-Stokes equations. Diffusion coefficient values were used for molecular size estimates based on the Stokes equation. The molecular diameters (De) calculated by the above equations are listed in Table XV to allow comparisons to be made.

TABLE XV

ESTIMATES OF THE MOLECULAR DIAMETER OF POLYETHYLENIMINE

Fraction	$\overline{M}_w$	Seely De, A.	Einstein-Stokes De, A.	Stokes De, A.	PEI Diffusing Through Membrane, %
1	20,000	69	66	74	2.0
3	18,000	66	62	69	1.3
4	11,100	57	52	55	1.6
5	10,400	55	51	53	5.6
7	5,350	43	40	38	15.6
9	2,140	33	28	25	45.7

The three estimates of the molecular size of PEI are in good agreement, considering the reliability of the data and the appropriateness of the models on which the equations used for the calculations are based. The Stokes and Einstein-Stokes equations are based on the same model whereas the Seely

equation is derived for a significantly different model. Their major difference is that the Stokes model is for solid spheres whereas the Seely model is for porous spheres having uniform permeability throughout. Because polymer molecules in solution may deviate considerably from the Stokes model as a result of the solvation and asymmetry of the molecule, the calculated diameters represent equivalent hydrodynamic spheres. They are the solid sphere sizes that have the same frictional coefficients as the molecules in solution that are being investigated.

Limited progress has been made in relating the molecular dimensions of branched polymers to their solution properties. Often the linear polymer of equal molecular weight is used as the reference point to relate the properties of branched polymers. For an ideal unrestricted linear polymer, Stockmayer and Zimm (106) have shown by calculation that one branch point decreases the radius of gyration (R_g) about 5%. Two random branch sites were shown to reduce the R_g approximately 9%.

Polyethylenimine has been shown to be highly branched; having branch sites on the average every 3-3.5 monomer units. For example, F-9 and F-1 according to these figures have 15 and 142 branch points, respectively, per molecule. Therefore, the R_g of PEI compared to a linear polymer of equal molecular weight is probably much less.

The equivalent hydrodynamic radius (R_e) of linear polymers, characterized by the random coil, has been related to their R_g. At present the best theory available shows that the R_e is about 2/3 the R_g (77). However, very highly branched molecules that immobilize most of the solvent within them and approach the properties of an impenetrable sphere may have an R_e approaching its R_g. In the extreme case, the R_e is larger than the R_g for solid spheres. If a

large proportion of solvent is immobilized within a molecule of spherical symmetry, the Stokes diameter may provide an accurate estimate of the outer dimensions of the molecule.

On the other hand, if the PEI molecule is moderately permeable, the Seely equation may provide the better estimate of the outer dimensions of the molecule. Table XV shows that for the same data ($[\eta]$ and $\underline{M}_{\underline{w}}$) the Seely diameters on the average are 7% larger than the Einstein-Stokes diameters. They are also larger than the independently determined Stokes diameters for Fractions 4, 5, 7, and 9. The apparent reason for this is that the PEI molecule is slightly permeable. However, the validity of the Stokes or the Seely equations to actually describe the solution size of the PEI molecule cannot be further justified.

The equilibrium dialysis results are also shown in Table XV. The amount of PEI diffusing through the membrane to the solvent side is given. It is expressed as the percentage of the original PEI on the solution side of the dialyzing membrane. These values do not corroborate the $\underline{De}$ calculated for PEI. They suggest that the solution size of the PEI molecule is possibly 20-25 A. larger than the average value of the Stokes, Einstein-Stokes, and Seely $\underline{De}$. This result is obtained by noting that F-1, 3, 4, and 5 having molecular weights greater than 10,000 do not readily diffuse through the dialysis membrane. However, F-7 has a significant number of molecules that diffuse through the membrane. Fraction 9 approaches the limiting value of 50% where all molecules easily diffuse through the membrane. The average $\underline{De}$ for F-9 is 28 A. This value is 20 A. less than the nominal pore size of the dialysis membrane — 48 A., a value that must be viewed with some reservation. These data suggest that the effective molecular size of the molecules of F-9 is approximately 48 A. This may be the case if a molecule of the same size as a pore aperture can diffuse into it.

The number of H ions adsorbed per PEI molecule was determined as a function of pH. It is expressed as the degree of protonation which is assumed to be equal to the ratio of the number of H ions adsorbed to the total number of amino groups present in solution. The point of zero charge on the PEI molecule was taken as pH 10.8 for calculation of the degree of protonation. This value was suggested by Sarkanen, et al. (65) and confirmed experimentally in the present study by light-scattering and mobility results. An inflection point was found to occur in the plot of R_{90} versus pH at about pH 10.8. The mobility was shown to be approximately zero at pH 11.

Changes in the molecular size of PEI occur in a 0.109N NaCl solution as the pH is lowered from 13 to 4. The decrease in the diffusion coefficient and increase in R_{90} as the pH is lowered from 13 to 7 support this conclusion. The increase in the R_{90} and negligible increase in mobility below pH 7 also suggest that molecular expansion occurs at acid pH.

Interpretation of the electrophoretic mobility results is based on the fact that little mobility increase is noted when the degree of protonation of the PEI molecule is increased from 34 to 66%. However, the mobility increased rapidly up to about 34% protonation. This indicates that the charge on the molecule increases to a greater extent than the expansion of the molecule.

CHARACTERIZATION OF PORASIL

The nitrogen gas adsorption BET surface areas of Porasil A, B, and C are 282, 60, and 76 $m.^2/g.$, respectively. The nitrogen gas adsorption isotherm (NAI) analyses results show that Porasil A, B, and C have 0.90, 0.10, and 0.24 cc./g. porous volumes, respectively, associated with equivalent pore

diameters between 14 and 600 A. The cumulative pore surface areas for Porasil A, B, and C are 91, 90, and 79% of the BET surface areas, respectively.

The mercury intrusion porosimetry (MIP) results indicate that "ink bottle type" pores are present in Porasil A, B, and C. Pore entry criteria, in this case, for rigid spherical molecules should be based on MIP analysis. The analyses show that the majority of the pore apertures in Porasil A are between 50 and 120 A., in Porasil B between 200 and 500 A., and in Porasil C between 130 and 340 A.

The BET surface areas and pore volume distributions for Porasil A and C are comparable to the manufacturer's specifications and previous investigations. The values found for Porasil B do not agree with the manufacturer's specifications or the results of previous studies.

If the elemental particles composing the spherical beads of Porasil A, B, and C are assumed to be spheres, then an estimation of their size can be calculated. The nitrogen gas adsorption BET surface area and the specific density of silica gel (2.20 g./cc.) (13) are used for the calculation.

The elemental particle sizes found for Porasil A, B, and C are 97, 454, and 358 A., respectively. These elemental particle sizes are comparable to the size of the equivalent pore diameters found by mercury intrusion porosimetry.

ADSORPTION OF POLYETHYLENIMINE ONTO SILICA GEL

The adsorption of PEI onto silica gel has been investigated with regard to the effect of pore entry criteria in determining equilibrium adsorption isotherms. The pore sizes of the silica gel and the molecular size of the PEI molecule were varied in adsorption experiments.

The adsorption of PEI onto Porasil A, which has the majority of its pore apertures less than approximately twice the diameter of the adsorbing molecule, is mainly controlled by the size of the molecule. In this case, solution conditions that decrease the size of the molecule allowing it to diffuse into the smaller aperture porous regions, increase the specific adsorption. Addition of simple electrolyte (up to 0.218N NaCl) that is known to cause a decrease in the size of cationic polymers in solution, greatly increases adsorption. Increases in pH from 4 to 11, which cause a decrease in the size of the PEI molecule, also greatly increase adsorption on Porasil A. A slight adsorption increase also occurs at the pH of maximum adsorption (pH 10.5-11.0) by addition of simple electrolyte (0.054N NaCl). This indicates that the size of the adsorbing molecule primarily controls the amount of adsorption onto Porasil A. Under these conditions a greater number of molecules may also adsorb per unit surface area as a result of the smaller size of the molecule if the size of the adsorbed molecule is approximated by its solution size.

The size of the molecule determines its ability to diffuse into the porous structure and adsorb. Further support is provided by the decrease in adsorption with an increase in molecular weight from 2140 to 18,000. Other investigators (34) have suggested that electrostatic repulsive forces between adsorbed molecules and molecules approaching the surface are responsible for the decrease in adsorption with increased molecular weight. However, the above adsorption was done in 0.109N NaCl solution, where electrostatic forces between molecules are suppressed. Therefore, the molecular size of PEI is the controlling factor determining adsorption.

In contrast, the adsorption of PEI onto Porasil B and C, which have the majority of their pore apertures greater than about twice the molecular diameters of the adsorbing molecules, shows only a slight specific adsorption

increase as the ionic strength is increased (up to 0.218N NaCl). In this case, the slight adsorption increase may be accounted for by the smaller molecular size and less lateral interaction between adsorbed molecules. This allows a greater packing density of molecules on the silica gel surface.

The adsorption dependence on pH is less for Porasil B and negligible for Porasil C compared to Porasil A. The specific adsorption on Porasil B increased significantly while that for Porasil C showed a negligible increase as the pH was increased from between 9 and 10 to between 10 and 11. Apparently, Porasil B contains a significant number of pores having apertures that become accessible to PEI molecules ($8{,}000 \leq \underline{M}_w \leq 20{,}000$) when their size is decreased by neutralization of the charge on PEI by addition of sodium hydroxide to raise the solution pH up to 10.8.

Porasil C, on the other hand, does not contain a significant amount of pores that become accessible to the PEI molecule as the solution pH is increased. Apparently, all pores are accessible to the DUPEI (see Fig. 21) at solution pH between 9 and 11.

The molecular weight dependence on Porasil C is the reverse of Porasil A. The specific adsorption increases with increased molecular weight from 2,000 to 10,400. This dependence is expected according to the theory of Felter and Ray (102) if the accessible surface area is constant.

Between 10,400 and 20,000 molecular weight the specific adsorption on a weight basis is nearly constant. This suggests that (1) the accessible surface area is decreasing (as the size of the molecule is increased its ability to diffuse into the porous regions is limited by its size) or (2) the flexibility of the PEI molecule is increased allowing it to flatten on the surface and

establish a maximum chain segmental attachment density. Repulsive interactions between adsorbed molecules and those approaching the surface (34) are discounted because the adsorption was done in 0.109N NaCl solution.

The present work and that of others (36, 37) suggest that the PEI molecule is a rather rigid spherical molecule at low degrees of charge. A flattening of this highly branched molecule (37) as it is adsorbed is unlikely. Therefore, the size of the PEI molecule compared with the size pores present probably controls adsorption. The size of the adsorbed molecule can be calculated from the adsorption data and the surface area determinations of the adsorbent.

An average diameter for the adsorbed molecule can be calculated by assuming (1) the total BET surface area for Porasil C is entirely accessible to PEI molecules of 20,000 molecular weight and less, (2) a spherical noninterpenetrating molecule is adsorbed, and (3) a close packed monolayer is formed on the silica gel surface. This packing arrangement has a projected surface area amounting to 90.6% of the area of a flat surface on which the monolayer rests. The following equations are used to calculate the diameter of the adsorbed molecule:

$$S = 1.11 \; X \; N \; A_m / M_w \qquad \text{and} \qquad (12)$$

$$d = (4 \; A_m / 3.14)^{\frac{1}{2}} \qquad (13)$$

where S is the total surface area of the adsorbent, X is the weight of polymer adsorbed per weight of adsorbent, N is the Avogadro number, A_m is the projected area of coverage per molecule, M_w is the molecular weight of the polymer, d is the diameter of the adsorbed molecule and 1.11 is the numerical constant introduced by the packing arrangement of uniform spheres. The first equation is solved for A_m using the adsorption data for F-1, 3, 5, 7, and 9 on Porasil C from standard aqueous solvent. Table XVI gives the results of these calculations

along with the average diameters of the PEI molecules in solution as calculated by the Seely, Einstein-Stokes, and Stokes equations.

TABLE XVI

DIAMETER OF PEI MOLECULE IN SOLUTION AND ADSORBED ONTO SILICA GEL

Fraction	Adsorbed Diameter, A.	Solution Diameter, A.
1	70	70
3	68	66
5	51	53
7	39	40
9	26	29

The calculated size of the adsorbed PEI molecule and the solution size show extremely good correlation. The close magnitude of these results suggest that the PEI molecule maintains much of its solution configuration when adsorbed (107). This physical picture limits the number of attachment sites to the adsorbent to a relatively small fraction of the primary and secondary amino groups located on chain segments at the extremity of the PEI molecule.

The specific adsorption per unit surface area (Γ_A) on Porasil A is much less than Porasil C. This apparently results for two reasons: (1) molecules are excluded from many pores because they are larger than the pore apertures and (2) the Γ_A within pores having dimensions slightly larger than the adsorbing molecules is much less than the Γ_A for a flat surface.

For example, in the limiting case, where the diameter of a rigid spherical molecule approaches the diameter of an infinitely long cylindrical pore, the theoretical Γ_A within the pore is approximately 27.6% of Γ_A of a monolayer on a flat surface. However, as the molecular size decreases in comparison to the pore size, the Γ_A within the pore theoretically increases and approaches the

value for a monolayer on a flat surface. This effect is probably the reason that the calculated exclusion pore sizes of Porasil A (Table XIV) are between 25 and 31 A. greater than the calculated molecular size. The exclusion pore sizes shown in Table XIV were calculated assuming that the $\Gamma_{\underline{A}}$ within pores was equal to the $\Gamma_{\underline{A}}$ of a flat surface, which was approximated by the $\Gamma_{\underline{A}}$ on Porasil C. Therefore, the calculated exclusion pore sizes are probably too large as a result of the lower $\Gamma_{\underline{A}}$ within smaller pores that are accessible to the PEI molecules, which was not taken into account.

The increased adsorption on Porasil A when going from 18,000 to 20,000 molecular weight is apparently caused by either an increase in the flexibility of the molecule or a limiting molecular size above which a majority of the pores are inaccessible. An increase in the flexibility of the molecule is unlikely; the molecule is highly branched and previous calculations indicate that the solution and adsorbed molecular sizes are nearly equal. The second possibility is that equal surface areas are accessible to F-1 and F-3. That is F-1 and F-3 are excluded from equal porous regions of Porasil A. Therefore, the $\Gamma_{\underline{A}}$ would be greater for the larger rigid spherical molecules adsorbed on equal surface areas that are accessible to both molecular sizes.

The exclusion of PEI molecules from many of the pores of Porasil A has been demonstrated as a cause for the much lower $\Gamma_{\underline{A}}$ on Porasil A compared to Porasil C. The molecular entrapment hypothesis — Jack in the Box Effect — proposed by Allan and Reif (3) to explain part of the irreversibility observed for the PEI-cellulose fiber system also seems like a plausible explanation that should apply equally well to the PEI-silica gel system. The Jack in the Box Effect was indirectly observed in two sets of data.

In the first set of data (Fig. 32), an increase in reversibility occurred at low equilibrium concentrations at low pH (2-3) with addition of simple electrolyte. A decrease in the size of the PEI molecule, allowing it a greater opportunity to diffuse out of the porous regions of silica gel, apparently accounts for the greater reversibility with respect to pH.

In the second set of data (Fig. 34), the Γ_A on Porasil A was found to be substantially greater at low pH (2-3) if the pH was initially high (between 10.5 and 11.0) then decreased to the lower pH and allowed to establish equilibrium. When the pH is raised, the size of the molecule decreases allowing it to diffuse into the smaller pores of Porasil A. As the pH is lowered the molecule expands and is trapped within the pores.

Much of the adsorption and reversibility data presented for the PEI-water-silica gel system suggests an ion-exchange adsorption mechanism involving electrostatic bonding forces between anionic silanol sites and cationic amino groups on PEI. At low pH (2-3), where the charge on PEI is high and the charge on the silica gel surface is negligible, little adsorption occurs. At high pH ($\geq$ 12), where the PEI molecule is uncharged and the silanol groups on the silica gel are fully ionized, little adsorption occurs. Adsorption, however, is partially reversible at both these pH extremes (Fig. 31, 32, and 34), when the pH is changed after the adsorption of PEI onto silica gel under favorable pH conditions (pH 9-11).

Negligible reversibility is observed at a neutral solution pH where the PEI molecule and the silica gel surface are both considerably charged. The adsorption forces are apparently quite strong. Elution with water or 0.218N NaCl solution at neutral pH did not cause substantial desorption.

Adsorption was found to be reversible with respect to molecular weight. The adsorption of higher molecular weight molecules was found to be favored over the adsorption of lower molecular weight molecules.

An attempt was made to examine a monolayer of PEI adsorbed on Porasil A to compare it to the original silica gel surface. The adsorption was done at pH 10.8 using DUPEI. At adsorption equilibrium the supernatant was decanted. The sample was rinsed with water and dried at 50°C. Transmission electron microscope micrographs of direct carbon replicas shadowed at 20° with platinum are shown in Fig. 38. The magnification factor is 60,000X.

The top micrograph shows the very rough porous nature of the surface of Porasil A. The bottom micrograph is for Porasil A having 0.46 mg. PEI adsorbed per square meter of surface area. The background surface roughness is clearly present through the adsorbed polymer layer. Many of the crevices and depressions of the surface are filled with polymer. However, the background surface topography appears essentially unchanged through the adsorbed polymer layer.

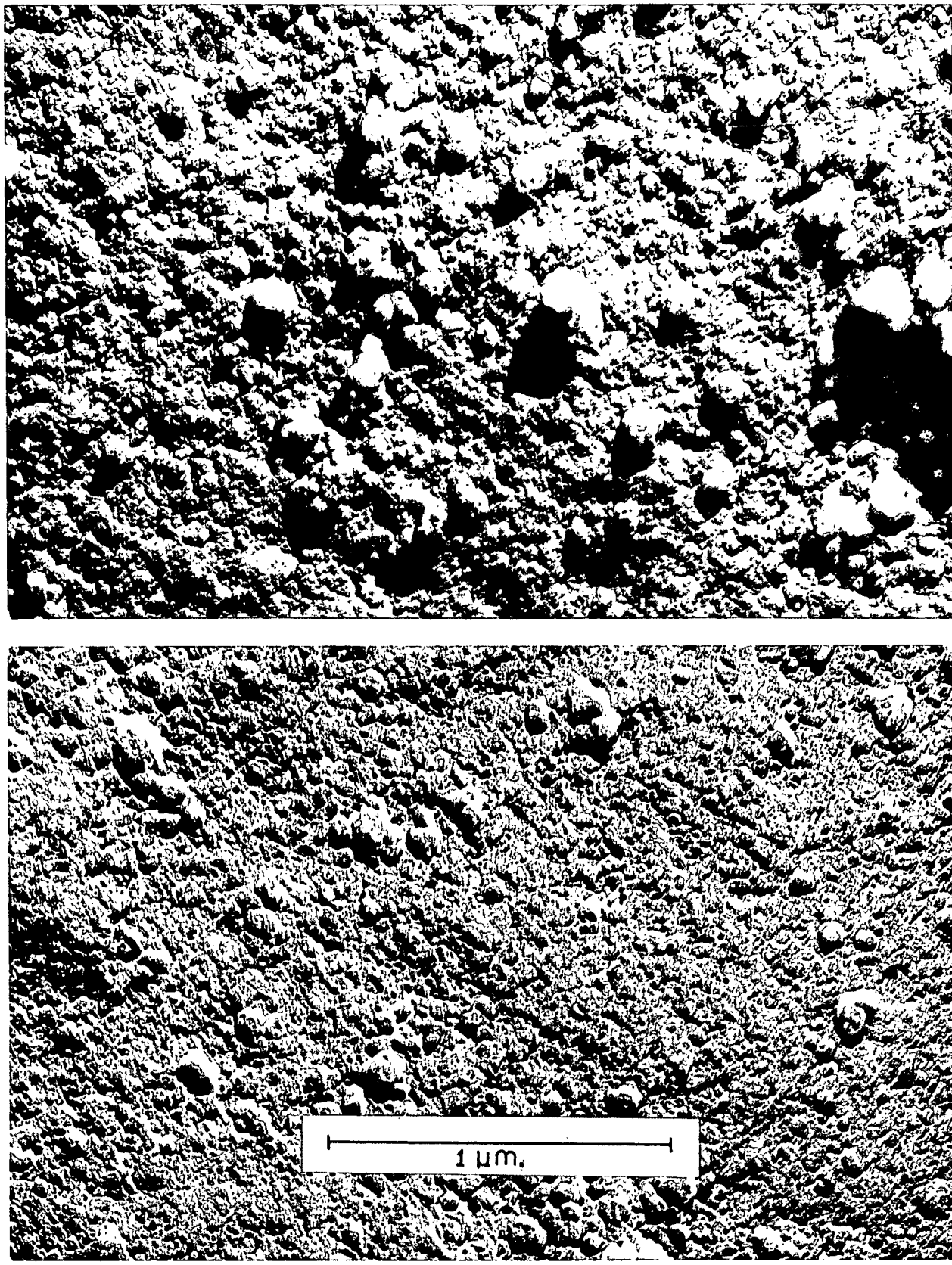

Figure 38. Top — Surface of Porasil A, Bottom — with Polyethylenimine Adsorbed

SUGGESTIONS FOR FUTURE RESEARCH

The present study has shown that the equilibrium adsorption of a cationic polyelectrolyte onto the anionic surface of a porous solid is directly determined by the relative size of the adsorbing molecule compared to the pore size in the adsorbent. Further work concerning the rate of diffusion of polymers in porous materials is of interest. Possible gains may be made in individual cellulose fiber quality by the penetration of polymer into the porous regions of fibers, while efficient sheet strength and surface property gains may be brought about by deposition of polymers on the outer surface of the cellulose fiber.

Continued interest also prevails concerning the mechanism of wet strength development and the mechanism of the flocculation of cellulose fibers by polymers. The recent work of Heinegard and Martin-Lof (34) has indicated that cationic polymers cause flocculation much like simple electrolytes. This is in contrast to the mechanism suggested by LaMer and coworkers (108) that proposes polymer bridging between flocculating particles. Their work (34) leads to a fresh approach to the design of polymers and their usage to enhance drainage, retention, and wet strength on the paper machine as well as improvements in the final sheet quality. A study of polymer structure and the conditions necessary to effect optimum use of wet-end additives to accomplish desired functions for greater fiber utility is an area where substantial economical and new product development gains can be realized. A basic study concerning the mechanism of wet strength development in fibrous webs by polymer additives can also help in conceiving new areas of fiber utility.

An expanded study concerning the exchange phenomenon and molecular weight partitioning equilibrium on highly porous adsorbents is also of interest. A study in this area may add further information to aid in the more efficient and economical use of polymers in the papermaking process.

ACKNOWLEDGMENTS

Many people have contributed greatly to the successful completion of this thesis. Recognition of the Board of Directors and member companies is given since they have created and continue to give support and hope for the future to The Institute of Paper Chemistry. The staff and faculty members are recognized for their service which continues to provide the opportunity for a graduate studies doctoral program.

Special mention is made of the Thesis Advisory Committee who provided much of their time, knowledge, and energies in my behalf. John W. Swanson served as chairman of the advisory committee and provided the initial enthusiasm, knowledge, and encouragement necessary that has inspired many students to undertake research concerning the phenomenon of polymer adsorption.

Robert A. Stratton also served on the committee, contributed substantially to the polyelectrolyte characterization work, and provided stimulating discussion as did Dale G. Williams concerning the complex interactions that may possibly occur in the system under investigation.

Special gratitude is extended to John A. Carlson who provided practical knowledge and operated the instruments for mobility, diffusion coefficients, and molecular weight determinations. Harold Swenson also was responsible for assistance in obtaining osmotic pressure measurements.

The characterization of silica gel was greatly aided by the electron micrographs provided by Russell A. Parham and Hilkka Kaustinen and the mercury intrusion data obtained by Seelye Nagel.

The author also wishes to thank his loving wife Carol for her patience, understanding and encouragement, that she enduringly extended throughout the thesis program.

NOMENCLATURE

A_m = projected area of molecule on flat surface

a = Seely molecular radius (81)

a' = cell length

BET = Brunauer, Emmett, and Teller (57)

C = concentration, mg./l.

C_e = equilibrium concentration, mg./l.

C_I = initial concentration, mg./l.

C_M = change in concentration for surface saturation

C_* = $C_I - C_e$

CVP = cumulative volume percent

CPSA = cumulative pore surface area

D = apparent diffusion coefficient at infinite time

D_o = diffusion coefficient at infinite time and dilution

$D(R_a)$ = distribution function, dV/dR_a

DUPEI = dialyzed unfractionated polyethylenimine (footnote on page 69)

d = diameter of molecule

E = electric field strength

EAI = equilibrium adsorption isotherm

EPD - equivalent pore diameter

F-1 = Fraction number 1, also F-3, F-4, F-5, F-7, F-9, and F-10

g_1 = weight of solvent

g_2 = weight of solute

J = fringe number

JBE = Jack in the Box Effect (3)

K = permeability

k = Boltzmann constant

$\underline{M}_w$ = weight average molecular weight

$\underline{M}_n$ = number average molecular weight

MIP = mercury intrusion porosimetry

$\underline{m}$ = mass of molecule

$\underline{N}$ = Avogadro's number

NAI = nitrogen gas adsorption isotherm

$\underline{n}$ = specific refractive increment

$\underline{P}$ = pressure applied

PA = Porasil A, also PB and PC

PEI = polyethylenimine

$\underline{q}$ = charge

$\underline{R}$ = gas constant

$\underline{r}^2$ = distance for axis of rotation squared

$\underline{R}_a$ = radius of straight cylindrical capillary

$\underline{R}_e$ = Stokes equivalent hydrodynamic radius

$\underline{\bar{r}}$ = average pore radius

SA = surface area

$\underline{S}$ = surface area of adsorbent

SEM = scanning electron microscope

$\underline{T}$ = temperature, Kelvin

TEM = transmission electron microscope

$\underline{V}$ = volume

$\underline{v}$ = electrophoretic mobility

$\underline{X}$ = weight adsorbate adsorbed per weight of adsorbent

$\underline{\gamma}$ = activity coefficient

$\underline{Z}$ = dissymmetry

$\Gamma_{\underline{A}}$ = specific adsorption, mg. PEI/m.^{2} Porasil

$\Gamma_{\underline{M}}$ = specific adsorption at surface saturation

$\Gamma_{\underline{w}}$ = specific adsorption, g. PEI/100 g. Porasil

ε = porosity

γ = surface tension of mercury

η = viscosity coefficient

θ = contact angle

λ = wavelength

$\bar{\nu}_1$ = specific volume of solvent

$\bar{\nu}_2$ = specific volume of solute

π' = osmotic pressure

π = 3.1416

ρ = density

LITERATURE CITED

1. Kindler, W. A. Adsorption kinetics in the polyethylenimine-cellulose fiber system. Doctor's Dissertation. Appleton, Wis., The Institute of Paper Chemistry, 1971. 112 p.

2. Trout, P. E., Tappi 34:539(1951).

3. Allan, G. G., and Reif, W. M., Svensk Papperstid. 74:2, 25(1971).

4. Silberberg, A., J. Chem. Phys. 46:105(1967).

5. Stone, J. E., Treiber, E., and Abrahamson, B., Tappi 52:108-10(1969).

6. Thode, E. F., Swanson, J. W., and Becher, J., J. Phys. Chem. 62:1036(1958).

7. Haselton, W. R., Tappi 38, no. 12:716-23(1955).

8. Sommers, R. A., Tappi 46, no. 9:562-9(1963).

9. Silberberg, A., J. Phys. Chem. 66:1872-907(1962).

10. Frisch, H. L., Simha, R., and Eirich, F. R., J. Chem. Phys. 21:365(1953).

11. Simha, R., Frisch, H. L., and Eirich, F. R., J. Phys. Chem. 57:584(1953).

12. Frisch, H. L., and Simha, R., J. Phys. Chem. 58:507(1959).

13. Handbook of chemistry and physics. 46th ed. Cleveland, Ohio, The Chemical Rubber Co., 1965-66.

14. Stamm, A. J. Wood and cellulose science. New York, The Ronald Press Co., 1964.

15. Anderson, J. F., Jr., and Wichersheim, K. A., Surface Sci. 2:252(1964).

16. McDonald, R. S., J. Phys. Chem. 62:1168(1958).

17. Stober, W., Kolloid. Z. 145:17(1956).

18. Fripial, J. J., and Uytterhoeven, J., J. Phys. Chem. 66:800-5(1962).

19. deBoer, J. H., and Vleesking, J. H., Koninkl, Ned. Akad. Wetenschap. Proc. B61:3(1958).

20. Agzam Khodzhaeu, D. A., Zhuravlev, L. T., Kiselev, A. V., Ivz., Akad. Nauk. SSSR, Ser. Khim. 6:1186-91(1968).

21. Alexander, G. B., Heston, W. H., and Iler, R. K., J. Phys. Chem. 58:453 (1954).

22. Van Lier, J. A., DeBruyn, P. L., and Overbeek, J. Th. G., J. Phys. Chem. 14:1675(1960).

23. Parks, G. A., Chem. Rev. 65:177(1965).

24. Beau, R., LePage, M., and DeVries, A. J., Appl. Polymer Symposia 8:137-55 (1969).

25. Dugger, D. L., J. Phys. Chem. 68:757(1964).

26. Prettre, M. Study weak mol. forces. 9th ed. 1966, (Publ. 1967). p. 523-97(Fr.); CA 70:61517r.

27. Vydra, F., and Stara, V., Collect. Czech. Chem. Comm. 33, no. 111:3883-8 (1968); Ger.; CA 70:31887u.

28. Hughes, R. E., and Von Frankenbury, C. A. In Annual reviews of physical chemistry. Vol. 14. p. 291. Palo Alto, Calif., Annual Reviews, Inc., 1963.

29. Patat, F., Killman, E., and Schliebener, C., Rubber Chemistry and Technology 39:36-87(1966).

30. Wet strength in paper and paperboard. TAPPI Monograph Series no. 29, New York, Technical Association of the Pulp and Paper Industry, 1965.

31. Swanson, J. W. In Consolidation of the paper web. Vol. 2. p. 741-72. Tech. Sect., Brit. Paper and Board Makers' Assoc., 1966.

32. Kindler, W. A., and Swanson, J. W. Some aspects of the adsorption of polyethylenimine in pulp fibers. Special Studies. Appleton, Wis., The Institute of Paper Chemistry. Unpublished work, 1967.

33. Howard, G. J., and McConnell, P., J. Phys. Chem. 71:2974-95(1967).

34. Heinegard, C., and Martin-Lof, S. The mechanism of the interaction between polyelectrolytes and cellulose surfaces. Gordon Research Conference on the Chemistry and Physics of Paper, 1971.

35. Millipore, Tech. Brochure TB-961, Millipore Filter Corporation, Bedford, Mass., 1961. 40 p.

36. The Dow Chemical Company, Tech. Bull. 192-63-71. PEI-The versatile polymer. Midland, Michigan, Dow Chemical Co., 1968. 24 p.

37. Dick, C. R., and Ham, G. E., J. Macromol. Sci. Chem. A4(6):1301-14 (Oct., 1970).

38. Kenchington, A. E., In Alexander and Block's Analytical methods of protein chemistry. Chap. 10. New York, Pergamon Press, 1960. 353 p.

39. Tanford, C. Electrochemistry in biology and medicine. Chap. 13. New York, John Wiley and Sons, 1955.

40. Shaw, O. J. Electrophoresis. London and New York, Academic Press, 1967. 144 p.

41. Bier, M. Electrophoresis theory, methods, and applications. New York, Academic Press, Inc., 1959. 563 p.

42. Beckman/Apinco Model H Electrophoresis-Diffusion-Instrument Instruction Manual, 1959.

43. Gosting, L. J. Measurement and interpretation of diffusion coefficients of proteins. In Advances in protein chemistry. Vol. XI. p. 429. New York, Academic Press, 1956.

44. Creeth, J. M., J. Am. Chem. Soc. 77:6428-40(1955).

45. Schachman, H. K. Ultracentrifugation in biochemistry. New York and London, Academic Press, 1959. 272 p.

46. Fujita, H. Mathematical theory of sedimentation analysis. New York and London, Academic Press, 1962. 315 p.

47. Wagner, R. H., ed. by Weissberger, A. Physical methods of organic chemistry. 2nd ed. Part I. p. 487-550. New York, Interscience, 1949.

48. Staverman, A. J., Rec. Trav. Chim. 70:344(1951).

49. Cannon, M. L., Manning, R. E., and Bill, J. D., Anal. Chem. 32:355-8(1960).

50. Doty, P., and Steiner, R. F., J. Chem. Phys. 20:85(1952).

51. Stacey, K. A. Light scattering in physical chemistry. London, Butterworths Scientific Publications, 1956. 230 p.

52. Brice-Phoenix Universal Light Scattering Photometer Manual, Phoenix Precision Instrument Company, Philadelphia, Pa. 40 p.

53. Swenson, H., and Kaustinen, H. Personal communication, 1970.

54. Materials Technology Laboratory, American Instrument Company, Inc., Silver Spring, Maryland.

55. Barrett, E. P., Joyner, L. G., and Halenda, P. P., J. Am. Chem. Soc. 73:373(1951).

56. American Instrument Company, Inc., Cat. No. 4-4680, Instruction No. 861-A, American Instrument Co., Inc., Silver Spring, Maryland.

57. Brunauer, S., Emmett, P. H., and Teller, E., J. Am. Chem. Soc. 60:209-10 (1938).

58. Ritter, H. L., and Drake, L. C., Ind. Eng. Chem. Anal. Ed. 17:782(1945).

59. Barrett, E. P., Joyner, L. G., and Skold, R., J. Am. Chem. Soc. 73:3155(1951).

60. Nelson, R., The Institute of Paper Chemistry, Appleton, Wis., 1968.

61. Rootare, H. M., Aminco Laboratory News, 4A-4H(1968).

62. Perrine, T. O., and Landis, W. R., J. Polymer Sci., Part A-15, no. 8:1993-2005(1967).

63. Henwood, A., and Garey, R. M., J. Franklin Inst. 221:4, 531(1936).

64. Analytical Group Method 52, Appleton, Wis., The Institute of Paper Chemistry, June 2, 1964.

65. Sarkanen, K. V., Dinkler, F., and Stannett, V., Tappi 49:4(1966).

66. Castellan, G. W. Physical chemistry. Reading, Mass. Addison-Wesley Publishing Co., 1966. 717 p.

67. Lawrence, J., and Conway, B. F., J. Phys. Chem. 75, no. 15:2353(1971).

68. Huizenga, J. R., Grieger, P. F., and Wall, F. T., J. Am. Chem. Soc. 72:2636(1950).

69. Lanpanje, S., Haebig, J., Davies, T., and Rice, S. A., J. Am. Chem. Soc. 83:1590-8(1961).

70. Dobbins, R. J., Tappi 53, no. 12:2284-90(1970).

71. Diamond, R. M., J. Phys. Chem. 67:2513(1963).

72. Adamson, A. W. Physical chemistry of surfaces. Los Angeles, Calif., U.S.C., Interscience Publishers, 2nd ed., 1967. 747 p.

73. Flory, R. J. Principles of polymer chemistry. Ithaca, New York, Cornell University Press, 1953. 671 p.

74. Daniel, E., and Alexandrowig, Z., Biopolymers 1:473-95(1963).

75. Davies, O. L. Statistical methods in research and production. New York, Hafner Publishing Company, 1961. 396 p.

76. Stokes, Sir G., Trans. Cambridge Phil. Soc. 8:287(1847); 9:8(1851).

77. Tanford, C. Physical chemistry of macromolecules. New York, London, Sydney, John Wiley and Sons, Inc., 1967. 710 p.

78. Nagasawa, M., and Fujita, H., J. Am. Chem. Soc. 86:3005-12(1964).

79. Kidam, O., and Katchalsky, A., J. Polymer Sci. 15:321-34(1955).

80. Morawetz, H. High polymers. Vol. XXI. Macromolecules in solution. New York, Interscience Publishers, John Wiley and Sons. 1965. 495 p.

81. Seely, T., J. Polymer Sci., Part A-1, 5:3029(1967).

82. Wetlaufer, D. B., Millic, S. K., Stoller, L., and Coffin, R. L., J. Am. Chem. Soc. 86:508(1969).

83. Arthur, H. Thomas Company, Dialyzing Tubing, 4465-A2, Philadelphia, Pa., 19105.

84. Craig, L. C., King, T. P., and Stracher, A., J. Am. Chem. Soc. 79:3729 (1957).

85. Zsigmondy, R., Z. Anorg. Allg. Chem. 71:356(1911).

86. Foster, A. G., Trans. Faraday Soc. 28:645(1932).

87. Kelvin, Lord, Phil. Mag. 42:368(1871).

88. deBoer, J. H., and Lippins, B. C., J. Catalysis 3:38(1964).

89. Waters Associates Inc. Chromatography packing bulletin. Framingham, Mass.

90. Barrer, K. M., McKenzie, N., and Reary, J. S. S., J. Colloid Sci. 11:479(1956).

91. Langmuir, F., J. Am. Chem. Soc. 40:1361(1918).

92. Freundlich, H. Colloid and capillary chemistry. London, Methuen, 1926.

93. Feitl, L., and Smolkova, K., J. Chromatography 65:249(1972).

94. Oth, A., and Doty, P., J. Phys. Chem. 56:43(1952).

95. Doty, P., and Steiner, R. F., J. Chem. Phys. 17:743(1949).

96. Koral, J., Uloman, R., and Eirich, F. R., J. Phys. Chem. 62:541(1958).

97. Lauria, R. J., Schmidt, W., and Eirich, F. R., 140th Meeting, American Chemical Society, Chicago, Illinois, Sept., 1971.

98. Traubs, I., Ann. 265:27(1891).

99. Greene, B. W., J. Colloid Interface Sci. 37, no. 1:144(1971).

100. Gouy, G., J. Phys. Theor. Appl. 9:457(1910); Ann. Phys. 7:129(1917).

101. Chapman, D. L., Phil. Mag. 25:475(1913).

102. Felter, R. E., and Ray, L. N., Jr., J. Colloid Interface Sci. 32, no. 2:349(1970).

103. Emery, P. H., Jr. Polymer adsorption and fractionation in the polystyrene-dichloroethane-carbon black system. Doctor's Dissertation. Appleton, Wis., The Institute of Paper Chemistry, 1965. 186 p.

104. Farrar, N. O. Partitioning and reversibility of polymer adsorption in the polystyrene, 1,2-dichloroethane-carbon black system. Doctor's Dissertation. Appleton, Wis., The Institute of Paper Chemistry, 1967. 93 p.

105. Laffend, K. The effect of acetyl content of glucomannan on its sorption onto cellulose and on its beater additive properties. Doctor's Dissertation. Appleton, Wis., The Institute of Paper Chemistry, 1967. 89 p.

106. Stockmayer, W. H., and Zimm, B. H., J. Chem. Phys. 17:1301(1949).

107. Higuchi, W. I., J. Phys. Chem. 65:487(1961).

108. LaMer, V. K., Kane, J. C., and Linford, H. B., J. Phys. Chem. 67:1977 (1963).

109. Teller, D. Sedimentation equilibrium of macromolecules. Doctor's Dissertation. Berkeley, Calif., University of California, 1965. 195 p.

110. Othe, A., Bull. Soc. Chim. Belges 63:393(1954).

APPENDIX I

DETERMINATION OF MOLECULAR WEIGHT BY SEDIMENTATION EQUILIBRIUM ANALYSIS

The weight average molecular weight ($\underline{M}_w$) is calculated from the concentration distribution of polymer in a centrifugal field by the following classical equation:

$$M_w = \frac{2\,RT}{\omega^2\,(1 - \bar{\nu}_2\,\rho)}\,\frac{d\,\ln\,C}{d(r^2)} \qquad (14)$$

where $\underline{R}$ is the gas constant, $\underline{T}$ is the absolute temperature, ω is the angular velocity of the rotor, $\bar{\nu}_2$ is the partial specific volume of polymer, ρ is the solution density, and $\underline{C}$ is the polymer concentration at distance $\underline{r}$ from the axis of rotation. The quantity $d\,\ln\,\underline{C}/d(\underline{r}^2)$ is obtained as the slope of a plot of $\ln\,\underline{C}$ versus $\underline{r}^2$. This quantity is used as a parameter relating to the nature of the polymer solution.

Studies have shown that for an ideal monodispersed system, $\ln\,\underline{C}$ versus $\underline{r}^2$ will be linear along the whole cell. For a nonideal monodispersed system, a curve of decreasing slope will be characteristic of this plot. For the polydispersed ideal system, the plot of $\ln\,\underline{C}$ versus $\underline{r}^2$ usually shows an increasing slope. For a polymer system that is nonideal and polydispersed the plot may be linear or of increasing or decreasing slope depending on the relative magnitude of each effect.

All sedimentation equilibrium runs on the ultracentrifuge were performed at 25°C. with rotor angular velocities from 20,108 to 44,775 r.p.m. depending on the molecular weight fraction. The partial specific volume of PEI at 25°C. at infinite dilution was taken as 0.708 cc./g. (1). The solution density at any given PEI concentration was calculated from the following expression:

$$\rho = (g_1 + g_2)/(g_1\bar{\nu}_1 + g_2\bar{\nu}_2) \qquad (15)$$

where g_1 is the grams of solvent, g_2 is the grams of polymer, and $\bar{\nu}_1$ and $\bar{\nu}_2$ are the partial specific volume of solvent and polymer, respectively. The partial specific volume of solvent (0.109N NaCl) at 25°C. was found in the literature (13) as 1.00156 cc./g.

The polymer concentration distribution in a centrifugal field was recorded utilizing Rayleigh optics on a Beckman Spinco Model E ultracentrifuge. Fringe numbers and positions were determined from film negatives of the Rayleigh interference patterns with the aid of an x-y microcomparator fitted with digital and card punch read-out devices. The concentration distribution across the cell expressed in fringe numbers was used to evaluate Equation (14) with the aid of a computer. Computations were done on an IBM 360 Model 44 computer using the sedimentation equilibrium analysis program by Teller (109). The program calculates the average M_w throughout the cell, at the meniscus, and at the bottom of the cell. Comparison of these values in conjunction with the sum of the absolute values of the deviation of ln C versus r^2 values from their regression line can be used to evaluate for linearity. If nonideality effects are considered negligible then a large deviation of ln C versus r^2 values from their linear regression line may be used as a measure of polydispersity.

Table XVII shows the results obtained for sedimentation equilibrium molecular weight determinations. The concentration of solution expressed as fringe number, the sum of the absolute values of the deviation from linearity, the rotor angular velocity, and the meniscus average and bottom of the cell M_w values are listed. The molecular weight shown at infinite dilution is the reciprocal of the least squares fit intercept of a plot of the reciprocal of the M_w versus fringe number.

TABLE XVII

WEIGHT AVERAGE MOLECULAR WEIGHT

Fraction	Fringe Number	DI[a] x 10^3	Rotor Angular Velocity, r.p.m.	Meniscus	Molecular Weight Average	Bottom	Infinite Dilution
1	4.52	5.84	20,108	16,595	16,369	16,828	19,840
	9.04	7.44		13,889	13,533	14,810	
	13.56	1.77		12,145	11,971	13,047	
	4.52	11.55	25,980	18,753	16,620	18,568	20,000
	9.04	6.96		12,663	13,517	15,812	
	13.56	5.79		13,913	12,089	15,146	
3	4.08	21.74	20,409	13,137	16,872	16,872	18,000
	7.38	9.20		16,408	18,871	22,501	
	12.15	8.26		14,584	16,587	20,282	
	15.79	6.71		14,605	16,537	18,200	
	18.15	2.36		18,364	17,476	17,674	
4	4.16	3.34	23,150	10,767	10,798	10,736	11,100
	9.05	5.24		8,288	9,409	10,049	
	13.81	4.16		8,614	9,601	9,940	
5	13.75	8.09	20,410	8,304	9,898	11,267	10,400
	19.40	5.63		9,140	9,814	9,782	
	27.01	6.12		8,927	9,472	10,549	
	31.71	4.91		7,772	9,240	10,143	
7	11.98	16.59	29,509	4,209	5,362	6,956	5,350
	16.81	13.38		4,350	5,183	6,718	
	21.64	11.45		4,604	5,282	6,302	
	26.11	8.01		4,699	5,263	5,555	
9	8.43	27.38	44,775	1,440	2,026	3,193	2,140
	13.36	22.99		1,456	1,988	3,675	
	18.26	18.70		1,464	1,964	2,795	
	25.65	15.83		1,395	1,846	2,762	

[a]Sum of the absolute value of the deviation of ln $\underline{J}$ versus $\underline{r}^2$ from linearity. The regression line was used as the reference line of linearity.

The $\underline{M}_{\underline{w}}$ at infinite dilution at the two rotor velocities shown for F-1 are within the experimental error of being equal. These values are essentially the same as Kindler (1) found for the highest molecular weight fraction of Dow Chemical Company's PEI Sample 633974. Dick and Ham (37) also have found that

20,000 is the highest molecular weight PEI obtainable without adding cross-linking agents.

The molecular weight of the whole PEI Sample 633974 was estimated by the manufacturer at 5000.

APPENDIX II

DETERMINATION OF MOLECULAR WEIGHT BY HIGH-SPEED MEMBRANE OSMOMETER

The number average molecular weight ($\underline{M}_n$) of a polymer in solution may be calculated from osmotic pressure measurements by employing the following classical equation:

$$M_n = RT/(\pi'/C)_{C\to o} \qquad (16)$$

where $\underline{R}$ is the gas constant, $\underline{T}$ is the absolute temperature, and π' is the osmotic pressure at polymer concentration $\underline{C}$. The reduced osmotic pressure ($\pi'/\underline{C}$) at $\underline{C} = 0$ is obtained as the intercept of a plot of $\pi'/\underline{C}$ versus $\underline{C}$.

Table XVIII gives the data points, concentration of PEI, and osmotic pressure. Figure 39 shows the $\pi'/\underline{C}$ versus $\underline{C}$ plots.

TABLE XVIII

OSMOMETRY DATA

PEI Fraction	Concentration, g./l.	π'	$\pi'/\underline{C}_{\underline{C}\to o}$ x 10^{-1} g./cm.^{2}	$\underline{M}_n$
3	0.232	0.31	1.431	17,500
	0.387	0.58		
	0.929	1.46		
	1.239	2.03		
5	0.381	0.78	1.976	12,680
	0.572	1.16		
	0.763	1.63		
	0.858	1.75		
	1.144	2.40		
	1.430	3.21		
	1.907	4.20		
7	0.0871	4.824	4.755	5,270
	0.116	4.824		
	0.174	4.882		

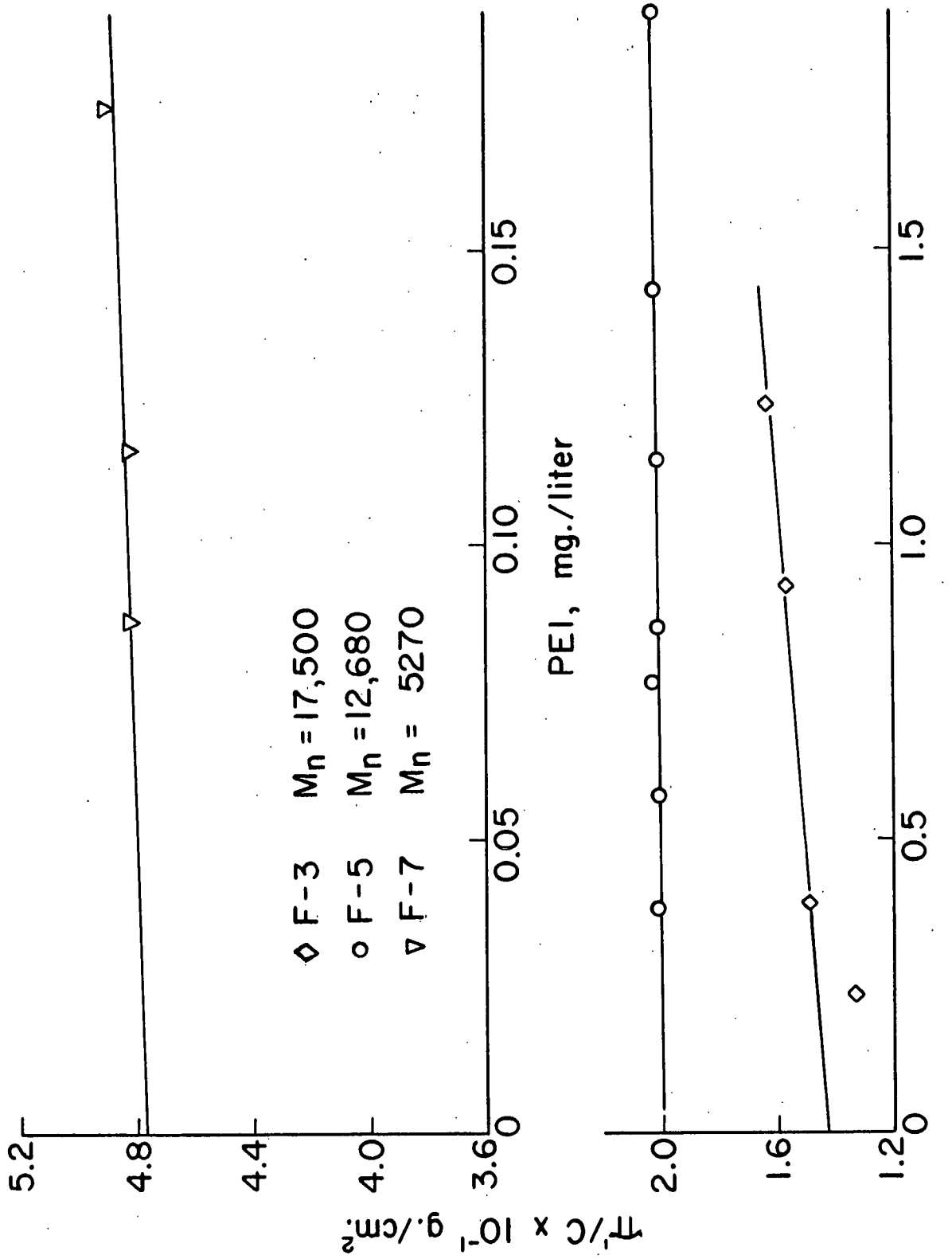

Figure 39. Specific Osmotic Pressure as a Function of Concentration

APPENDIX III

TABLE XIX

DIFFUSION COEFFICIENTS OF POLYETHYLENIMINE

Fraction	Average Fringe Number	Apparent $\underline{D} \times 10^6$, cm.^{2}/sec. at $\underline{t} = \infty$	Limiting $\underline{D}_o \times 10^6$, cm.^{2}/sec. at $\underline{t} = \infty$, $\underline{C} = 0$
1	9.40	0.612	0.601
	13.40	0.672	
	18.12	0.567	
	20.81	0.638	
	26.85	0.672	
3	7.37	0.980	0.947
	11.67	0.910	
	15.79	0.950	
	18.16	0.870	
	24.38	0.970	
4	10.83	0.800	0.843
	15.12	0.798	
	20.83	0.798	
	23.43	0.810	
	29.86	0.741	
5	13.75	1.098	1.060
	19.40	1.064	
	27.01	1.116	
	31.63	1.062	
7	11.98	1.378	1.334
	16.81	1.329	
	21.64	1.299	
	26.11	1.394	
9	8.43	1.777	1.829
	13.36	1.750	
	18.27	1.673	
	25.65	1.670	

APPENDIX IV

TABLE XX

VISCOSITY DATA

Fraction	Concn., %	Reduced Viscosity, η_{sp}/C, cc./g.	Intrinsic Viscosity $[\eta]$ with 95% Confidence Limits, cc./g.	Slope of $\eta_{sp/C}$ vs. C
1	1.427	11.56	11.33 ± 0.24	0.243
	1.282	11.73		
	0.976	11.58		
	1.427	11.66		
	0.936	11.64		
	0.678	11.46		
	0.436	11.39		
3	1.613	12.90	10.59 ± 0.17	1.436
	1.403	12.67		
	1.613	12.83		
	1.403	12.60		
	1.152	12.25		
	0.849	11.79		
	0.609	11.44		
4	3.235	14.10	10.24 ± 0.37	1.213
	2.813	13.55		
	2.311	12.96		
	1.703	12.27		
	3.200	14.21		
	2.782	13.74		
	2.285	13.00		
	1.684	12.36		
5	2.025	11.94	9.86 ± 0.24	1.056
	1.761	11.72		
	1.446	11.45		
	1.066	10.99		
	0.698	10.48		
	2.025	12.06		
	1.446	11.26		
	0.698	10.71		
7	1.309	10.00	9.80 ± 0.19	0.143
	1.077	9.96		
	0.563	9.92		
	1.507	9.99		
	1.309	10.00		
	1.077	10.00		
	0.793	9.82		

TABLE XX (Continued)

VISCOSITY DATA

Fraction	Concn., %	Reduced Viscosity, η_{sp}/C, cc./g.	Intrinsic Viscosity [η] with 95% Confidence Limits, cc./g.	Slope of $\eta_{sp/C}$ vs. C
9	0.729	7.77	7.49 ± 0.39	0.794
	0.854	8.46		
	0.991	8.32		
	1.126	8.54		
	1.239	8.30		
	0.582	7.93		
	0.529	7.64		
	0.438	7.81		
	0.364	8.06		
	0.233	7.63		

APPENDIX V

MOLECULAR DIMENSION CALCULATIONS BY THE SEELY EQUATION

Several theories and models exist which relate viscosity and molecular weight to the intramolecular structure of polymers. Most are based on a linear polymer. The various equations that result may be regarded at best to be estimates of the molecular dimensions and not absolute. Seely (81) has derived an equation based on the model of a hypothetical polymer molecule viewed as a porous sphere. An equation was derived for the case where fluid flow within the sphere obeys Darcy's law while the creeping motion equations are used to describe fluid flow outside the sphere. The porosity, permeability, and radius of the sphere are considered and related to the hydrodynamic properties of dilute solutions. The final equation developed has the following form:

$$[\eta] = A/(1 + B\, M_w^{-2/3}) \ . \tag{17}$$

The constants A and B are given by

$$A = 5/[2(1 - \varepsilon)\rho] \quad \text{and} \tag{18}$$

$$B = 10K\ (3.33\pi\ N/A)^{2/3} \ , \tag{19}$$

where ε is the porosity, ρ is the density, and K is the permeability and N is Avogadro's number. For a porous spherical molecule of mass m, the radius of the sphere a may be related to m by the following:

$$m = (4/3)\ \pi\ a^3\ \rho\ (1 - \varepsilon) \ . \tag{20}$$

If N molecules are present and Equation (18) is substituted into (20), the molecular radius, in angstroms when the $[\eta]$ is expressed in cc./g., is given by

$$a = 0.542\ (M_w A)^{1/3} \ , \tag{21}$$

The Seely equation is easily applied to $[\eta]$ and the molecular weight data. If the equation adequately describes the hydrodynamic behavior of polymers in dilute solutions then a plot of the $[\eta]^{-1}$ versus $\underline{M}_w^{-2/3}$ will show linearity. The intercept and slope give $\underline{A}^{-1}$ and $\underline{BA}^{-1}$, respectively. The permeability and porosity of the macromolecule are calculated using Equations (12) and (13) when the density of the polymer is known. A density value of 1.41 g./cm.^{3} was used in porosity and permeability calculations (1).

The correlation coefficient for the $[\eta]^{-1}$ versus $\underline{M}_w^{-2/3}$ plot is 0.97. Figure 40 shows the least squares fit of the Seely equation through the data points. The porosity, permeability, and the hydrodynamic radius as a function of $\underline{M}_w$ for a number of branched and/or cross-linked polymers including the results obtained for PEI are shown in Table XXI (81).

TABLE XXI

MOLECULAR PARAMETERS RESULTING FROM SEELY EQUATION

	$\underline{M}_w$ Range	Porosity	Permeability, $\underline{K}$, cm.^{2}	Hydrodynamic Radius, $\underline{a}$, as a function of $\underline{M}_w$
Dextran moderately branched	4.2×10^5-2.7×10^6	0.982	3.52×10^{-13}	$2.5\ \underline{M}_w^{1/3}$[a]
Dextran highly branched	4.0×10^4-2.4×10^5	0.964	1.05×10^{-13}	$2.0\ \underline{M}_w^{1/3}$
Glucomannan triacetate	1.25×10^4-3.2×10^5	0.998	3.58×10^{-13}	$2.8\ \underline{M}_w^{1/3}$
Lignosulfonic acid in 0.5N NaCl	1×10^4-7×10^4	0.699	7.5×10^{-15}	$1.02\ \underline{M}_w^{1/3}$
PEI in 0.1N NaCl	2×10^3-2×10^4	0.860	1.8×10^{-15}	$1.26\ \underline{M}_w^{1/3}$

[a] Values confirmed by light scattering.

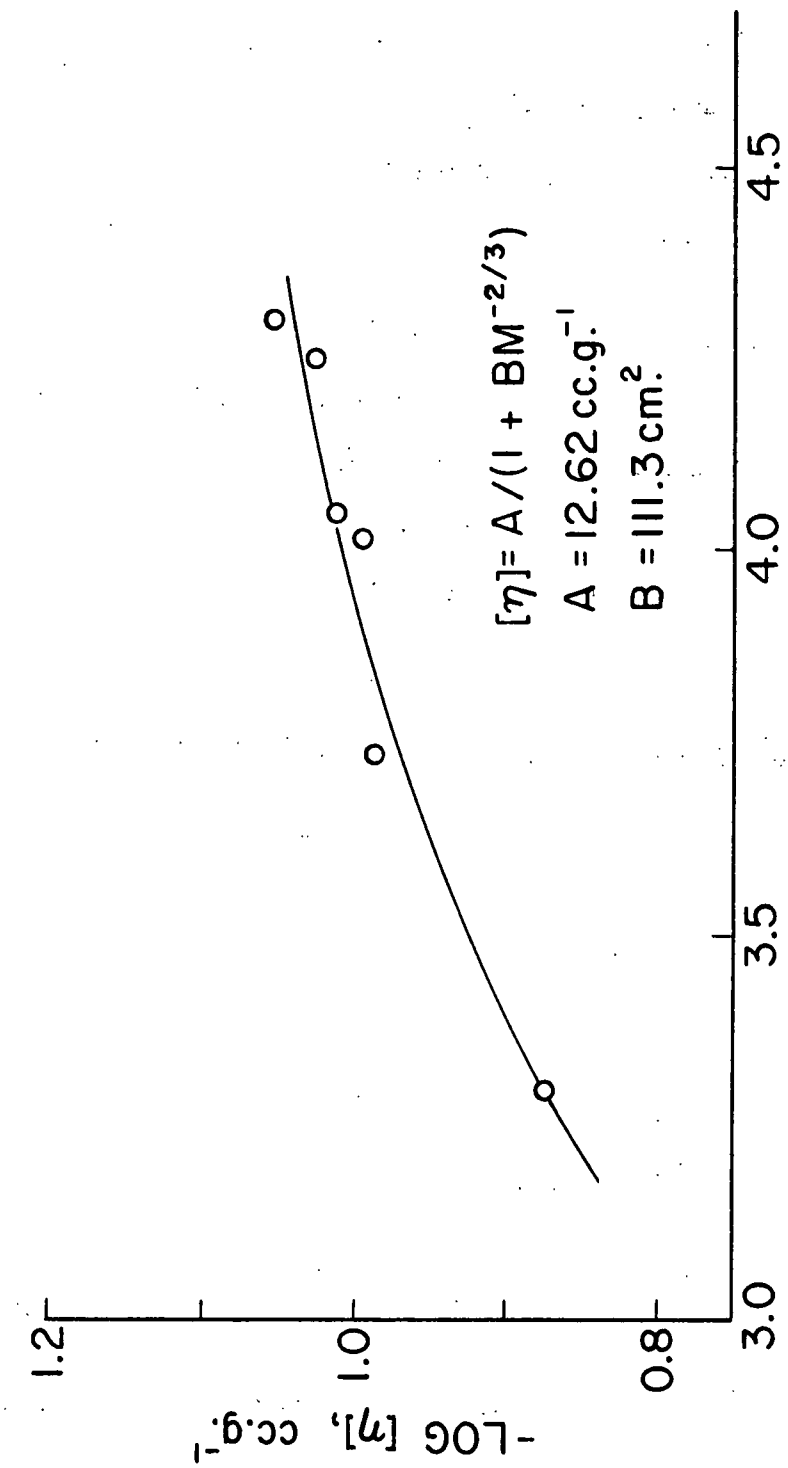

Figure 40. Seely Relation Fit to Polyethylenimine Intrinsic Viscosity and Molecular Weight Data

The differences in the two dextran molecules listed are the molecular weight ranges and the degree of branching. Dextrans are believed to be somewhat stiff macromolecules. The higher degree of branching is reflected by the slightly lower porosity and permeability (K). The hydrodynamic radius as a function of M_w also reflects this structure. The molecular dimensions obtained by light scattering are in good agreement with values determined above for the moderately branched dextran (81).

The glucomannan triacetate molecule compared to the dextrans is seen to be slightly more rigid with a little higher ε and K. The hydrodynamic radius relationship as a function of M_w also shows the increased stiffness. A coefficient of 2.8 compared to 2.5 and 2.0 for the dextrans was obtained for the glucomannan triacetate molecule.

The lignosulfonic acid molecule in 0.5N NaCl has a very compact structure compared to the dextrans and glucomannan triacetate molecules. This is reflected by the low K and ε compared to the above cited macromolecules.

The porosity coefficient obtained for the PEI macromolecule is lower than the dextran molecule but not nearly as low as the lignosulfonic acid molecule. The permeability coefficient K is of great interest. It is about 2 orders of magnitude less than the dextran molecule and about one-fourth the value obtained for the lignosulfonic acid molecule. These two parameters, ε and K, suggest what has been concluded previously for the PEI macromolecular structure from the polymerization mechanism and degree of branching studies (37).

The porosity coefficient shows that only 14% of the volume within the equivalent sphere is polymer and that 86% of the volume is filled with solvent. The very low permeability, however, indicates that little fluid flow occurs

through the molecule. Thus, the motion of the fluid within the molecule is best described by the motion of the molecule itself. The PEI macromolecule can be described as being very close to an impenetrable spherical molecule. To fit both the ε and $\underline{K}$ obtained, a very highly branched molecular structure is supported, with relatively close branch sites that should give rise to low permeability. The uniformity of structure in three dimension is implied since a nearly impenetrable structure is supported. The association of counterions within the sphere of the PEI macromolecule may enhance the structuring of solvent and be a contributing factor in causing the molecule to have a very low permeability.

APPENDIX VI

DISSYMMETRY DETERMINATIONS OF PEI SOLUTION AS A FUNCTION OF pH

The dissymmetry (Z) of the PEI macromolecule as a function of pH of the PEI solutions used for Rayleigh scattering determinations is shown in Fig. 41. The Z values obtained are mostly below 1.0. This behavior is commonly found for polyelectrolytes, especially when simple electrolyte is present (50, 94, 95, 110). Dissymmetry values below unity are explained by some investigators as resulting from the electrostatic interaction between charged sites and the binding of counterions which produce a nonrandom system. It should be emphasized that little information concerning the size and shape of polyions are obtained when Z values are less than unity. It is often noted, however, that viscosity and dissymmetry determinations show good correlation. It is interesting to note that close correlation is found between the viscosity and dissymmetry values as a function of pH. The viscosity data were obtained in the literature (3) and are shown in Fig. 41 with the dissymmetry values.

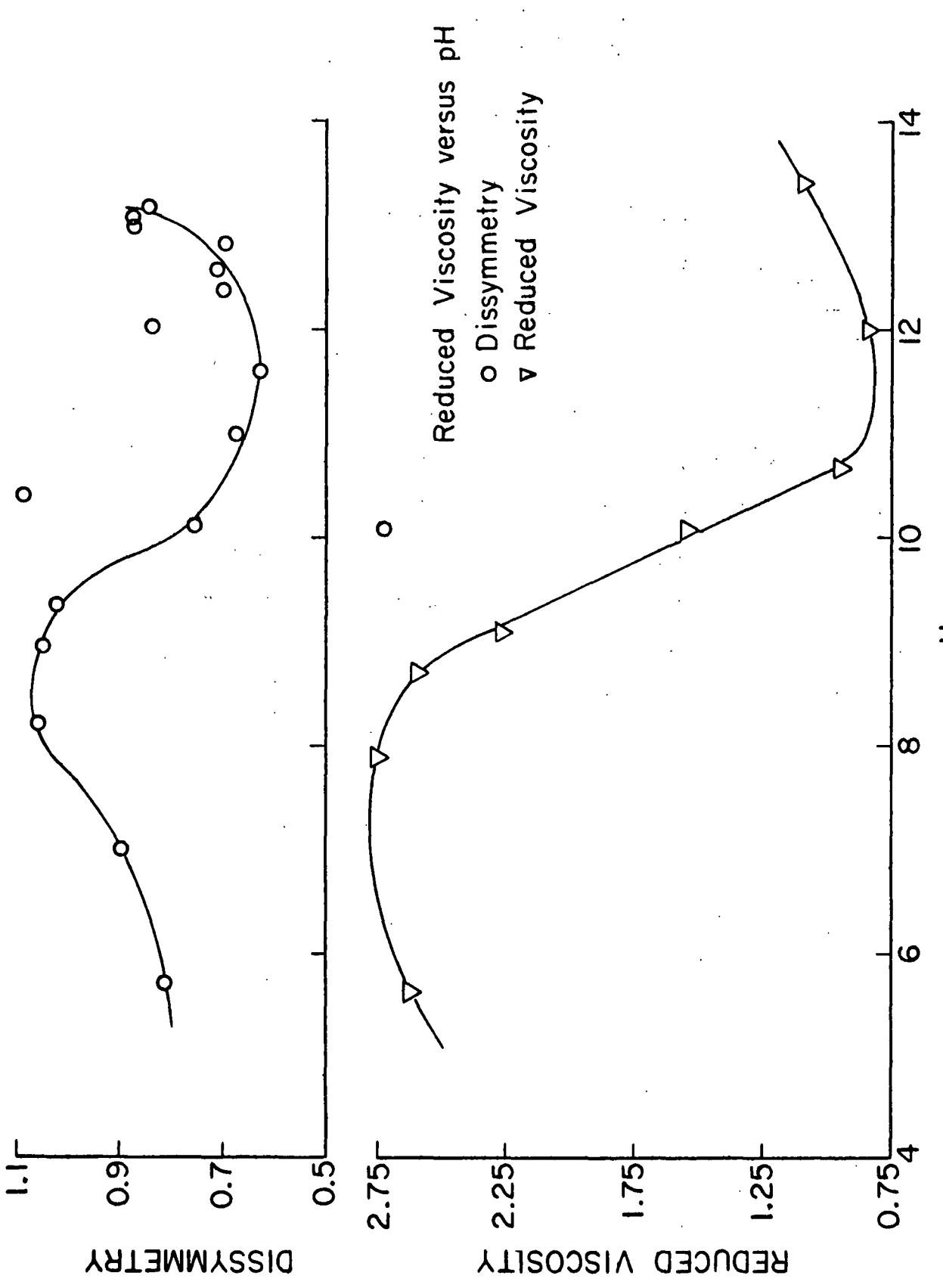

Figure 41. Reduced Viscosity and Dissymmetry of PEI as a Function of pH. Dissymmetry Versus pH. PEI F-3 0.167% in 0.109N NaCl. $\underline{D} = [(\underline{G}_{45°\,obs}/\underline{F}_{45°}) - \underline{G}'_{45°\,obs}/\underline{F}'_{45°})]/[(\underline{G}_{135°\,obs}/\underline{F}_{135°})-(\underline{G}'_{135°\,obs}/\underline{F}'_{35°})]$. $\underline{G}_{45°}$, $\underline{G}_{135°}$, = Light Scattered at 45° and 135°, $\underline{F}_i$ is the Product of Transmission of Filters'; Indicates Solvent Scattering

APPENDIX VII

TRANSMISSION ELECTRON MICROGRAPHS OF POROSIL A, B, AND C

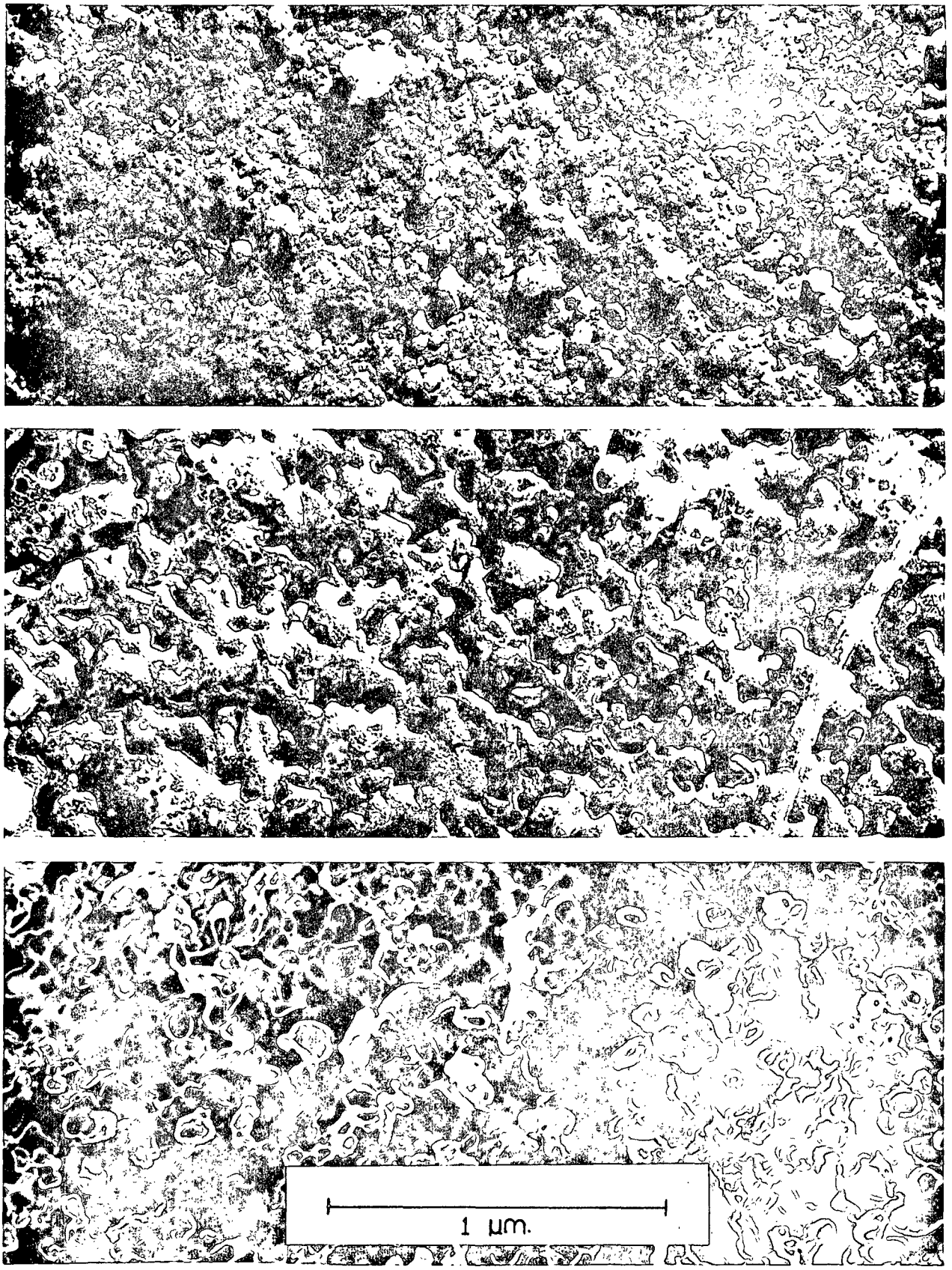

Figure 42. Top — Surface of Porasil A, Middle — Porasil B, Bottom — Porasil C

APPENDIX VIII

CALCULATION OF MINIMUM ACCESSIBLE SURFACE AREA OF POROSIL A FROM MERCURY INTRUSION POROSIMETRY AND NITROGEN GAS ADSORPTION

Table XXII lists the mercury intrusion porosimetry (MIP) and nitrogen gas adsorption isotherm pore analysis results. The area, cumulative area, volume, and cumulative volume percentages as a function of equivalent pore diameter (EPD) ranges are listed (59). An example of the method used to calculate the accessible surface area follows.

The cumulative volume percentage (CVP) for MIP indicates that 69.1% of the porous volume is accessible through restrictions (apertures) characterized by EPD < 120 A. In contrast, the nitrogen isotherm results suggest that only 26.5% of the pore volume corresponding to 41.1% of the porous surface area (SA) is characterized by EPD < 120 A.

Since nearly equal total pore volumes were found for Porasil A for pores $\leq$ 600 A. by both methods (69.1 − 26.5 = 42.6%) then 42.6% of the total porous volume accessible through restrictions of 120 A. EPD is actually best characterized by much larger pore sizes. If a minimum surface area model is selected, this would mean in the above case the largest pores present are considered to comprise the 42.6% of the total pore volume. On this basis, a minimum accessible surface area is calculated. For the filling of the largest pores, 42.6% (CVP) corresponds to 29% of the total surface area. This figure is obtained in the following way. From the NAI results on a CVP basis, filling of (100 − 42.6 = 57.4%) of the total pore volume starting with the smallest pores, corresponds to a cumulative pore SA of 71% of the surface area. This means that (100 − 71 = 29%) 29% of the surface area is representative of 42.6% of the total volume when the largest pores present are considered to be the dimensions of the ink bottle cavity.

TABLE XXII

PORE SURFACE AREA AND VOLUME DISTRIBUTIONS FROM MERCURY POROSIMETRY AND NITROGEN ADSORPTION ISOTHERMS

Porasil A

Equivalent Pore Diameter, A.	Nitrogen Adsorption		Mercury Intrusion		Nitrogen Adsorption		Mercury Intrusion	
	Area, %	Cumulative Area, %	Area, %	Cumulative Area, %	Volume, %	Cumulative Volume, %	Volume, %	Cumulative Volume, %
14-20	0.0	0.0	--	--	0.0	0.0	--	--
20-30	0.0	0.0	--	--	0.0	0.0	--	--
30-40	0.0	0.0	--	--	0.0	0.0	--	--
40-50	0.0	0.0	2.57	2.57	0.0	0.0	1.16	1.16
50-60	3.3	3.3	7.25	9.82	1.3	1.3	3.98	5.14
60-70	0.0	3.3	10.38	20.20	0.0	1.3	6.73	11.87
70-80	9.8	13.1	19.58	39.78	5.2	6.5	14.64	26.51
80-90	6.0	19.1	19.38	59.16	3.6	10.1	16.42	42.93
90-100	7.7	26.8	13.27	72.43	5.2	15.3	12.58	55.51
100-120	14.3	41.1	12.40	84.83	11.2	26.5	13.60	69.11
120-140	14.5	55.6	5.21	90.04	13.2	39.7	6.78	75.89
140-160	13.0	68.6	2.94	92.98	13.8	53.5	4.40	80.29
160-180	11.7	80.3	1.54	94.52	14.2	67.7	2.61	82.90
180-200	6.4	86.7	0.83	95.35	8.6	76.3	1.60	84.50
200-300	11.9	98.6	2.36	97.71	19.8	96.1	5.86	90.46
300-400	1.1	99.7	1.17	98.88	2.7	98.8	4.12	94.48
400-500	0.2	99.9	0.62	99.50	0.8	99.6	2.76	97.24
500-600	0.1	100.0	0.50	100.0	0.4	100.0	2.76	100.0

Thus, a minimum of 70.1% (41.1 + 29.0 = 70.1) of the total surface area is accessible to rigid molecules having less than 120 A. diameter. A 120 A. diameter molecule would have access to (100 − 70.1 = 29.9%) 29.9% or (29.9% x 282 = 84) 84 $m.^2/g.$ of Porasil A. Since a minimum surface area is assumed, it is likely that the accessible surface areas calculated may be slightly low. However, Table XIII may be viewed on a semiquantitative basis.

APPENDIX IX

TABLE XXIII

PORE SURFACE AREA AND VOLUME DISTRIBUTIONS FROM MERCURY POROSIMETRY AND NITROGEN ADSORPTION ISOTHERMS

Porasil B

Nitrogen Adsorption

Equivalent Pore Diameter, A.	Pore Area, %	Pore Cumulative Area, %	Pore Volume, %	Cumulative Pore Volume, %
14-20	19.8	19.8	4.9	4.9
20-30	30.6	50.4	9.9	14.8
30-40	12.4	62.8	5.8	20.6
40-50	6.7	69.5	4.1	24.7
50-60	4.6	74.1	3.5	28.2
60-70	1.7	75.8	1.5	29.7
70-80	3.3	79.1	3.3	33.0
80-90	2.1	81.2	2.4	35.4
90-100	1.6	82.8	2.1	37.5
100-120	2.2	85.0	3.2	40.7
120-140	1.9	86.9	3.3	44.0
140-160	1.4	88.3	2.9	46.9
160-180	1.1	89.4	2.6	49.5
180-200	0.8	90.2	2.2	51.7
200-300	3.2	93.4	10.5	62.2
300-400	2.5	95.9	11.3	73.5
400-500	1.9	97.8	10.9	84.4
500-600	2.2	100.0	15.6	100.0
		Mercury Intrusion		
150-200	5.76	5.76	2.82	2.82
200-250	16.56	22.32	10.40	13.22
250-300	19.53	41.85	15.38	18.60
300-350	16.21	58.06	14.71	33.31
350-400	12.36	70.42	12.94	46.25
400-450	8.81	79.23	10.46	56.71
450-500	6.42	85.65	8.51	75.22
500-550	4.70	90.35	6.90	82.12
550-600	3.17	93.52	5.10	87.22
600-650	2.11	95.63	3.69	90.89
650-700	1.59	97.22	2.99	93.88
700-750	1.05	98.27	2.12	96.00
750-800	0.71	98.98	1.54	97.54
800-850	0.57	99.55	1.34	98.88
850-900	0.45	100.00	1.12	100.00

TABLE XXIV

PORE SURFACE AREA AND VOLUME DISTRIBUTIONS FROM MERCURY POROSIMETRY AND NITROGEN ADSORPTION ISOTHERMS

Porasil C

Nitrogen Adsorption

Equivalent Pore Diameter, A.	Area, %	Cumulative Area, %	Volume, %	Cumulative Volume, %
14-20	2.1	2.1	0.2	0.2
20-30	30.5	32.6	4.5	4.7
30-40	12.2	44.8	2.6	7.3
40-50	6.2	51.0	1.7	9.0
50-60	4.0	55.0	1.3	10.3
60-70	0.1	55.1	0.0	10.3
70-80	3.8	58.9	1.8	12.1
80-90	1.5	60.4	0.8	12.9
90-100	1.1	61.5	0.7	13.6
100-120	1.6	63.1	1.0	14.6
120-140	1.4	64.5	1.1	15.7
140-160	1.0	65.5	0.9	16.6
160-180	0.9	66.4	1.0	17.6
180-200	0.7	67.1	0.9	18.5
200-300	5.7	72.8	8.9	27.4
300-400	11.2	84.0	24.2	51.6
400-500	8.9	92.9	24.3	75.9
500-600	7.1	100.0	24.1	100.0
		Mercury Intrusion		
125-150	15.26	15.26	9.35	9.35
150-175	17.60	38.86	12.61	21.96
175-200	12.87	45.73	10.71	32.67
200-225	9.98	55.71	9.36	42.03
225-250	10.16	65.87	10.71	52.74
250-275	9.98	75.85	11.57	64.31
275-300	7.64	83.49	9.74	74.05
300-325	5.32	88.81	7.35	81.40
325-350	4.05	92.86	6.06	87.46
350-275	2.49	95.35	3.98	91.44
375-400	1.49	96.84	2.43	93.87
400-425	1.27	98.11	2.32	96.19
425-450	0.52	98.63	1.00	97.19
450-475	0.34	98.97	0.68	97.87
475-500	0.29	99.26	0.52	98.39
500-525	0.24	99.50	0.45	98.84
525-550	0.22	99.72	0.42	99.26
550-575	0.20	99.92	0.39	99.65
575-600	0.08	100.00	0.35	100.00

APPENDIX X

EQUILIBRIUM ADSORPTION DATA

The tables contained within consist of adsorption data for the PEI-water-silica gel system taken under various experimental conditions. Constant agitation and temperature (25°C.) were maintained. Except where specified, the data were taken at 72 hours adsorption time.

When appropriate, the data required to construct equilibrium isotherms are given together with the calculated values necessary to check for compliance to the Langmuir equation. The symbols have the same meanings as in the text, C_I is the initial PEI concentration in an adsorption run, C_e is the equilibrium PEI concentration, C_* is the PEI concentration change with adsorption, Γ_w is the specific adsorption, g. PEI/100 g. silica gel. The pH given is at C_e. The units for C_I and C_e are milligrams per liter. The quantity C_e/C_* is unitless.

Unless otherwise stated, adsorption runs were done in an aqueous solution containing 0.109N NaCl and 4.25×10^{-5}N NaOH. Forty milliliters of solution were used in adsorption runs. Fifty milligrams of Porasil A, 120 mg. of Porasil B, and 480 mg. of Porasil C were used in the appropriate adsorption runs.

TABLE XXV

ADSORPTION OF F-10 ON PORASIL B

Adsorption time, hr.	72			720			
C_I, mg./l.	C_e, mg./l.	C_e/C_*	Γ_w, g./100 g.	C_e	C_e/C_*	Γ_w	pH
142.7	57.2	0.669	2.85	54.2	0.612	2.95	8.27
283.5	188.5	1.98	3.16	182.7	1.81	3.36	9.18
425.3	324.9	3.24	3.34	315.2	2.86	3.67	9.38
567.0	452.8	3.96	3.80	449.9	3.84	3.90	9.35
709.0	589.2	4.92	3.99	615.7	6.60	3.107	9.33
850.6	735.3	6.38	3.84	735.9	6.42	3.82	9.34
992.6	880.3	7.84	3.74	875.0	7.44	3.92	9.38

TABLE XXVI

ADSORPTION OF DUPEI ON POROSIL A, B, AND C FROM WATER

Time, hr.	84			216			240		
C_e	C_e/C_*	Γ_w	C_e	C_e/C_*	Γ_w	C_e	C_e/C_*	Γ_w	pH
				Porasil A					
84.8	7.925	0.856	81.9	6.022	1.088	84.3	7.527	0.896	8.80
172.3	9.214	1.496	168.8	7.604	1.776				9.04
250.4	6.936	2.888	245.4	5.971	3.288	246.6	6.180	3.192	9.18
327.0	5.945	4.400	324.4	5.632	4.608	324.1	5.598	4.632	9.28
406.8	5.754	5.656	402.1	5.333	6.032	401.8	5.308	6.056	9.37
492.0	6.074	6.48	480.8	5.215	7.376	491.4	6.022	6.528	9.40
562.7	5.269	8.544	546.4	4.439	9.848	583.9	6.821	6.848	9.43
				Porasil B					
23.9	0.334	2.384	22.4	0.306	2.434	20.0	0.265	2.514	9.40
110.5	1.373	2.681	115.2	1.520	2.524	113.4	1.461	2.584	9.64
198.3	2.248	2.937	199.1	2.278	2.910	200.6	2.335	2.860	9.60
289.9	3.148	3.067	285.8	2.971	3.204	283.7	2.886	3.273	9.67
375.6	3.686	3.393	366.5	3.302	3.696	364.4	3.222	3.766	9.70
471.4	4.640	3.383	457.2	3.948	3.856	458.4	4.000	3.816	9.71
582.7	6.713	2.890	554.1	4.802	3.843	564.4	5.370	3.500	9.80
				Porasil C					
0	0	0.796	0	0.000	0.796	0	0	0.796	9.28
0	0	1.592	0	0.000	1.592	0.471	0.002	1.580	9.41
4.1	0.0145	2.353	1.77	0.006	2.373	0.784	0.003	2.380	9.53
35.9	0.1037	2.884	6.48	0.017	3.129	3.240	0.009	3.156	9.64
40.4	0.0924	3.642	46.0	0.106	3.596	42.1	0.097	3.628	9.78
114.9	0.2508	3.817	108.1	0.232	3.874	109.9	0.237	3.859	9.80
191.5	0.4006	3.983	187.4	0.389	4.010	189.1	0.394	4.003	9.80

TABLE XXVII

ADSORPTION OF DUPEI ON PORASIL A FROM WATER AS A FUNCTION OF pH

pH	C_e, mg./liter[a]	Adsorbed, %
4.29	104.4	2.81
4.90	101.5	5.46
7.15	103.0	4.14
7.10	104.4	2.81
8.88	97.8	8.93
9.80	75.7	29.5
10.40	19.5	81.9
10.47[b]	2.2	98.0
10.69	5.2	97.0
10.70	2.1	98.1
10.81	2.2	98.0
11.00	2.4	97.6
11.50	17.4	83.8
11.92	100.8	6.10
12.18	107.4	0.0
12.38	107.4	0.0
12.75	107.4	0.0
13.1	107.4	0.0

[a] The initial concentration of all solutions was 107.4 mg./l. of DUPEI.

[b] The final equilibrium PEI concentration below pH 10.40 was determined spectrophotometrically. The final equilibrium concentration above pH 10.47 was determined by an organic nitrogen determination on 25.0 ml. of solution.

TABLE XXVIII

ADSORPTION OF DUPEI ON POROSIL A, B, AND C FROM WATER AT THE pH OF MAXIMUM ADSORPTION

NaOH, $\underline{N}$[a] x 10^2	$\underline{C}_I$	$\underline{C}_e$	$\underline{C}_e/\underline{C}_*$	$\Gamma_{\underline{w}}$	pH
		Porasil A			
1.125	Blank	--	--	--	10.55
1.000	47.8	5.01	0.117	3.42	10.58
0.875	95.5	11.2	0.133	6.74	10.65
0.750	143.2	29.5	0.260	9.10	10.61
0.625	191.0	58.0	0.436	10.64	10.69
0.625	286.5	136.4	0.909	12.00	10.70
0.625	382.0	231.8	1.543	12.02	10.71
0.625	573.0	417.2	2.678	12.46	10.72
0.625	764.0	598.0	3.602	13.28	10.79
		Porasil B			
1.000	Blank	--	--	--	10.50
0.875	95.5	20.0	0.264	2.51	10.74
0.750	191.0	66.6	0.535	4.14	10.78
0.625	286.5	148.5	1.076	4.60	10.77
0.500	382.0	240.1	1.692	4.73	10.65
0.375	477.5	326.4	2.159	5.03	10.55
0.250	573.0	418.7	2.713	5.14	10.42
0.125	669.5	515.3	3.34	5.14	10.20
		Porasil C			
1.375	Blank	--	--	--	--
1.250	215.0	6.73	0.030	1.73	10.80
1.125	322.0	7.23	0.023	2.62	10.79
1.000	430.0	28.9	0.072	3.34	10.87
0.875	537.0	81.0	0.178	3.80	10.80
0.750	644.0	156.4	0.321	4.06	10.78
0.500	752.0	237.4	0.461	4.29	10.80

[a]Normality of sodium hydroxide in adsorption solution.

TABLE XXIX

ADSORPTION OF DUPEI ON PORASIL A AT MAXIMUM ADSORPTION pH

0.0544N NaCl

NaOH, N[a] x 10^2	C_I	C_e	C_e/C_*	Γ_w	pH
1.125	Blank	--	--	--	10.52
1.125	95.5	12.7	0.153	6.62	10.61
1.125	191.0	61.0	0.469	10.40	10.62
0.750	286.5	137.9	0.928	11.89	10.58
0.750	382.0	219.5	1.351	13.00	10.55
0.750	477.5	306.4	1.791	13.69	10.58
0.750	573.0	405.4	2.419	13.41	10.60
0.750	669.5	492.3	2.778	14.18	10.50
		0.1094N NaCl			
1.125	Blank	--	--	--	10.53
1.125	95.5	40.7	0.745	4.38	10.65
1.125	191.0	63.9	0.503	10.17	10.70
0.750	286.5	139.9	0.954	11.73	10.65
0.750	382.0	225.1	1.435	12.55	10.60
0.750	477.5	314.6	1.929	13.04	10.50
0.750	573.0	405.4	2.419	13.41	10.58
0.750	669.5	495.2	2.841	13.94	10.60

[a]Concentration of sodium hydroxide in adsorption solution.

TABLE XXX

ADSORPTION OF F-7 ON PORASIL A, B, AND C AS A FUNCTION OF IONIC STRENGTH

NaCl, N	C_e,[b] mg./liter	Γ_w, g./100 g.	pH
	Porasil A		
0.005	178.5	1.21	9.00
0.005	--[a]		
0.041	138.8	4.38	9.10
0.041	--[a]		
0.074	119.0	5.97	9.12
0.074	--[a]		
0.109	108.0	6.82	9.15
0.109	--[a]		
0.144	99.6	7.52	9.05
0.144	--[a]		
0.170	94.0	7.97	9.10
0.170	--[a]		
0.211	92.5	8.09	9.15
0.211	--[a]		
	Porasil B		
0.005	136.1	1.91	9.63
0.041	129.0	2.15	9.65
0.074	126.4	2.24	9.64
0.109	118.7	2.49	9.61
0.144	126.4	2.24	9.62
0.170	126.1	2.24	9.63
0.211	124.3	2.30	9.65
	Porasil C		
0.005	93.0	3.35	9.55
0.041	83.0	3.68	9.55
0.074	81.3	3.74	9.58
0.109	76.3	3.91	9.58
0.144	79.2	3.80	9.60
0.170	79.8	3.79	9.60
0.211	79.0	3.82	9.42

[a] Blank Porasil A and solvent.

[b] C_I = 194 mg./liter.

TABLE XXXI

ADSORPTION OF FRACTIONS 1, 3, 4, 5, 7, AND 9 ON PORASIL A

Fraction	$\underline{M}_w$	$\underline{C}_I$	$\underline{C}_e$	$\underline{C}_e/\underline{C}_*$	Γ_w	pH
1	20,000	94.6	76.0	4.086	1.49	8.73
		141.9	114.9	4.026	2.16	8.89
		189.2	158.2	5.103	2.48	9.01
		236.8	201.8	5.832	2.77	9.08
		288.0	246.3	5.910	3.34	9.15
		378.3	324.9	6.084	4.27	9.30
		567.4	493.5	6.679	5.91	9.40
		94.0	74.5	3.821	1.56	8.69
		141.0	115.8	4.595	2.02	8.85
		188.0	157.6	5.184	2.43	9.00
		234.9	206.0	7.128	2.31	9.10
		281.9	241.0	5.892	3.27	9.20
		375.9	334.1	7.992	3.34	9.28
		536.8	497.3	7.478	5.32	9.41
3	18,000	96.8	83.7	6.389	1.05	8.59
		160.0	132.6	4.814	2.19	8.89
		193.6	169.4	7.000	1.94	8.95
		242.0	219.2	9.614	1.82	9.05
		290.4	262.8	9.522	2.21	9.12
		387.2	348.5	9.005	3.01	9.20
		580.8	530.9	10.639	3.99	9.30
		96.8	87.8	9.650	0.73	--
		145.0	130.8	9.083	1.12	--
		193.6	173.8	8.780	1.58	--
		242.0	220.1	10.05	1.75	--
		290.4	267.2	11.57	1.85	--
		387.2	364.7	16.21	1.80	--
4	11,100	187.3	155.3	4.853	2.56	--
		280.1	243.0	6.550	2.97	--
		374.6	318.8	5.713	4.46	--
		468.3	401.2	5.979	5.37	--
		562.0	484.9	6.289	6.17	--
		749.3	668.7	8.297	6.45	--
		46.6	33.0	2.427	1.09	8.23
		93.2	72.8	3.568	1.63	8.59
		139.8	116.4	4.974	1.87	8.82
		186.3	154.7	4.896	2.53	9.01
		279.5	239.5	5.988	3.20	9.22
		372.7	321.1	6.223	4.13	9.30
5	10,400	98.3	68.3	2.277	2.40	8.65
		147.4	108.7	2.809	3.01	8.90
		196.5	148.5	3.004	3.84	9.00
		245.7	189.4	3.364	4.50	9.11
		294.8	232.4	3.724	4.99	9.20
		393.1	311.4	3.812	6.54	9.30
		589.6	483.4	4.552	8.50	9.35

TABLE XXXI (Continued)

ADSORPTION OF FRACTIONS 1, 3, 4, 5, 7, AND 9 ON PORASIL A

Fraction	M_w	C_I	C_e	C_e/C_*	Γ_w	pH
7	5,350	96.8	47.1	0.948	3.98	--
		145.2	74.2	1.045	5.68	--
		193.6	102.2	1.118	7.31	--
		242.0	138.8	1.345	8.26	--
		290.4	172.0	1.453	9.47	--
		387.2	253.4	1.894	10.70	--
		580.8	425.7	2.745	12.41	--
9	2,140	96.4	10.3	0.120	6.89	8.45
		144.6	29.2	0.253	9.23	8.88
		192.8	73.0	0.485	10.38	9.05
		241.1	104.6	0.766	10.92	9.20
		289.3	150.8	1.089	11.08	9.30
		385.7	239.8	1.644	11.67	9.40
		578.6	413.9	2.513	13.18	9.55

TABLE XXXII

ADSORPTION OF PEI FRACTIONS 1, 3, 5, 7, AND 9 ON POROSIL C

Fraction	M_w	C_I	C_e	C_e/C_*	Γ_w^a	pH
1	20,000	49.2	1.23	0.026	1.92	7.74
		98.5	9.57	0.108	3.56	8.04
		147.8	45.7	0.448	4.08	8.33
		197.0	90.6	0.852	4.26	8.49
		246.2	136.4	1.242	4.39	8.62
		295.5	184.9	1.672	4.42	8.70
3	18,000	48.1	2.20	0.048	1.84	7.83
		96.2	8.35	0.095	3.51	8.11
		144.4	41.7	0.406	4.11	8.43
		192.5	86.9	0.823	4.22	8.62
		240.6	135.8	1.296	4.19	8.67
		288.8	182.9	1.727	4.24	8.78
5	10,400	48.2	2.94	0.065	1.81	7.87
		96.5	5.40	0.059	3.64	8.16
		144.8	44.2	0.439	4.02	8.46
		193.0	86.7	0.816	4.25	8.60
		241.2	131.8	1.204	4.38	8.74
		289.5	180.4	1.653	4.36	8.81
7	5,350	47.9	1.96	0.043	1.84	7.88
		95.8	13.3	0.161	3.30	8.17
		143.6	54.2	0.606	3.58	8.43
		191.5	97.5	1.037	3.76	8.64
		239.4	144.1	1.512	3.81	8.79
		287.2	191.0	1.985	3.85	8.80
9	2,140	48.6	1.96	0.042	1.87	7.72
		97.2	28.0	0.405	2.77	8.02
		145.8	63.0	0.761	3.31	8.36
		194.8	111.2	1.330	3.34	8.30
		243.1	158.1	1.860	3.40	8.46
		291.7	197.9	2.110	3.75	8.56

[a] 100 Mg. of Porasil C was present in adsorption runs.

APPENDIX XI

ADSORPTION REVERSIBILITY

The tables contained in this Appendix list adsorption reversibility data. Table XXXIII lists the specific adsorption at adsorption equilibrium and after elution with aqueous solvent at the various pH and sodium chloride contents stated. The initial adsorption runs were carried out in 40.0 ml. of aqueous solution containing 0.109$\underline{N}$ NaCl and $4.25 \times 10^{-5}\underline{N}$ NaOH at a constant temperature of 25°C. and a constant rate of agitation.

Table XXXIV lists the $\Gamma_{\underline{w}}$ of the reestablished adsorption equilibrium. Initially, the EAI for DUPEI on Porasil A was established at about pH 10.5 to 10.8. The pH was then lowered to about pH 2 and allowed to come to equilibrium. The reversibility of adsorption with respect to pH was investigated at the three ionic strength levels listed.

Table XXXV gives EAI data for separate adsorption runs for F-1 on Porasil A at low pH (from about pH 2 to 3) and at the maximum adsorption pH. The reestablished EAI data are also given. The low pH run was adjusted to the pH where maximum adsorption occurs. The high pH run was readjusted to a low pH and allowed to come to equilibrium.

Table XXXVI gives the data for the displacement of adsorbed DF-10 ($\underline{M}_{\underline{w}} \simeq$ 1500) by F-3 ($\underline{M}_{\underline{w}} \simeq 18{,}000$). The equilibrium adsorption data for the adsorption of F-10 on Porasil B from aqueous 0.109$\underline{N}$ NaCl and $4.25 \times 10^{-5}\underline{N}$ NaOH solution are given. The supernatant was replaced by F-3 in the same solvent. The replacement adsorption isotherm data at 139 and 260 hr. are listed. The equilibrium concentrations of the dialysis of 5 ml. of supernatant against 5.0 ml. solvent are listed.

The weight % of DF-10 and F-3 adsorbed, DF-10 displacement originally adsorbed and the increase in adsorption with addition of F-3 are listed.

TABLE XXXIII

DESORPTION BY ELUTION WITH SOLVENT

	Conditions	Acid[a], ml.	Γ_w[b], g./100 g.	Γ_w[c]
1.	Adsorption —	0.47	0.203	1.560
	F-1 on Porasil A	--	--	2.016
		5.34	2.296	2.432
		6.34	2.722	2.312
2.	Desorption —	7.24	3.114	3.272
	distilled water exchanged	--	--	3.344
	10 times over 120 hr.	11.28	4.852	5.320
1.	Adsorption —	2.39	0.865	1.088
	F-4 on Porasil A	3.75	1.450	1.632
		4.95	1.967	1.872
2.	Desorption —	5.99	2.414	2.528
	0.218N NaCl solution exchanged	7.35	3.000	3.200
	6 times over 108 hr.	9.45	3.860	4.128
1.	Adsorption —	6.01	1.076	2.947
	F-10 on Porasil B	8.55	1.537	3.357
		8.74	1.560	3.666
2.	Desorption —	10.29	1.840	3.899
	0.109N NaCl solution adjusted to	10.69	1.920	3.107
	pH 12.00 with NaOH — solvent	11.29	2.030	3.820
	exchanged 7 times over 120 hr.	12.09	2.17	3.916

[a] Milliliter of HCl, 5.0×10^{-3}N, used to titrate ammonia distilled over into boric acid solution.

[b] Specific adsorption PEI g./100 g. Porasil after elution with solvent.

[c] Specific adsorption at equilibrium.

TABLE XXXIV

REVERSIBILITY WITH RESPECT TO pH AS A FUNCTION OF IONIC STRENGTH

NaCl, N[a]	C_I, mg./liter	C_e[b], mg./liter	C_e/C_*	Γ_w[c], g./100 g.	pH[d]
0.000	46.6	13.2	0.395	2.672	1.75
	93.1	51.6	1.24	3.320	1.75
	139.6	98.1	2.36	3.320	1.72
	186.2	143.5	3.360	3.416	1.81
	279.3	222.4	3.908	4.552	1.81
	744.9	609.2	4.489	10.856	2.45
0.054	93.1	82.8	8.04	0.82	1.80
	186.2	151.4	4.351	2.78	1.90
	279.3	221.2	3.807	4.65	1.90
	372.4	290.8	3.564	6.53	1.90
	465.6	360.6	3.434	8.40	1.95
	558.7	447.5	4.024	8.90	2.15
	652.8	498.2	3.223	12.37	2.15
0.109	93.1	72.3	3.48	1.66	1.80
	186.2	149.7	4.10	2.92	1.90
	279.3	223.0	3.96	4.50	1.90
	372.4	291.9	3.63	6.44	1.95
	465.6	362.6	3.520	8.24	1.95
	558.7	443.4	3.846	9.22	2.10
	652.8	518.2	3.849	10.77	2.35

[a] Concentration of NaCl in adsorption solution.

[b] Reestablished DUPEI solution concentration.

[c] Specific adsorption of DUPEI g./100 g. Porasil A.

[d] Final solution pH.

TABLE XXXV

REVERSIBILITY WITH RESPECT TO pH

Run	Initial Adsorption Equilibrium[a]					Reestablished Equilibrium[b]			
	C_I	C_e	C_e/C_*	Γ_w	pH	C_e	C_e/C_*	Γ_w	pH
1	Blank	--	--	--	10.38	--	--	--	2.40
	49.4	13.8	0.388	2.85	10.50	7.6	0.176	3.45	2.30
	98.9	33.3	0.508	5.25	10.40	61.0	1.525	3.20	2.20
	148.5	68.9	0.866	6.37	10.40	103.7	2.160	3.84	2.20
	198.3	106.6	1.162	7.34	10.30	146.4	2.676	4.38	2.12
	248.1	141.7	1.332	8.51	10.40	197.1	3.670	4.30	2.25
	297.8	201.8	2.102	7.68	10.38	227.4	3.124	5.82	2.18
	397.0	257.2	1.840	11.18	10.40	315.8	3.724	6.78	2.60
	545.9	386.8	2.431	12.73	10.45	424.5	3.385	10.03	2.70
2	Blank	--	--	--	2.60	--	--	--	10.60
	49.4	33.6	2.126	1.26	2.60	0.0	0.0	3.98	10.60
	98.9	76.6	3.434	1.78	2.68	21.8	0.281	6.22	10.70
	148.5	123.1	4.846	2.03	2.70	52.1	0.537	7.76	10.72
	198.3	170.6	6.159	2.22	2.90	95.4	0.921	8.29	10.80
	248.1	215.1	6.518	2.64	2.90	100.8	0.681	11.85	10.70
	297.8	286.3	2.489	0.92	3.90	159.1	1.145	11.11	10.85
	397.0	340.3	6.001	4.54	4.00	253.9	1.757	11.56	10.75
	545.9	481.7	7.503	5.14	7.35	388.9	2.452	12.69	10.72

[a] Adsorption of F-1 PEI on 50.0 mg. Porasil A from 40 ml. of adsorption solution after 72 hr.

[b] Change pH by addition of acid or base reestablished equilibrium at 72 hr.

TABLE XXXVI

DISPLACEMENT OF LOW MOLECULAR WEIGHT POLYETHYLENIMINE BY HIGH MOLECULAR WEIGHT

				Adsorption of F-10 on Porasil B			Time Allowed for Equilibrium, hr.
C_I, mg./liter	49.1	98.0	147.0	196.0	294.0	392.0	--
C_e, mg./liter	2.95	6.48	10.3	63.6	156.1	257.8	134
Γ_w, g./100 g.	0.923	1.83	2.73	2.65	2.76	2.68	134
				Replacement Equilibrium Addition of F-3			
C_I, mg./liter	49.3	98.6	147.2	196.5	295.0	393.6	--
C_e, mg./liter	5.3	37.4	84.6	124.3	215.6	315.2	139
C_e	1.2	36.5	81.9	123.7	213.9	312.9	260
Γ_w, g./100 g.	0.879	1.22	1.25	1.44	1.59	1.57	139
Γ_w	0.961	1.24	1.30	1.46	1.62	1.61	260
				Dialysis of Supernatant			
Solution side C_I	5.30	37.4	84.6	124.3	215.6	315.2	--
Solution side C_e	4.71	22.7	53.7	86.3	180.8	280.8	120
Solvent side C_e	0.59	14.7	30.9	38.0	34.8	34.8	120
				Final Replacement Adsorption			
Weight % of total adsorbed, DF-10	50.5	41.2	38.7	29.8	37.9	37.0	
Weight % of total adsorbed, F-3	49.5	58.8	61.3	70.2	62.1	63.0	
Weight % of DF-10 replaced, initially adsorbed	1.64	31.3	43.7	53.9	40.2	41.4	
Weight % adsorption increase with addition of F-3	95	66.7	68.7	64.7	63.6	63.1	